2002

Evaluation of Dynamic Properties of a Carbon-Carbon Composite at Elevated Temperatures.

Sean Patrick Bunker

Recommended Citation

Bunker, Sean Patrick, "Evaluation of Dynamic Properties of a Carbon-Carbon Composite at Elevated Temperatures." (2002).
Electronic Theses and Dissertations. 294.
http://digitalcommons.library.umaine.edu/etd/294

EVALUATION OF DYNAMIC PROPERTIES

OF A CARBON – CARBON COMPOSITE

AT ELEVATED TEMPERATURES

By

Shaun Patrick Bunker

B.S. University of Maine, 2001

A THESIS

Submitted in Partial Fulfillment of the

Requirements for the Degree of

Master of Science

(in Mechanical Engineering)

The Graduate School

The University of Maine

August, 2002

Advisory Committee:

Michael Peterson, Assistant Professor of Mechanical Engineering, Advisor

Vince Caccese, Associate Professor of Mechanical Engineering

Lawrence Thompson, Research Engineer, Applied Thermal Science Inc.

EVALUATION OF DYNAMIC PROPERTIES

OF A CARBON – CARBON COMPOSITE

AT ELEVATED TEMPERATURES

By Shaun Patrick Bunker

Thesis Advisor: Dr. Michael Peterson

An Abstract of the Thesis Presented
in Partial Fulfillment of the Requirements for the
Degree of Master of Science
(in Mechanical Engineering)
August, 2002

Methods for in-situ monitoring of high temperature composite materials are important in a number of technological applications. In this work a method is developed that makes use of solid cylindrical waveguides to monitor the change of elastic properties and the oxidation reaction of carbon-carbon composites with change in temperature. The apparatus is designed to allow ultrasonic measurements to be performed in a controlled atmosphere at temperatures up to $1100^{\circ}C$. Signal processing required to obtain quantitative information is considered for the experimental apparatus described.

ACKNOWLEDGMENTS

I would first like to express my appreciation for my "thesis group", Miao Sun and Anthony Puckett for their patience, guidance, suggestions and encouragement during this intense process. I could not have completed this work without them.

I would also like to thank my advisor, Dr. Michael "Mick" Peterson for the chance to work on this project.

Many thanks go out to Sheryl Brockett and Richard Mewer who gave me the "It will all be over with soon" speech many times. I would like to thank them both for the encouragement and strength they provided me.

Last but certainly not least, I would like to express my thanks and love to Michelle for the support, understanding and encouragement I needed to finish this work. I couldn't have done it without you.

TABLE OF CONTENTS

LIST OF TABLES

LIST OF FIGURES

Chapter 1

INTRODUCTION

1.1 Motivation

Advancement of technologies such as those proposed for a number of new missile and satellite technology programs are pushing the thermal requirements of materials to new levels. These programs will require components to operate on high-maneuvering targets in a severe aero-thermal environment. A variety of new materials must be engineered in order to survive these severe environments while performing their individual tasks. Composite materials are currently being designed to meet these demanding criteria. These recently developed materials require a thorough knowledge of their mechanical properties as well as their failure mechanisms. Evaluation and monitoring techniques must be developed to aid in the design and fabrication of such materials. The composite material that will be considered in this work is made up of carbon fiber reinforced carbon.

Carbon-carbon composites are appropriate materials for applications that require high specific strength at elevated temperatures. Currently, limited information is available in the open literature that focuses on the behavior of the mechanical properties of carbon-carbon composites at elevated temperatures. Significant effort has been directed toward the development of protective coatings used on carbon-carbon composites. The interest in coatings is due to the reaction between carbon and oxygen at high temperatures that result in loss of material. Typically these protective coatings have a limited life, so the oxidation reaction of carbon-carbon composites is of great

1

importance. Limited information exists on the effects this reaction has on the modulus and other mechanical properties of carbon composites without coatings. This thesis will focus on monitoring the change in modulus of carbon – carbon composites with temperature and will consider the effects of the oxidation process on the elastic modulus of the material.

1.2   Carbon – Carbon Composites

Carbon-carbon (C/C) composites are materials that consist of carbon fibers embedded in a carbonaceous matrix. The particular carbon composite analyzed in this work is composed of a 3-dimensional, orthogonal, carbon fiber weave. The woven fiber preform is coated with the matrix material using chemical vapor infiltration to provide initial structure to the material. After depositing a thin layer of matrix on the fibers, the material is impregnated with a "thermoset" polymer resin and then heat treated in an inert atmosphere. This resin infusion process is repeated several times in order to increase the density of the matrix. At each step the heating turns the resin into a carbon matrix of increasing density. Repeating the procedure several times reduces the porosity of the material as the resin is forced into the pores of the matrix. The final product is a carbon fiber reinforced anisotropic carbon matrix composite that has a high strength to weight ratio. The material is used in applications for temperatures well above 1000°C. In fact, the strength of C/C composites increases with increasing temperature up to 2200°C because of the improved coupling between fiber and matrix [Rozak, 1984]. Figure 1.1 resembles the 3-dimensional orthogonal weave of the C/C composite studied in this work. The interstices in the weave are filled with the carbon matrix.
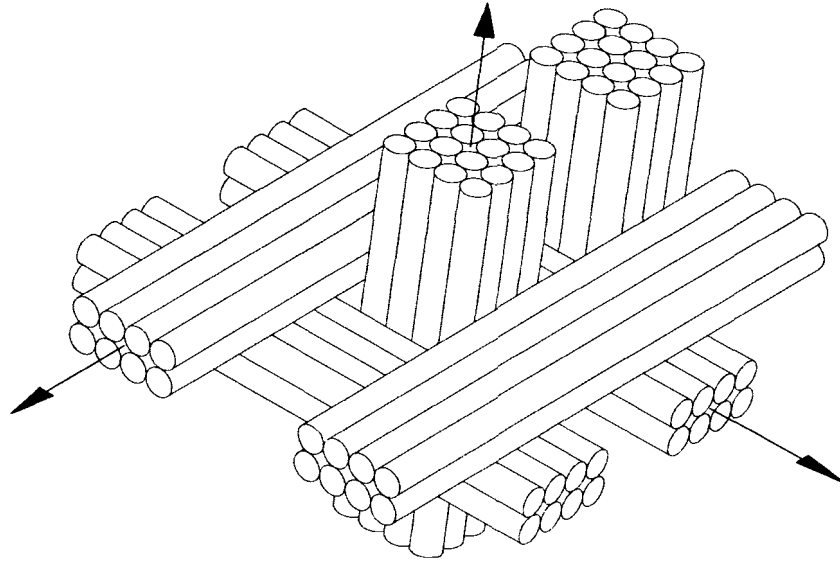
Figure 1.1. Sketch of 3 – dimensional carbon fiber weave.

The C/C composite specimens studied in this work are anisotropic materials, which have properties that are different in all directions at any given location. The anisotropy of the material leads to mechanical properties that must be considered carefully. Because of the 3-dimensional orthogonal weave, the original block of the material is nominally orthotropic with three planes of symmetry. Due to small size of the specimens cut from the original block and any irregularities within the weave, the specimens are considered to be anisotropic. The elastic properties of C/C composites cannot be represented by two terms as in isotropic material. Instead, at least nine elastic components of the stiffness tensor are required. Because of the uncertainty in the sample orientation and lay-up, as many as twenty-one independent elastic constants may be required [Sun, 2002]. In this work the C_{11} term is the single elastic constant that is monitored. This is the elastic constant that corresponds to the normal modulus of the C/C

composite in one of the primary axes of the material. Figure 1.2 is a photo of a sample of the C/C composite studied in this work.
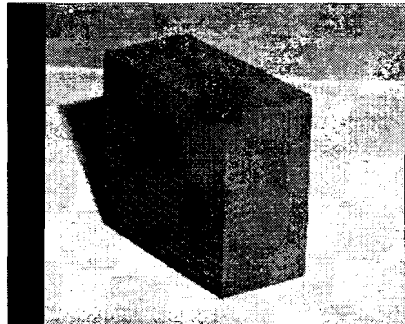
Figure 1.2. A piece of the actual C/C composite studied in this work.

One major limitation to carbon - carbon composites is the oxidation at high temperatures. The reaction between the carbon and oxygen occurs at elevated temperatures. Carbon readily reacts with oxygen at temperatures above 400°C. This reaction results in a rapid material loss (primarily of the matrix) and degradation of the mechanical properties of the material. As the material reacts with the oxygen, both the strength and the modulus of the material will change as structural material is lost. Consequently, protective coatings are often deposited on the C/C composite in order to prevent this reaction from occurring in high temperature environments. While in current applications of C/C composites these protective coatings are normally used, they typically crack and otherwise degrade in use. When intact, the coatings form a diffusion barrier that keeps oxygen from reacting with the carbon. Because of the mechanical properties, this coating lowers the overall strength to weight ratio but helps extend the life of the C/C component. Numerous experiments have been conducted in order to study and improve these protective coatings [Savage, 1993]. However, a continuing need exists to perform experiments to better understand the oxidation process. Currently, no

in-situ method exists to study the effects on mechanical properties of oxidation of C/C composites.

This work is focused on devising a method to monitor the oxidation process and to study the affects on the carbon-carbon composites. The overall goal is to measure and record the changes in material properties during controlled oxidation experiments. These results can then be compared to modulus – temperature experimental results obtained from mechanical testing in an inert atmosphere to better understand how oxidation affects the modulus as well as exploring the potential for using modulus as a measure of oxidation. With this modulus information, as well as strength testing at specific levels of oxidation, engineers will be able to apply a finite life design of carbon – carbon composites.

1.3   Applications of Carbon-Carbon Composites

Developed for aerospace applications, carbon-carbon composites exhibit low density, high thermal conductivity, low thermal expansion and excellent mechanical properties at elevated temperatures in excess of 2000°C. These materials are ideal for rocket nozzles and re-entry nose tips, diverter valves and have been used in the nose and leading edges of the NASA space shuttle seen in figure 1.3.
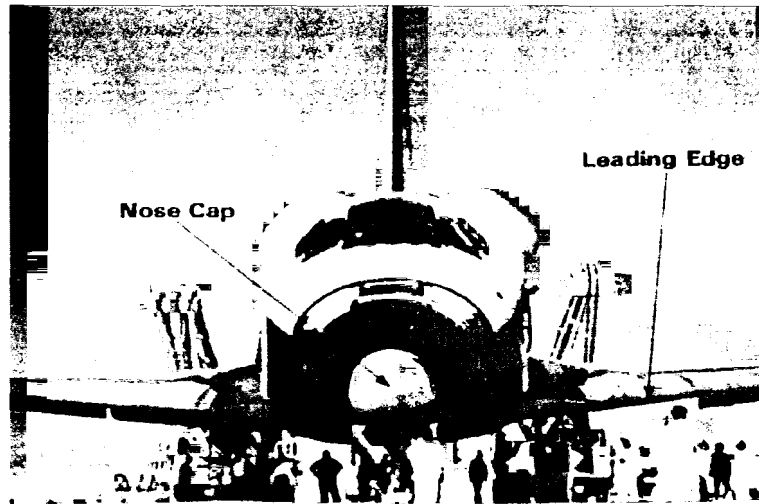
Figure 1.3. The NASA Space Shuttle and the use of C/C composites [Savage, 1993].

Commercial applications of this technology exist in areas such as aircraft brake systems, race car brake systems and other high temperature, high strength applications [Peterson, 2002]. C/C composites have demonstrated the ability to retain strength, and to resist wear when sliding against another C/C component. C/C composite brakes allow higher operational temperatures and produce the same amount of stopping distance without generating unwanted additional weight. Compared to their metallic counterparts, C/C composite brakes save the Boeing 747 almost 800 kg of excess mass [Savage, 1993]. Although the cost of C/C composites for aircraft brakes is high, the high strength, high specific heat, and large weight savings make them very cost effective for such applications. Figure 1.4 is a picture of an aircraft braking system containing C/C composite brake pads that have been sectioned.
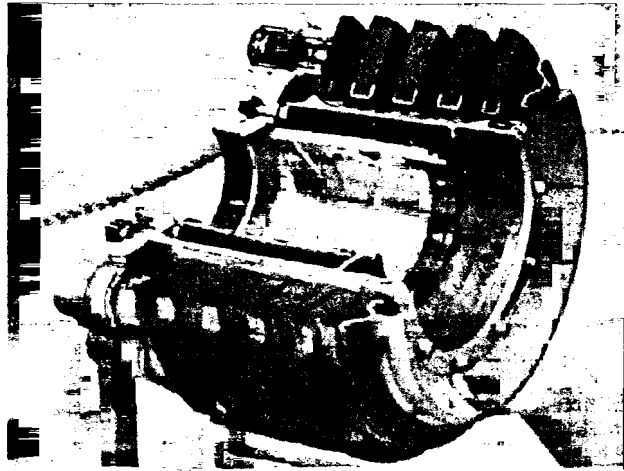
Figure 1.4. Sectioned C/C brakes from a commercial airliner [Savage, 1993].

C/C composites have also been manufactured into mechanical fasteners. These fasteners are used in high temperature applications that require high strength, high heat resistance. C/C composites are a good choice for such applications because of the ability to retain their mechanical properties at elevated temperatures.
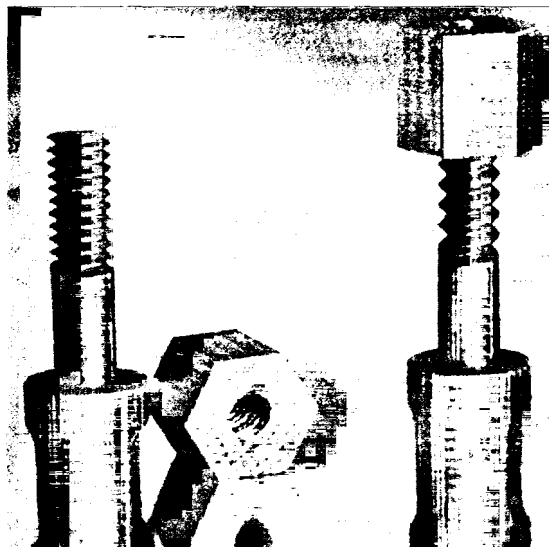
Figure 1.5. High temperature mechanical fasteners [Savage, 1993].

Among other aerospace applications, C/C composites can be used as rocket nozzles. Extremely hot gases pass through these nozzles that act as divergent exits. The

materials in these applications are short lived, but the static and dynamic loading are combined with very intense heating [Savage, 1993]. The exit nozzles are typically coated to delay oxidation and degradation of the component. If the component were to fail, the trajectory could no longer be properly controlled and the rocket targeting would be lost. Thus the C/C composite exit nozzle must possess excellent stability and strength under extreme conditions for a specified amount of time. However, the operational time is usually no more than one minute. A sketch of the rocket motor and nozzle is shown in figure 1.6.

The motivation for C/C composites as aircraft engine components has recently accelerated. Many countries are exploring the potential to construct hypersonic aircraft capable of flying at speeds of up to mach 5 [Savage, 1993]. C/C composites are extremely appealing in these applications due to their toughness at extreme temperatures. The strength to weight ratio of the C/C composites compared to alternative materials is an added bonus for this newly developing application. However, further progress in design applications will be facilitated
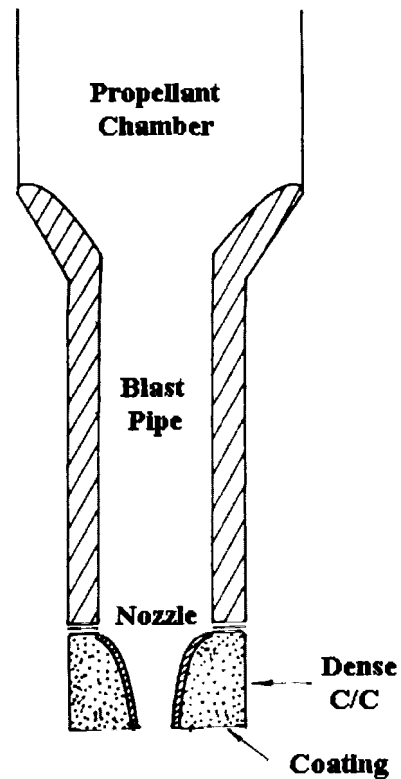
Figure 1.6. Rocket nozzle.

by a more thorough knowledge of their mechanical properties and the oxidation behavior at elevated temperatures.

8

1.4 Need for In-Situ Properties

Design for finite life for applications such as diverter nozzles, requires a thorough knowledge of the residual properties of a material. In high temperature design applications, C/C composites can be used as high strength components without adding the weight or complexity of oxidation resistant coatings. These components can maintain their physical properties in an oxidizing environment for a specified time. Similar applications include exhaust components for fighter aircraft and structures for space defense satellites [Carbon, 1995].

New in-situ monitoring methods are required to help materials researchers to better understand the mechanisms and reactions of C/C composites at elevated temperatures. Currently ex-situ methods exist that measure the material properties of C/C composites without destroying the sample as well as destructive testing. These methods require that a sample be removed from the testing environment during different stages of oxidation. Once a sample has been removed from the heated environment, the sample can no longer be tested. In order to acquire substantial knowledge of these material properties of a composite, several samples must be tested. Depending on the testing method, testing many samples can take a very long period of time.

In order to determine the degree of oxidation, a sample is weighed before and after an experiment. Degree of oxidation is usually reported based on the weight loss during the experiment. The technique developed in this work, will allow a sample to be tested in-situ. The oxidation process will not only be based on weight loss, it will also be controlled by the amount of oxygen allowed into the testing environment. The apparatus

will allow a controlled amount of air into the testing environment while the elastic properties are actively monitored. Also, an inert gas can be used to test the change in modulus with temperature. This will allow multiple tests to be performed on the same sample if the inert atmosphere tests are performed prior to oxidation. This method will prove to be beneficial in the studying of dynamic properties of materials in an elevated temperature environment by allowing the properties to be monitored in-situ and reaction processes including oxidation and densification to be measured in real time.

1.5   Alternative Technologies

A number of techniques exist for measuring the elastic properties of a solid. Examples of these methods that are widely used are the ultrasonic immersion testing, static or mechanical test methods and vibration testing. Some of these alternative approaches are briefly discussed in the following sections.

1.5.1   Mechanical Testing Methods

Mechanical testing methods present perhaps the most well established methods for obtaining the elastic properties of a material. In addition, mechanical testing is the only practical method of obtaining strength information on materials. The scale of the specimens is dependent on a number of issues associated with the acceptable length scales of materials and edge effects in the sample preparation methods. Using modern three or four point bend fixtures it is possible to obtain visco-elastic properties as well as strength for small (less than 60 mm long) beams cut from composite materials. In addition it is possible with mechanical testing to perform the tests at elevated temperatures. Kimura and co-authors [1982] found the change in modulus with

10

temperature of a C/C composite 3mm x 10mm x 60mm long using this four point bending technique. Young's modulus of a sample was measured from the stress strain relations recorded from the experiment and compared to another sample evaluated at a higher temperature. While static testing in mechanical fixtures is possible, larger specimens create significant cost and complexity to develop even the basic elastic properties of an anisotropic sample.

Other static testing methods that have been used on composite materials are compression and tensile testing. Much like the three and four point bending technique, these tests measure stress and strain of a sample with an applied load. Stress and strain are measured by monitoring the change in length of a specimen. This is achieved by attaching strain gages to the sample or by monitoring the displacement of sample. Unfortunately in high temperature applications, most strain gages cannot withstand the extreme temperatures. Clamp on extensometers with the electronics located outside of the furnace are typically used and make it possible to obtain the modulus in the direction of the strain [Walls, 2002]. Clamping components needed for tensile testing also create significant problems when testing in elevated temperatures so the standard test is compression. However in this configuration extensive high temperature compression testing is possible at temperatures as high as 3000°C. For anisotropic material multiple samples oriented at different directions to the fiber directions are required for full characterization.

1.5.2 Dynamic Testing

Dynamic methods are an important alternative to mechanical testing methods. Unlike mechanical testing methods, dynamic testing is typically limited to the acquisition of elastic properties. These methods range from standard methods such as dynamic mechanical analysis (DMA) to more recent techniques such as resonance spectroscopy measurements [Dual, 2001]. Standard dynamic mechanical analysis is used in commercial instruments for characterizing polymers. In this method a small sample is tested dynamically in a very similar manner to the mechanical test methods. DMA uses either sweep of temperature or frequency to acquire the elastic and visco-elastic properties of the material. Composite materials are typically tested in a three-point bend fixture. DMA is typically limited to the same temperature range considered in this work, 1100 –1400°C.

Resonance spectroscopy is a more general method than DMA since it allows the full visco-elastic tensor of a general anisotropic material to be obtained. Resonance spectroscopy makes use of a known regular geometry and excites resonance modes through the material thickness for a specific frequency range [Demarest, 1971 & Ohno, 1976]. The typical sample is a regular parallelepiped with dimensions on the order of 3-5 mm. Unlike DMA and mechanical testing, resonance spectroscopy has only been used for a limited temperature range. While it is possible to perform these tests at elevated temperature, resonant spectroscopy uses transducers that must be placed outside of the furnace. Most importantly, when compared to DMA or mechanical testing, resonance spectroscopy allows the full visco-elastic tensor to be recovered from a single sample. This allows materials with significant inhomogeneity and anisotropy to be investigated.

1.5.3 Ultrasonic Methods

Ultrasonic methods, the current approach, have been used to extensively measure the elastic properties of composite materials [Dual, 2001 & Huger, 1999]. The approach that is perhaps best accepted is immersion testing of samples. Bulk wave transit-time measurements are utilized as the principal mechanism for characterizing the elastic response of a material [Kline, 2001]. Water is used as a coupling between specimen and transducer. Because water is the immersion medium, only longitudinal waves are generated at the source. Mode conversion is used to excite transverse waves in the composite. Specimens of various sizes can be tested using this technique if a water tank is available to perform the experiments. Like resonant spectroscopy, the full visco-elastic tensor can be obtained from a single sample using an optimization technique. However, also like resonant spectroscopy, only a small range of temperatures can be used. The working fluid can be varied in temperature within a small range. An alternative, air or inert gas coupled ultrasonics is also possible, but greatly reduces the signal to noise ratio and can increase the complexity significantly.

Another technique that has recently been the subject of much interest has been laser generation and the detection of ultrasound. Laser generation is a very promising technique for testing material properties in high temperature environments. However, the use of laser ultrasound will require significant additional understanding before measurements at elevated temperatures can be developed. Perhaps the most promising approach is a hybrid approach that would make use of laser generation of ultrasound with a buffer rod used for the detection of the ultrasound. Laser detection of ultrasound on a

black surface in the presence of significant particulate matter as well as convective air currents presents significant challenges.

1.6 Ultrasonic Theory

A typical human being can hear sound in the range of 2 Hz to 20 kHz. Frequencies higher than this are considered ultrasonic. The typical frequency range normally used for ultrasonic nondestructive testing is 100 kHz to 50 MHz. In this work 1MHz central frequency transducers are used which results in a wavelength of 5mm, depending on the material tested.

Piezoelectric transducers are typically used for nondestructive ultrasonic testing. A sketch of an ultrasonic transducer and its components is shown in figure 1.7. The mechanical energy is transmitted from the transducer into the waveguide. Three main components of an ultrasonic transducer are the active element, backing and an impedance matching plate. The active element is a piezoelectric ceramic. This material converts the electrical energy into the ultrasound. The backing is a highly dense material that controls the vibration of the transducer by absorbing the energy radiating from the back face of the active element and thus shaping the pulse.

Ultrasonic transducers have a maximum exposure temperature, the Curie temperature of the piezoelectric material. If transducers are exposed to temperatures past their Curie temperature, the active element loses its properties and becomes nonfunctional. In order to assure that the transducers do not get damaged, it is necessary to keep the transducers below their Curie temperature.

14
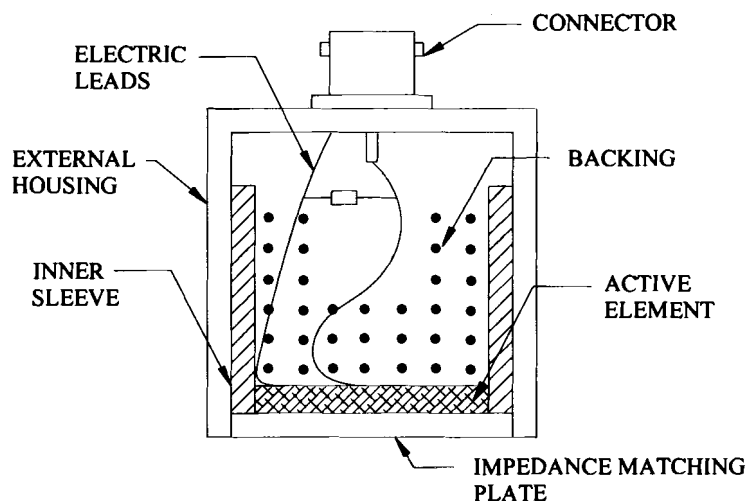
Figure 1.7. A sketch of the components of an ultrasonic transducer.

1.7 Waveguides

Ultrasonic waveguides or buffer rods are used to transmit the ultrasonic wave into

the furnace and through the carbon-carbon composite. The waveguides prevent damage

to the ultrasonic transducers. This technique was previously used to monitor the reaction

bonding of Silicon Nitride [Peterson, 1994]. In this work, solid cylindrical rods are used

to guide an ultrasonic signal from a transducer, to a sample and into a receiving

transducer. Cylindrical rods have boundaries that have strong impedance mismatch to

the surrounding medium. Waves impinging on these boundaries are reflected back in the

structure, thus the structure is said to be a waveguide [Dual, 2001]. Appropriate signal

processing techniques are used to remove the effects of the waveguides and to calculate

the phase velocity from the ultrasonic signal through the sample [Peterson, 1994]. While

the waveguides transmit the signal, the waves in the sample can be approximated as a 1-

D signal.

The group velocity of an ultrasonic wave at normal incidence between transducers, waveguides and C/C composite sample is measured. In order to maintain normal incidence, the contact surfaces of the waveguides and sample must be parallel and flat. The parallel surface conditions ensure that longitudinal waves propagate through the setup. The velocity of the ultrasonic wave is calculated by recording the time for a signal to propagate through the sample.

Longitudinal waves propagate through the C/C composite specimen. To obtain the changes in material properties of the specimen, measurements are most effectively performed in the principle material axes. Orienting the specimen in a principle material axis reduces the complexity of the received signal. The general three-dimensional differential wave equation is written as [Cracknell, 1980]:

$$\frac{\partial^2 u}{\partial x^2} + \frac{\partial^2 v}{\partial y^2} + \frac{\partial^2 w}{\partial z^2} = \frac{1}{c^2} \cdot \frac{\partial^2 u}{\partial t^2} \tag{1.1}$$

where $u, v \& w$ are the wave displacements in the positive x, y & z-directions respectively, c is the velocity of the signal and t is time. Equation 1.1 can be reduced to the one-dimensional case:

$$\frac{\partial^2 u}{\partial x^2} = \frac{1}{c^2} \cdot \frac{\partial^2 u}{\partial t^2} \tag{1.2}$$

due to the wave propagation occurring in only one direction (x-direction) along a principal material axis. The one-dimensional case is not valid for the waveguides, but can be applied to the specimen because of the dimensions of the specimen. It is assumed that the effect of the waveguides is removed. A general solution to equation 1.2 can be written as:

16

$$u(x,t) = A_1 \cdot e^{i \cdot (k \cdot x - \omega \cdot t)} + A_2 \cdot e^{-i \cdot (k \cdot x + \omega \cdot t)} \qquad (1.3)$$

where A_1 is the amplitude of a wave propagating in the positive x-direction, A_2 is the amplitude of the wave propagating in the negative x-direction, t, is the time, k, the wave number, can be related to the wavelength, λ, and frequency, f, by:

$$k = \frac{2 \cdot \pi \cdot f}{\lambda} \qquad (1.4)$$

or alternatively is the angular frequency, ω, divided by the wave velocity, c. The wave velocity can be calculated by dividing the sample thickness by the total time for a signal to propagate through the sample.

Relating the wave velocity to material properties such as Young's modulus is one of the objectives of this work. For example, the modulus of type 316L stainless steel is monitored in this work along with a C/C composite. As the temperature of a sample of stainless steel increases, the modulus decreases. For an isotropic solid material, such as type 316L stainless steel, wave velocity is related to the material density and Young's modulus by the following generalized equation:

$$c = \sqrt{\frac{E \cdot (1 - \upsilon)}{(1 + \upsilon) \cdot (1 - 2 \cdot \upsilon) \cdot \rho}} \qquad (1.5)$$

where E is Young's modulus, ρ is the material density, υ is Poisson's ratio, and c is the calculated wave velocity through the sample. Referring to equation 1.5, if the modulus of a stainless steel sample decreases as temperature increases, the wave velocity, c, should also decrease, providing the density does not drastically change as well. The flexure modulus of a carbon composite slightly increases with temperature [Savage, 1993]. If this is the case for the C/C composites studied in this work, the modulus should slightly

increase, assuming that the density of the material remains the same. Rearranging equation 1.5, the change in modulus of an isotropic material corresponding to the change in temperature can be expressed as the following:

$$\Delta E = E(T_1) - E(T_2) = \frac{(1+\upsilon)\cdot(1-2\cdot\upsilon)}{(1-\upsilon)}\cdot\left[[\rho(T_1)]\cdot[c(T_1)]^2 - [\rho(T_2)]\cdot[c(T_2)]^2\right] \qquad (1.6)$$

where T_1 is the lower temperature and T_2 is the higher temperature and c is the wave velocity through a sample at these temperatures and ρ is the respective material density at these temperatures. The density of a material will slightly change with increase in temperature if the volume or weight of the material changes. In the case of an isotropic material such as type 316L stainless steel, the density decreases linearly from 7900m^3/kg at room temperature to 7500m^3/kg at 1000°C. The modulus calculations using a constant density are compared to the modulus calculations using varying density in the results discussion of 316L stainless steel. The equations for calculating the change in modulus of an anisotropic material, such as the C/C composite, will be discussed in chapter 4.

1.8   Thesis Statement

A method is developed for testing carbon-carbon composites that allow the changes in elastic properties with increase in temperature to be evaluated as well as the effect of oxidation to be monitored in real time. Methods for in-situ monitoring of high temperature composite materials during oxidation are important in a number of technological applications. The apparatus in this work makes use of solid cylindrical waveguides and is designed to allow for ultrasonic measurements through a sample. The specimen can be in either an inert atmosphere or a controlled oxidizing environment with varying temperatures. The velocity of an ultrasonic wave will be measured in a carbon-

carbon composite. This work will also include preliminary work on the attenuation in the sample and the on the signal processing required to obtain quantitative information from the experimental apparatus described.

Adequate evidence is needed to demonstrate that the above technique can provide correct and accurate material property information. In order to accomplish this task, preliminary tests are conducted using a material that has known modulus - temperature characteristics. The material chosen for these preliminary test is stainless steel type 316L, where temperature data up to $850^{\circ}C$ is available from several sources.

Chapter 2

EXPERIMENTAL APPARATUS

2.1   Introduction

A primary focus of this work is the design and assembly of an apparatus for in-situ testing of carbon-carbon (C/C) composites at high temperatures. The apparatus allows the changes in elastic properties with change in temperature of a C/C composite to be monitored. In particular, it is possible to monitor the oxidation of a C/C composite in real time. The apparatus used consists of a high temperature tube style furnace, an ultrasonic pulse generator, transmitting and receiving ultrasonic transducers, and the setup required to contain and seal the monitoring system. The apparatus on each side of the furnace is essentially the same, although the left side will be described. The next few sections will go into some detail about the different parts and describe their purpose.

2.2   Furnace Setup

Monitoring the changes in elastic properties of carbon-carbon (C/C) composites with change in temperature is possible using elastic waves. The experiments that monitor these changes are conducted with the ultrasonic transducers located outside of the furnace and waveguides to transmit the signal. The furnace is a conventional tube type, 3-zone furnace (Lindberg Model 55346, Watertown WI) that has three individual embedded alloy heating elements (type LGO), located near the center. The furnace is capable of producing temperatures up to 1100°C. The three heating elements surround a 40mm outer diameter (32mm inner diameter) mullite tube (Anderman Ceramics, model EWF .610, London UK) that runs horizontally through the furnace extending out the right and

20

left hand sides. Alumina fiber insulation also surrounds the mullite tube through the furnace. The mullite tube allows the entire apparatus, shown in figure 2.1 on the following page, to be sealed from the outside of the furnace. This allows the C/C composite to be held in a controlled atmosphere furnace. Without the tube extending out of the furnace, sealing the C/C composite sample inside a high temperature atmosphere is difficult.
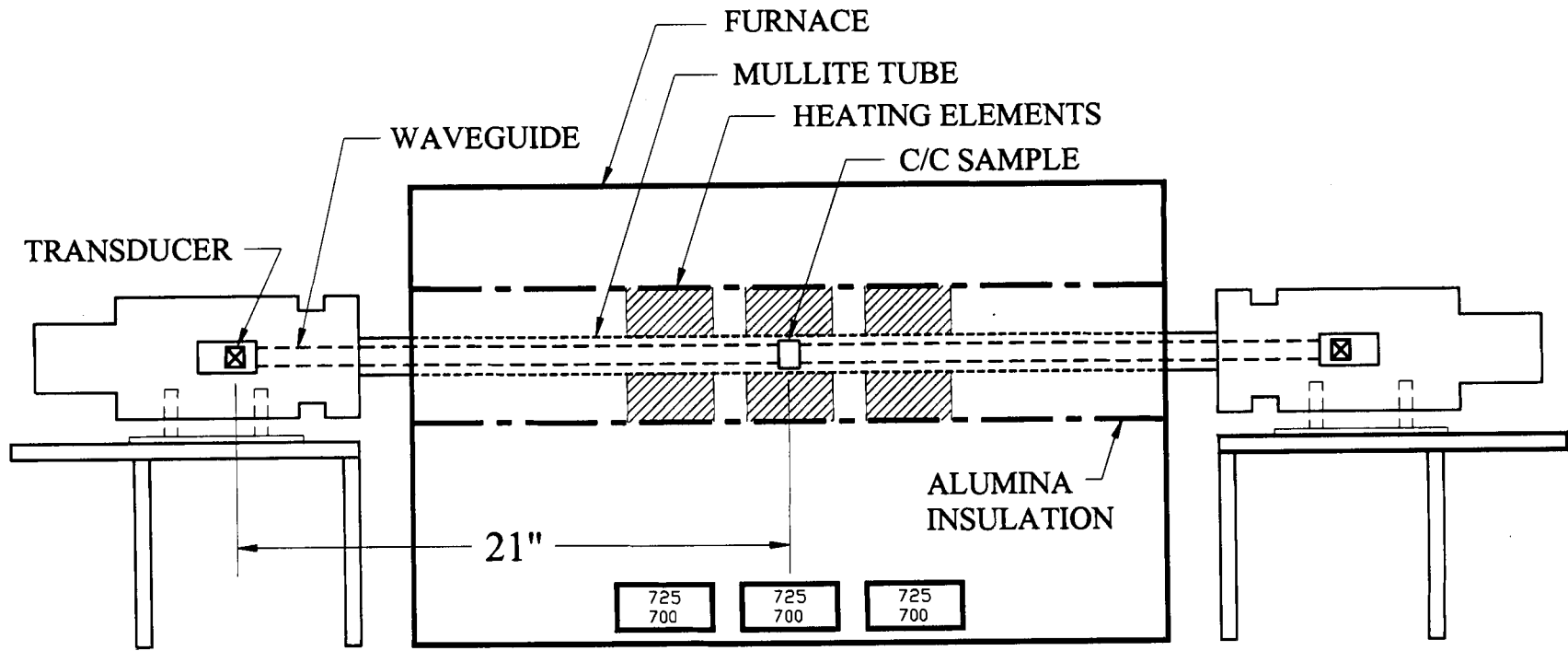
Figure 2.1. A sketch of the furnace employed in this work.

2.3 Ultrasonic Transducers

The transducers used in this work are broadband nominal 1 MHz (central frequency units) contact transducers (Panametrics model V103, Waltham MA). Standard room temperature transducers are used in this work rather than high temperature transducers. High temperature transducers still have a Curie temperature significantly lower than the temperatures of interest in these experiments. High temperature transducers are also significantly less efficient than their room temperature counterparts. Room temperature transducers are able to transmit large signal amplitudes, which are ideal for this application. Large signal amplitudes are required because of the attenuation that occurs in the C/C sample and through the dry coupling that is used between waveguides and the sample.

Initial testing was performed on the transducers to check the frequency response of the transducers. One transducer, acting as the transmitting transducer, was connected to a spike pulser (Panametrics model 5072PR, Waltham MA) while the receiving transducer was connected directly to an oscilloscope (Tektronix model TDS520A, Beaverton OR) without using a pre-amp. A piece of aluminum, 50mm thick was used as the reference material. The recorded signal was processed to generate the response of the setup. The spectrum that was provided with the transducers is similar to that obtained, assuring that they are functional. A picture of the initial transducer testing setup with the aluminum is shown in figure 2.2. Figure 2.3 shows the response of the ultrasonic transducers.
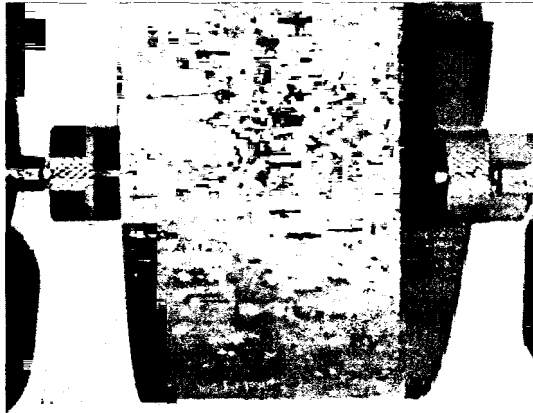
Figure 2.2. Initial testing setup of ultrasonic transducers through aluminum.
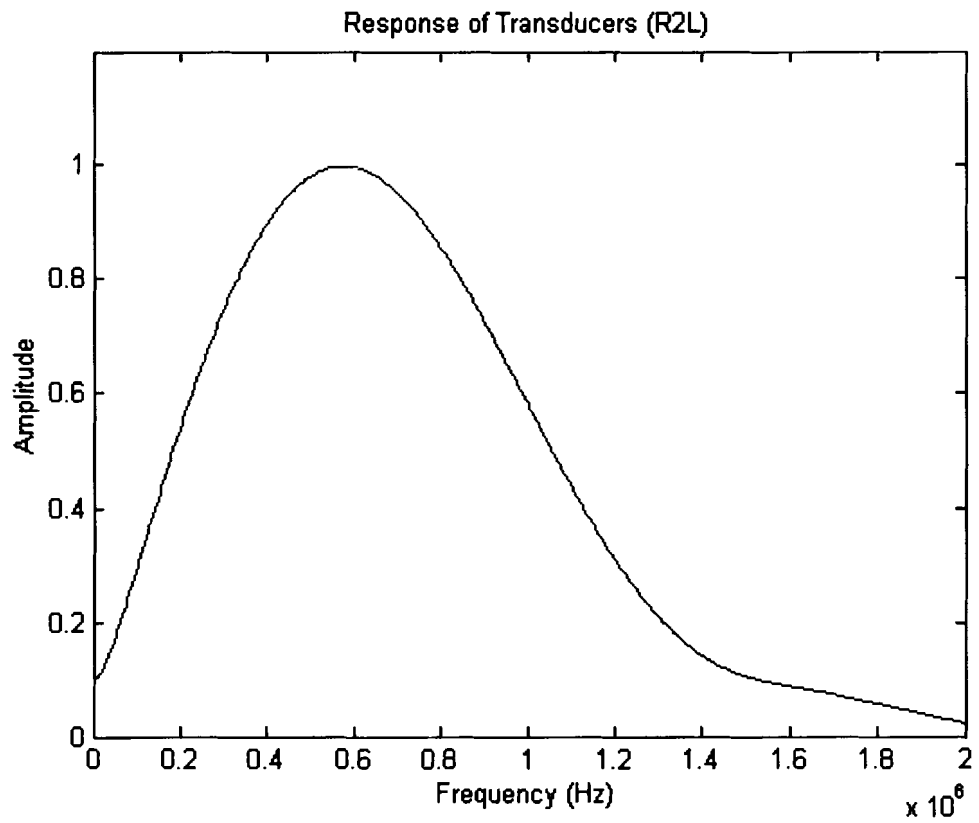
Figure 2.3. Response of the ultrasonic transducers.

2.4 Possible Waveguide Materials

Ultrasonic measurements can be performed at temperatures much higher than the allowable working temperature of the transducers when using waveguides. Unfortunately the required waveguides result in a received signal that is quite complex. The process for removing the effect of the waveguides and the coupling between the sample and waveguides are described in chapter 4. However changes in attenuation, strength and stiffness with change in temperature should still be considered when choosing the material for the waveguides.

The waveguide material is selected primarily on the ability to retain sufficient stiffness at temperatures up to 1100°C. The waveguides should be resilient at elevated temperatures due to the pressure load obtained when the waveguides are intermittently in contact with the sample. The material should have relatively low ultrasonic attenuation at the temperatures of interest. If the waveguides attenuation change is low, the attenuation change will be generated from the sample and the dry coupling between the sample and waveguides.

The choices for the waveguide materials were selected by using the material information from several material property charts and graphs, obtained from the Cambridge Engineering Selector (CES) software. Some examples of the graphs used are compressive strength vs. temperature, relative cost vs. temperature and loss coefficients vs. temperature. The loss coefficient measures the degree to which a material dissipates vibrational energy [Ashby, 1999]. The loss coefficient is another way to describe the attenuation of a material. It is desired to keep the loss coefficient as small as possible

25

when selecting the waveguide material. The compressive strength vs. temperature, fracture toughness vs. temperature and relative cost vs. temperature charts are shown in figures 2.4, 2.5 and 2.6, respectively.

The base criteria for this application was relatively high compressive strength at temperatures up to 1100°C and low material cost. The choices that met the criteria for this particular application are labeled in these charts as machinable glass, silicon and thorium based products. Fused quartz is a "machinable glass" and also meets the criteria. Silicon and thorium based products are relatively expensive compared to the machinable glass materials which make them less attractive selections. Sapphire was another possible choice for waveguide material but was also found to be extremely expensive compared to fused quartz when ordering long cylindrical rods.

Due to the intermittent contact between the rods and the sample, it is preferable to use a material that can be easily replaced at relatively low cost. Therefore, fused quartz was the material chosen for this waveguide application. Fused quartz is inexpensive and has adequate compressive strength at high temperatures. Fused quartz also has ample thermal properties such as high resistance to thermal shock at the temperatures experienced in this work. Quartz is also easily machinable and can be cut to the desired length using a tile saw. Fused quartz will also soften at the higher temperatures experienced in this work, which will improve the contact between waveguide and sample. The modulus of the fused quartz waveguides slightly increases with temperature [Fukihara, 1999], which will affect the velocity of the signals propagating through the setup with varying temperatures. This is discussed further in chapter 5.
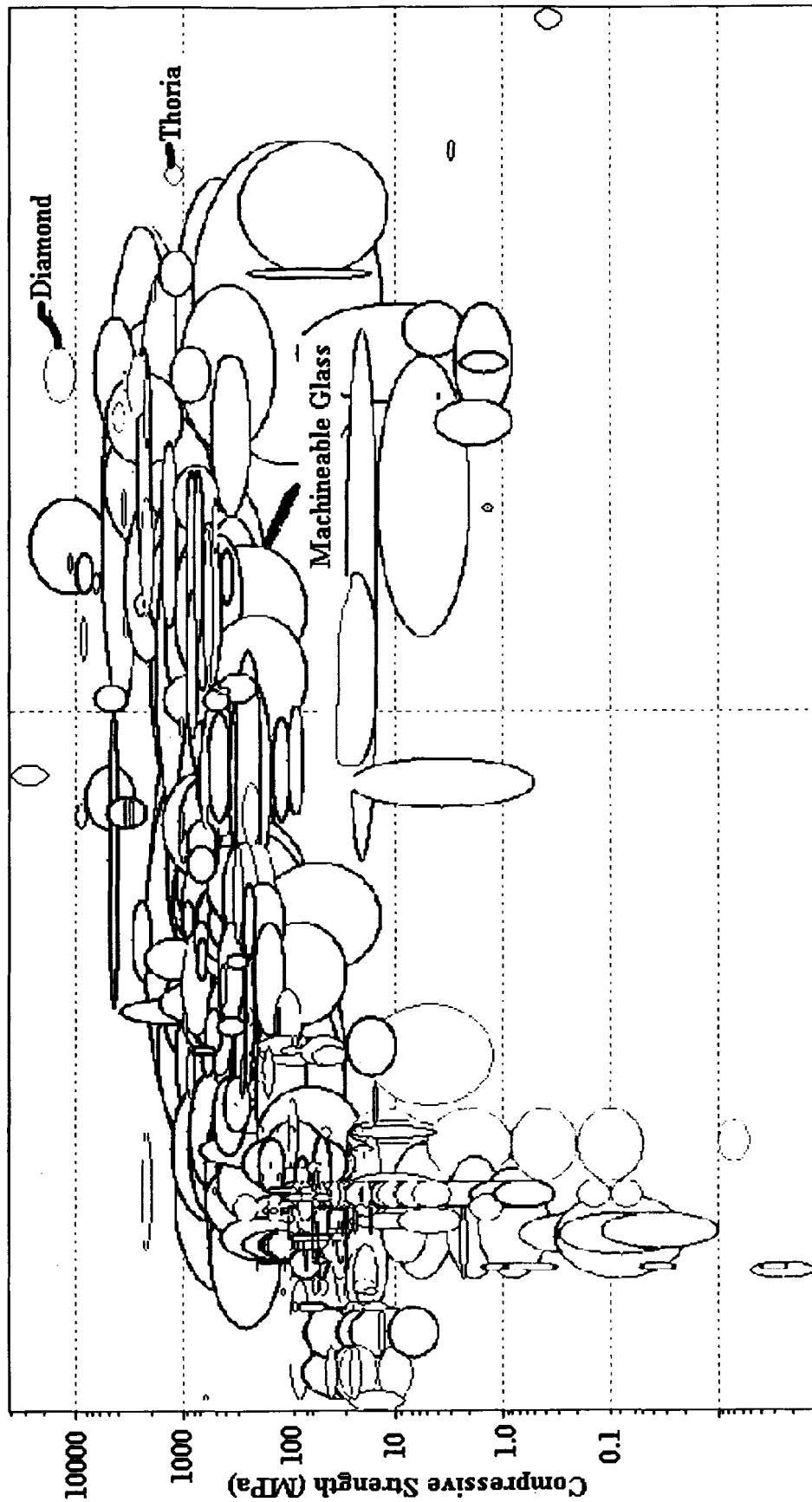
Figure 2.4. Compressive strength vs. temperature chart for possible waveguide material.

27
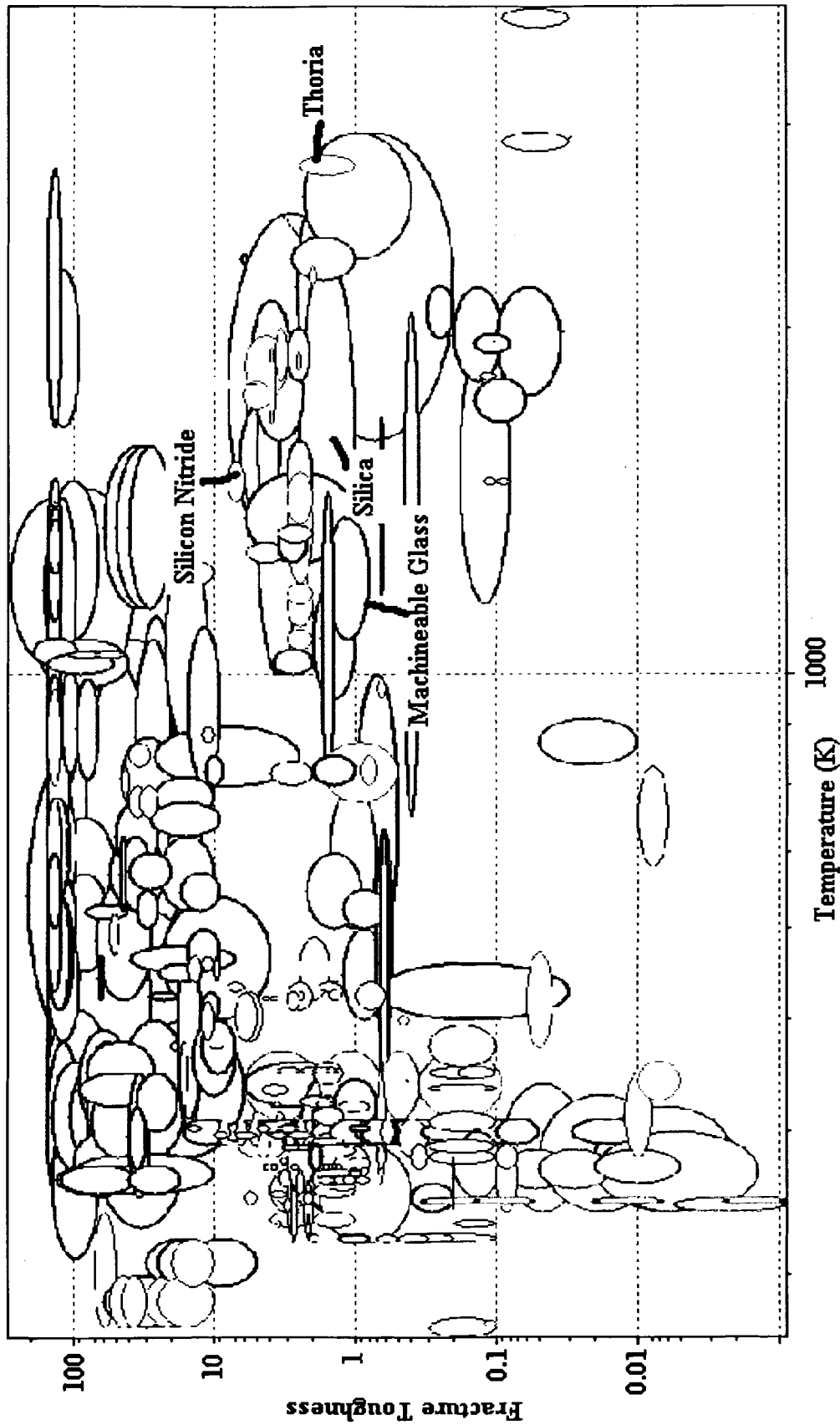
Figure 2.5. Fracture toughness vs. temperature chart for possible waveguide material.
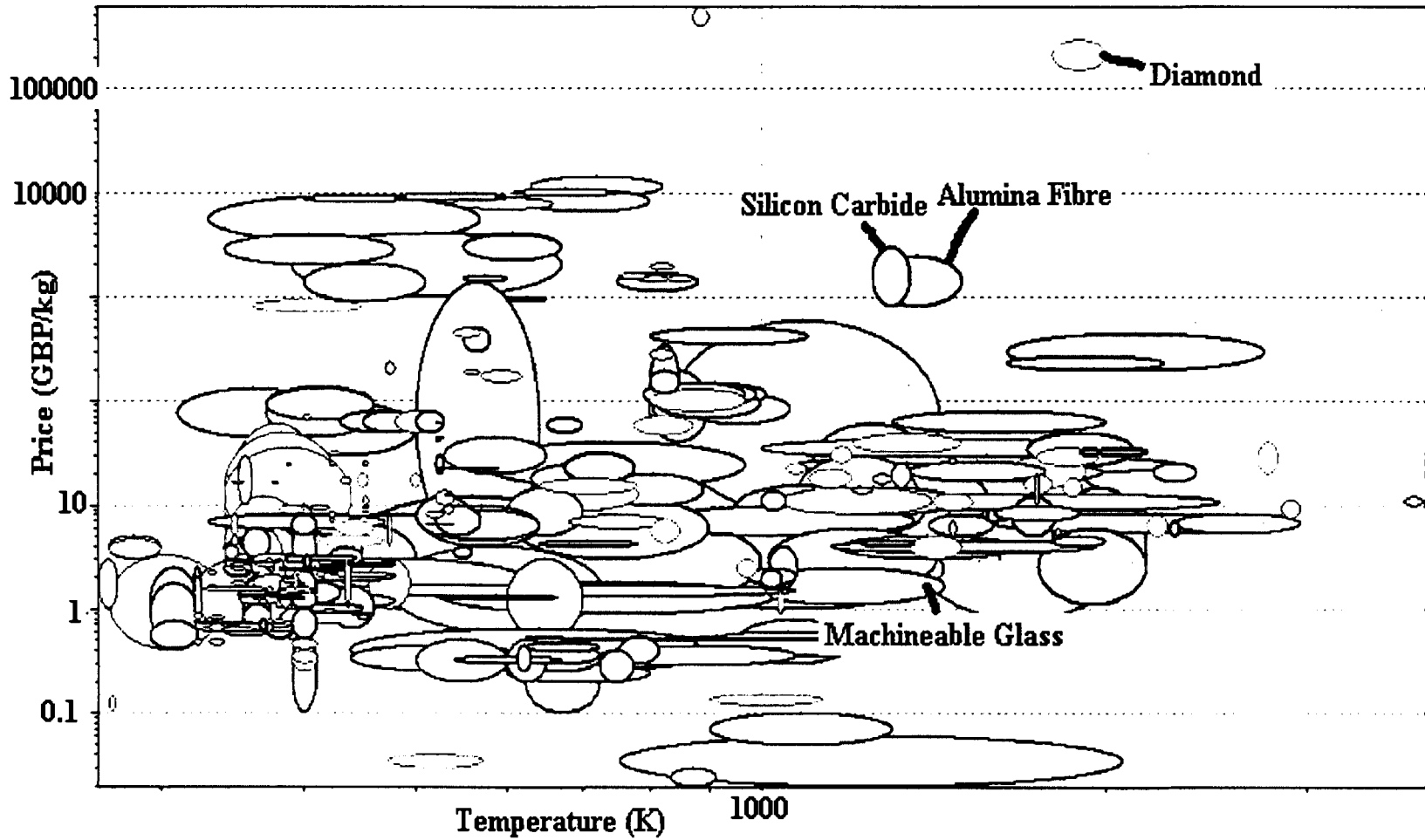
Figure 2.6. Cost vs. temperature chart for possible waveguide material.

2.5 Endcap Setup

There are three major components to the apparatus that are located outside of the furnace on the left and right hand sides. These components, shown in figure 2.7, are the endcaps, the water-cooling system and the endcap housing foundation. The setup contains smaller more detailed working mechanical components that are fastened to the endcaps and held in place by the endcap housing foundation.
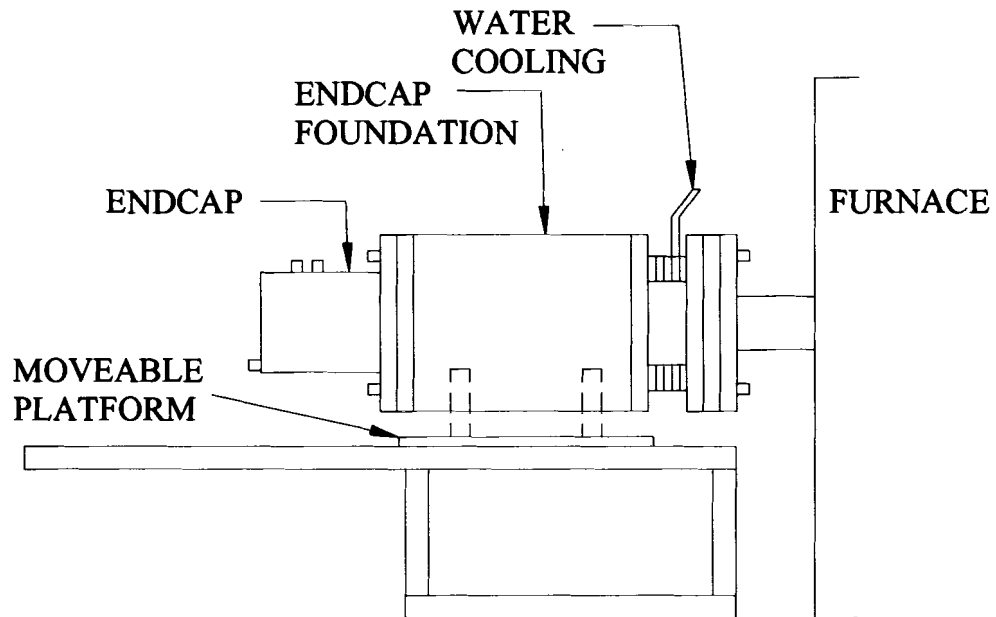
Figure 2.7. A sketch of the three major components outside of the furnace.

This setup is held by a setscrew on two cradles, made from Plexiglas, that are fastened to an adjustable platform, also shown in figure 2.7. The purpose of the endcaps is to house the ultrasonic transducers and allow for proper sealing of the entire apparatus while protecting the transducers from the extreme heat of the furnace tube. The individual components will be described in the following sections. Each side of the furnace has similar endcaps and components, thus only the left-hand side of the furnace will be discussed.

2.5.1 Water-Cooling System

One of the most important components of the apparatus is the water-cooling system. The waveguide and the environment are cooled before they contact the ultrasonic transducer. The water-cooling setup is located between the exit of the furnace tube and the endcap housing foundation, shown in figure 2.7. The water-cooling system consists of copper piping wound around a cylinder that houses ball bearings, which support the waveguide. Figure 2.8 is a sketch of the water-cooling setup showing the water inlet and exit and the location of the bearings.
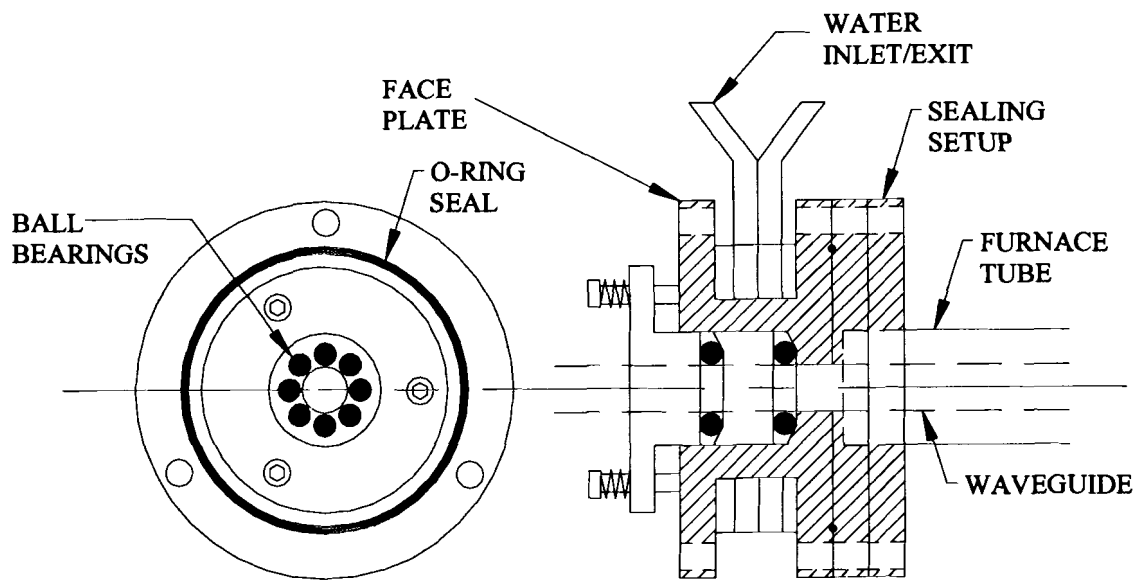
Figure 2.8. Water-cooling setup with ball bearings.

The ball bearings help cool the waveguide through conduction from the water that passes through the copper piping. The copper piping is sized to provide ample cooling to the waveguide and the surrounding environment. The faceplate of the water-cooling setup has a chamfer that is ¼ inch deep machined with a ¼ inch ball nose endmill around the perimeter of the plate to provide a seat for an o-ring seal. When the water-cooling

system is fastened to the sealing setup (described in section 2.5.4), the o–ring becomes compressed and provides an airtight seal between the two.

The ball bearings are held in place with a piece of aluminum that was machined to fit into the cylinder and secured with three screws and springs. The springs keep constant pressure on the piece of aluminum that ensures the ball bearings are held in place and properly support the waveguide. If excess torque is applied to the screws, more pressure is applied to the bearings and more force is applied to the waveguide. This force would constrict the inward and outward movement of the waveguides. Therefore, the torque is applied to the screws to support the waveguides without restricting their movement.

2.5.2 Air Cylinders

Intermittent contact between waveguide and sample is required to allow the sample to be evenly heated when no ultrasonic measurements are being taken and to obtain reference signals. Air cylinders, with a 1inch range, are used to move the waveguides into contact with the sample and to retract them. The air cylinders are placed in the endcaps and fastened to a faceplate as shown in figure 2.9. The faceplate is used to hold the air cylinders and to provide a proper seal for this portion of the setup.

The faceplate has a ¼inch deep chamfer machined using a ¼inch ball nose endmill around the perimeter to provide a seat for an o–ring seal. The o–ring seal is compressed when the endcap is bolted to the faceplate and endcap housing foundation. The intermittent contact between waveguide and sample is obtained by attaching the ultrasonic transducer setup to the end of the air cylinder rod. This endcap has a sealed

port that allows the transducer cable on the inside to connect to a cable from the outside. There are two other ports that connect the air cylinder to their proper hookups.
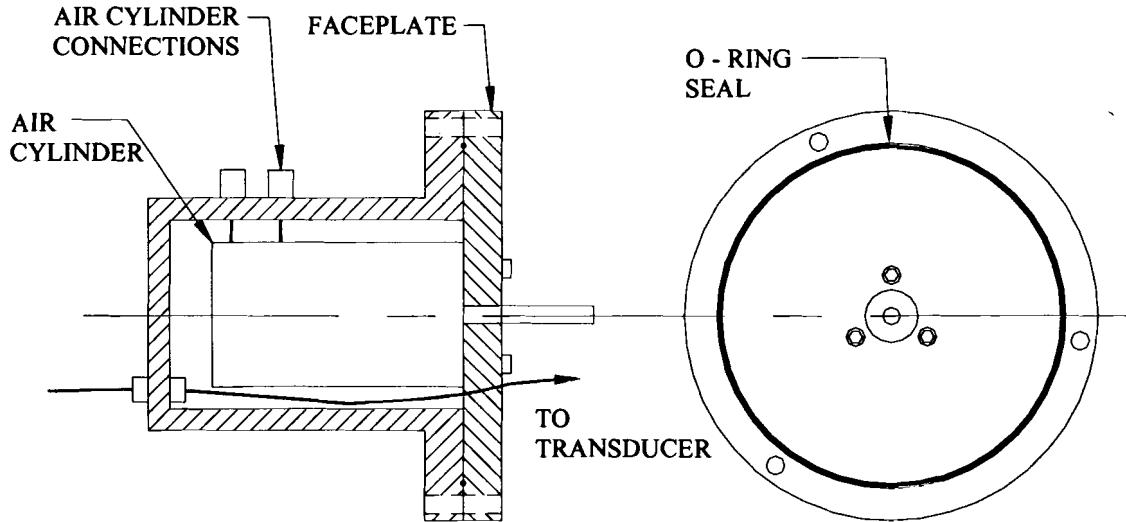
Figure 2.9. The endcap configuration with the air cylinder.

Preliminary experiments were performed using compressed air as the working gas in the air cylinders to test the cylinders for possible leaks into the setup. A C/C composite sample was placed inside the furnace and the entire apparatus was sealed, evacuated, backfilled with an inert gas and heated to 1000°C. It was concluded that the cylinders leaked air into the apparatus from the visible oxidation experienced by the C/C composite sample after prolonged exposure in a controlled environment. It is for this reason that the same gas used for the inert atmosphere will be used as the working gas for the air cylinders.

2.5.3   Ultrasonic Transducer Setup

The ultrasonic transducers are secured in a clamp that holds one end of the waveguide against the face of the transducer. This clamping setup was then attached to the air cylinder rod as shown in figure 2.10.
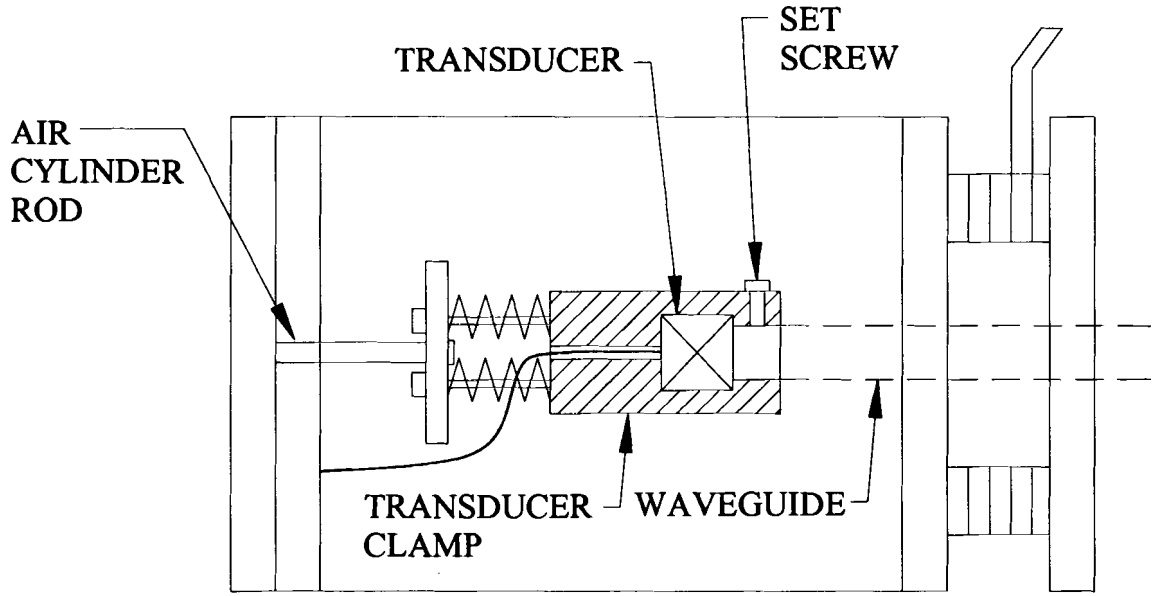
Figure 2.10. Ultrasonic transducer setup with clamp attached to air cylinder rod.

The transducer clamp has a small through hole that allows the transducer cable to exit and connect to the port located at the rear of the endcap. The clamp is connected to a plate with three screws and springs that is connected to the air cylinder rod with a single bolt. The holes on this plate were machined slighter larger than the diameter of the screws to allow the screws of the transducer clamp to move freely through the plate. This allows the springs to absorb any unwanted excessive force generated by the air cylinder while moving the transducer setup. The springs act as a safety feature to prevent damage to the quartz waveguide when using intermittent contact.

The waveguide enters the endcap housing foundation through the water-cooling system. During installation, the ultrasonic transducer is secured in the clamp and the waveguide is then firmly pressed against the face of the transducer and secured with the setscrew. If excess torque is applied to the setscrew, the end of the quartz waveguide will shatter. A coupling is used between the waveguide and transducer to provide an

improved surface contact between the two. A high temperature, vacuum grease (Dow-Corning, #976, Midland MI) is used as the coupling in this application. After the waveguide and transducer are secured in the clamp and fastened to the air cylinder rod, the entire setup is fastened to the endcap and secured to the endcap housing foundation. The whole transducer setup can be extended or retracted one full inch from the sample.

2.5.4 Endcap Housing Foundation and Sealing

The water-cooling system and the endcap setup, described in the previous sections, are fastened to the endcap housing foundation. This foundation is a large brass cylinder with a 114.3mm (4-½ inches) outer diameter and a 63.5mm (2-½ inches) inner diameter and is 165mm (6.5 inches) long. A chamfer was machined around the perimeter on each end of the foundation using a ¼ inch ball nose endmill that is ¼ inch deep, to provide a seat for an o–ring seal. When the endcap and water-cooling setup are fastened to the foundation, the o–ring seals compress and the setup becomes airtight. Some of the vacuum grease that was used as coupling between the waveguide and transducer is applied to the o–rings to ensure a sealed setup. Three holes were drilled and tapped 1inch deep around the perimeter of each end of the foundation to allow ¼–20inch screws to be used to fasten the endcap and water-cooling setup. A single hole was also drilled and tapped for a ¼ - 20 inch setscrew ¾ inches deep on the base of the foundation to secure the foundation to the moveable platform. Figure 2.11 is a sketch of the endcap housing foundation resembling the location of the holes and o-ring chamfer.
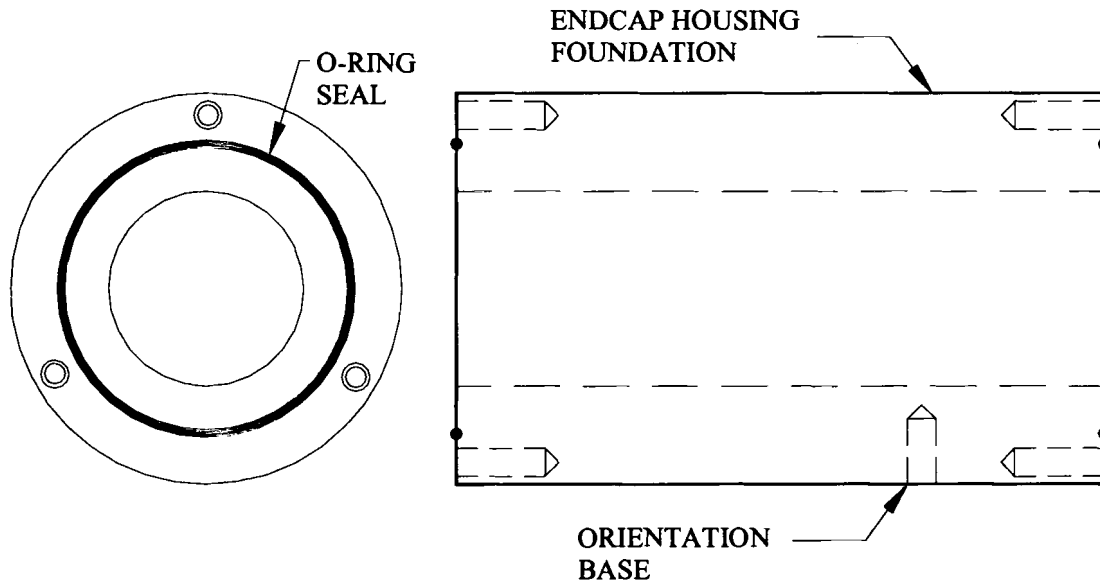
Figure 2.11. The endcap housing foundation.

The entire setup described in the previous sections is sealed around the furnace tube that extends out of the sides of the furnace. The setup used to seal the endcap components around the furnace tube is similar to the setup used on the endcap housing foundation. Two faceplates were machined to hold and compress a high temperature o–ring seal around the furnace tube. The faceplates are fastened to the water-cooling setup using three bolts. The o–ring seal is compressed around the furnace tube when the faceplates are secured together. A chamfer was machined around the inner diameter of one faceplate to prevent the high temperature o–ring seal from spreading away from the furnace tube. This design forces the seal to compress against the furnace tube. The sealing faceplates are shown in figure 2.12.
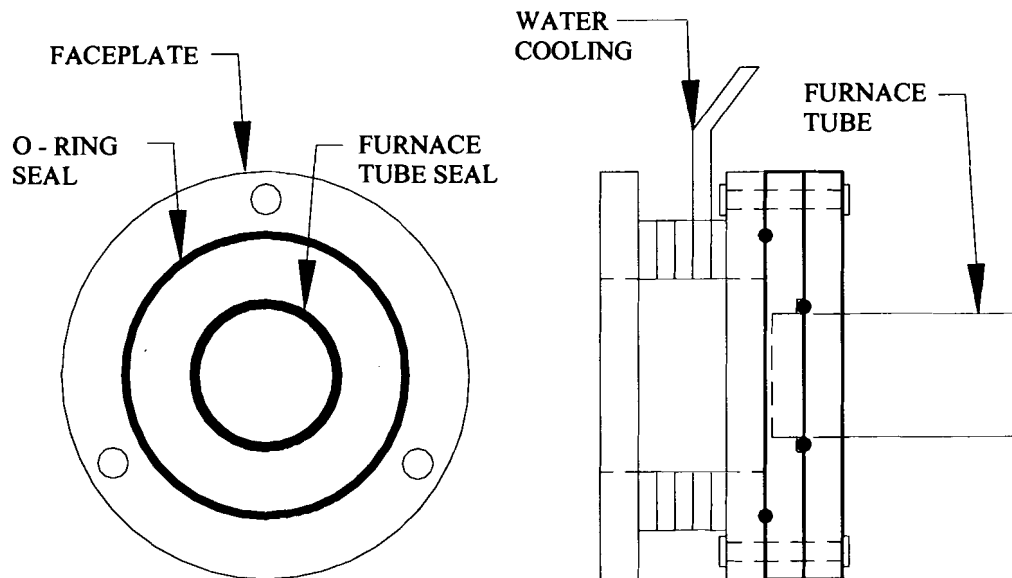
Figure 2.12. The faceplates that seal the setup around the furnace tube.

The faceplate closest to the furnace also has a small chamfer around the perimeter that holds a small copper pipe that is joined to the water-cooling system. The left hand image of figure 2.13 shows the white high temperature o–ring that seals the endcap setup around the furnace tube shown in the right hand image. A picture of the entire setup is shown in figure 2.14.
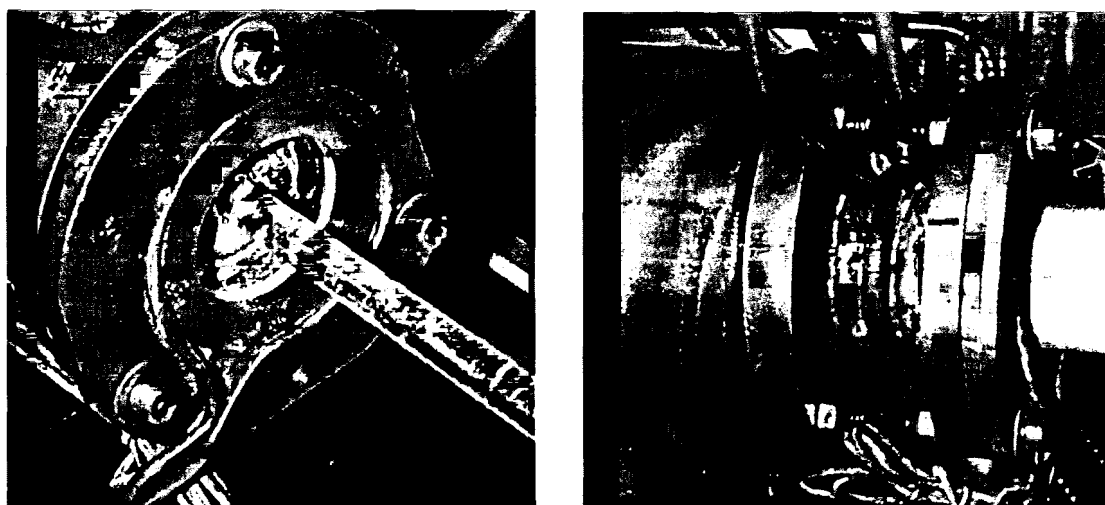
Figure 2.13. Inner high temperature seal (left) sealed around the furnace tube.
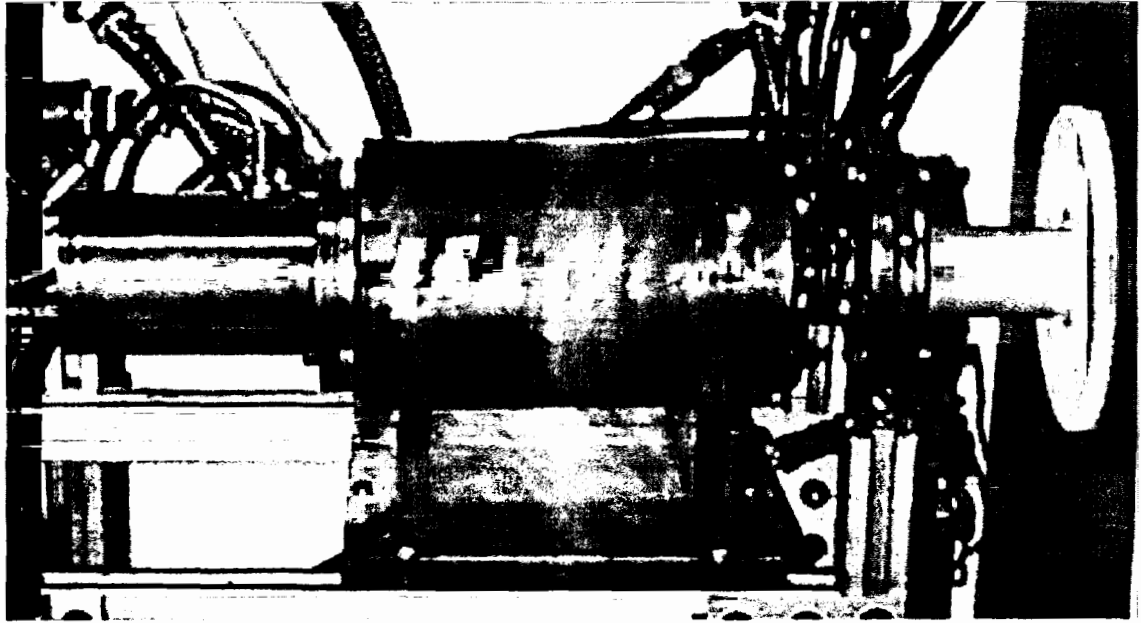
Figure 2.14. The entire left hand endcap setup sealed around the furnace tube.

2.6   Waveguide Deflection

The proposed waveguide technique allows a signal to propagate through a sample located inside the furnace while the ultrasonic transducers are located outside the furnace. The transducers and waveguides must be aligned on center in order for the transmitted signal to propagate through the setup. The waveguides normally 58.5cm (23inches) in length. They are clamped at one end and supported with a ball-bearing setup under a water-cooling system. This leaves almost 43.5cm of waveguide material unsupported as shown in figure 2.15. Due to the tolerance in the clamping components around the waveguide, the free end of the waveguide cannot be supported as shown in figure 2.15.

38
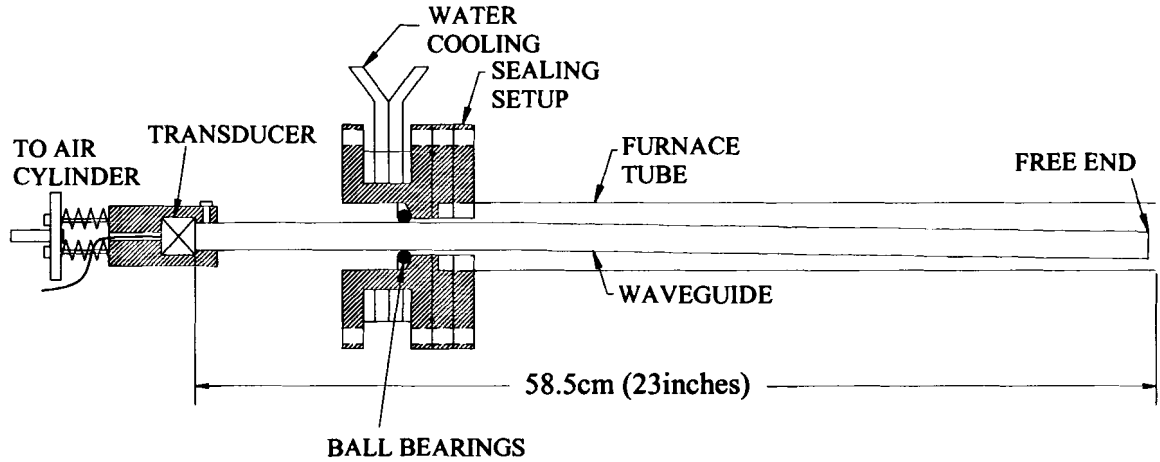
Figure 2.15. Waveguide and clamping setup showing bearing location.

In order to avoid creep deflection of the waveguide, an alumina fiber tube is used

to support the fused quartz waveguide. The outer diameter of the alumina tube is the

same as the inner diameter of the furnace tube. The inner diameter of the alumina tube is

the same diameter as the waveguide diameter. Each side of the furnace has an alumina

tube that supports the waveguides. The total length of each alumina tube is 5cm

(~2inches) less than the total length of furnace tube divided in half. This leaves an

opening between the alumina tubes for a composite sample. Figure 2.16 is a sketch of

how the alumina tube, waveguide and sample interact. It also shows the general location

of the ball bearings, air cylinder, C/C sample and the platform that secures it.
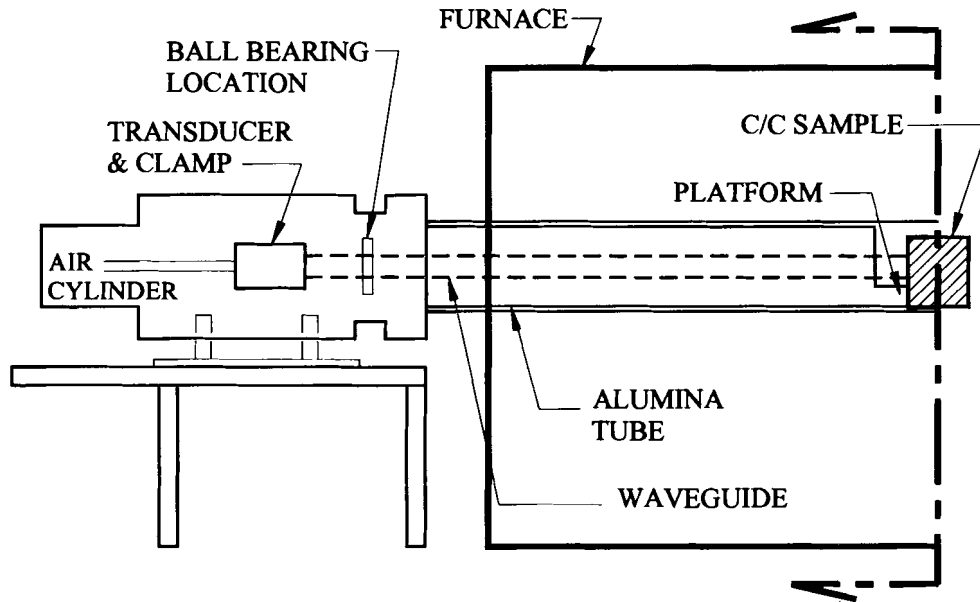
Figure 2.16. A sketch of the alumina tube and waveguide setup.

This setup allows the sample to rest directly on the furnace tube between small platforms that were cut from one end of each alumina tube. The platforms secure the sample using the bottom portion and allow the remaining portion of the sample to be evenly heated. The sample could be insulated from the heat if the alumina tubes were used to secure the entire width of the sample. Figure 2.17 are pictures that show the interaction between the alumina tubes, waveguides and a C/C composite sample. The left hand figure shows the waveguides in contact with a sample. The waveguides are withdrawn from the sample in the right hand figure. These figures show the setup with a C/C sample but were taken outside of the furnace tube. This entire setup slides into the furnace tube, which will be described along with the furnace preparations in chapter 3.
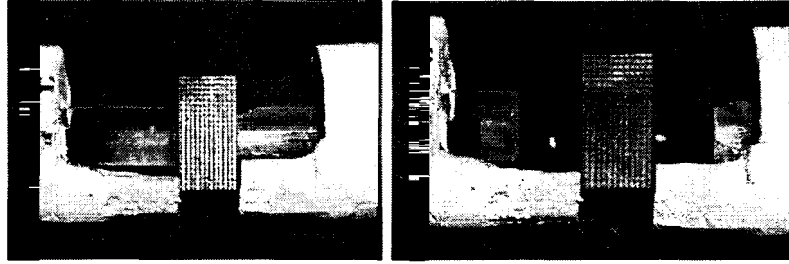
Figure 2.17. Alumina tubes, waveguides and C/C sample.

2.7 Testing of Water-Cooling System

While the sample is held at the center of the furnace tube and monitored at temperatures ranging from room temperature to 1100°C, the ultrasonic transducers outside of the hot zone must remain below the Curie temperature of the piezoelectric material. Therefore, the temperature outside of the hot zone of the furnace where the transducers are located, as well as the temperature at the center of the furnace where the sample is held, must be monitored.

The furnace has three independent heating elements, located near the center, with separate digital controllers. The controllers have two temperature readouts, one for the setting point and one for the furnace temperature. The temperature inside the furnace tube will not necessarily be the same as the controller readouts because of the mullite tube and spacing of the elements. A preliminary test was performed, without the transducers or a sample, to determine the temperature gradient inside the furnace, the temperature at the center of the furnace and the temperature at the transducer mounting location. This preliminary test also determined if the digital controllers display the correct temperature on the inside of the furnace. The spacing of the three individual heating elements and the mullite tube is shown in figure 2.1.

41

A preliminary test of the furnace recorded temperatures on the left hand side of the furnace, the center, and the left hand transducer location. Six K-type thermocouples (Omega, #XC-20-K, Stamford CT) were attached to a quartz waveguide using a two–part high temperature quick set epoxy (Manco Inc, #TM-51, Avon OH). The first thermocouple was attached to the quartz rod at the left end of the furnace and used as a reference. The other thermocouples were attached every 10cm (~ 4inches) on the left hand quartz rod, shown in figure 2.18, and placed inside the furnace tube. A seventh thermocouple was placed at the left hand transducer mounting location. The temperature at this location was monitored to see if it exceeded the Curie temperature of the transducers. The wiring for all of the thermocouples exit out of the left hand end of the furnace and were connected to a multiple channel temperature-measuring device (Newport Electronics, Model INFBT10-0001-TC, Santa Ana CA). Figure 2.18 shows the preliminary temperature test with the placements of the thermocouples.

The apparatus was sealed from the atmosphere to simulate an experiment and the furnace was heated to its maximum temperature of 1100°C. After the furnace idled at 1100°C for one hour, the temperature was recorded at each of the seven thermocouples.
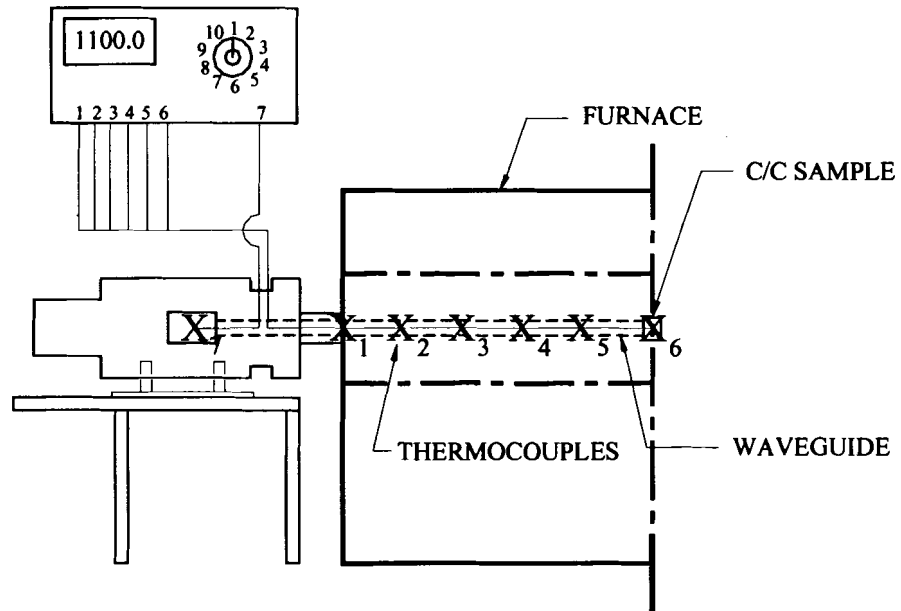
Figure 2.18. The preliminary temperature testing setup with thermocouples.

After the thermocouple readings are recorded, the furnace temperature was lowered in 100°C increments and left to idle for one hour at each temperature. The process was repeated down to 300°C. The temperature readings recorded at 800°C to 1000°C are shown in table 2.18. Figure 2.19 is a graphical representation showing the temperatures recorded at the thermocouple positions one through six.

From figure 2.19, the temperature near the center of the furnace is quite close to the set point. Table 2.1 shows the temperatures recorded at each thermocouple location. The temperature at the transducer location never went above 46°C. The Curie temperature of the transducers is slightly above 60°C. Thus the cooling system on the furnace appears to be sufficient to prevent damage to the transducers from the heat of the furnace.

Furnace Setting	Recorded Thermocouple Temperatures (°C)						
800°C	30.4	209.5	665.92	795	810.21	810.2	808.47
900°C	37.4	243	754	890.7	905.9	905.25	903.69
1000°C	38.9	281.2	846.6	987.7	1003.4	1002.2	1001
1100°C	46	324.5	939.2	1085	1102.6	1101.6	1100.7
Position (in)	trans.	0	4	8	12	16	20

Table 2.1. Detailed thermocouple recordings inside the furnace tube.
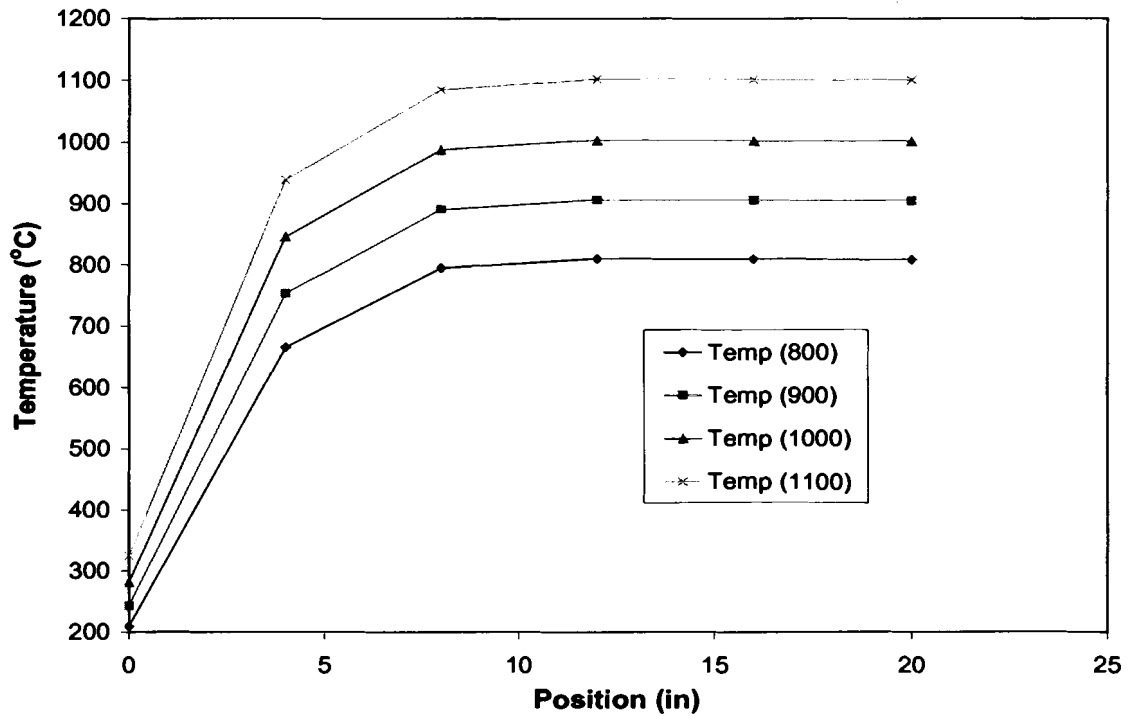
Figure 2.19. Change in furnace temperature with change in position through tube.

From the sample position, at 20 inches, in table 2.1, the difference between the set point and the recorded temperatures is small, ~ 1%. The difference is even smaller, 0.06% at elevated temperatures. At 800°C, the recorded thermocouple temperature is within 9°C of the actual furnace setting. At 1100°C, the recorded thermocouple temperature is within 1°C of the actual furnace setting. When performing experiments with C/C composites, the temperature at the center of the furnace can be recorded from

the controllers with minimal error. The transducers in the end-cap housing will be sufficiently cooled by the water-cooling system.

2.8   Equipment Setup

A total of six ultrasonic signals are needed to acquire the changes in material properties of the sample. The instrumentation and setup will be described and the settings needed to perform the experiments will be discussed.

2.8.1   Pulser, Oscilloscope and Pre-amp

An ultrasonic signal is used to monitor the elastic modulus change with temperature in the sample. A conventional spike pulser (Panametrics Model 5072PR, Waltham MA) is used to create the energy that is converted to an ultrasonic signal within the piezoelectric material of the transmitting transducer. The spike pulser is shown in figure 2.20.
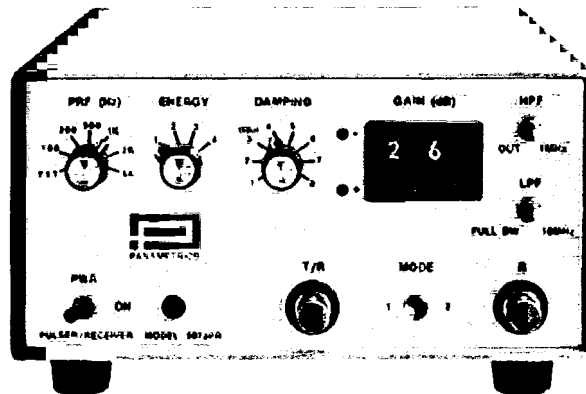
Figure 2.20. Conventional spike pulser used in this work.

The energy from the spike pulser is used at the highest setting possible, in this case the pulser energy was set at "4", or 400 volts. The energy is needed due to the attenuation of the signal when propagating through the waveguides and sample. The damping on the

45

pulser is adjusted to lower the noise of the received signal, in this case the damping is set at "3" or 50 ohms. The spike pulser is also used to receive pulse-echo signals required for future signal processing. This pulser has a built in pre-amp that was set to 50db of gain when receiving pulse-echo signals.

For through transmission signals, a receiving transducer is connected to a separate pre-amp (Panametrics 5660C, Waltham MA), shown in figure 2.21. The separate pre-amp improves the signal isolation which is needed due to the low signal to noise ratio. The dry coupling between the sample and waveguides and the vacuum grease between the waveguides and transducers combine to attenuate the signal significantly. Without the use of the pre-amp, the received signal would be very minute and difficult to detect, compared to the initial transmitted signal. The pre-amp used in this work has two gain settings, 40db and 60db. The through transmission signals recorded in this work are amplified using the 60db gain.
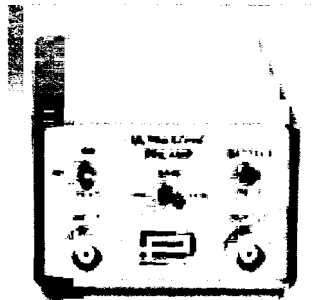
Figure 2.21. Ultrasonic pre-amp used in this work.

The amplified signal is sent to an oscilloscope (Tektronix Model TDS 520A, Beaverton OR). It is critical that the proper settings on the oscilloscope be used to enable the received ultrasonic signal, which changes over the course of the experiment, to be acquired for later analysis. The oscilloscope used in this work is shown in figure 2.22.
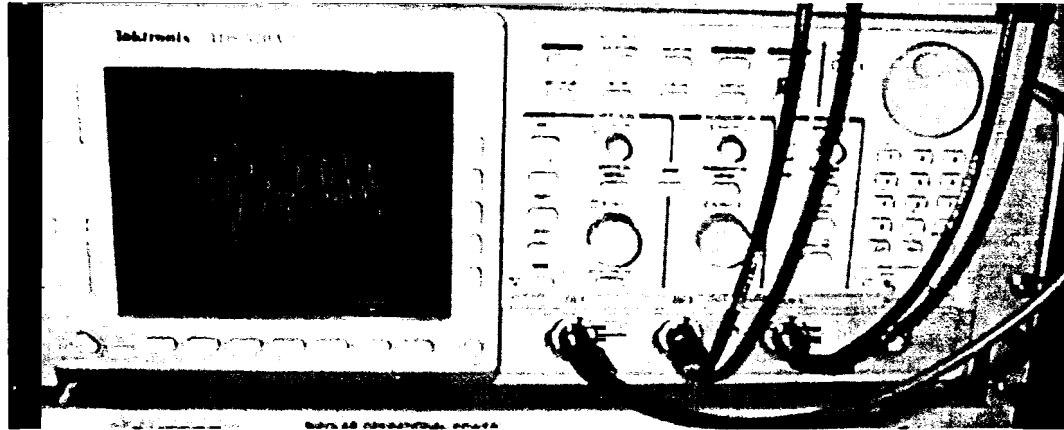
Figure 2.22. Actual oscilloscope used in this work.

The oscilloscope is used with the following settings:

- 0%   Trigger position
- 15000 points per record
- 250   Mega samples per second
- 195   μsec time delay

Signal averaging is set at 50 signals which is necessary to improve the signal to noise ratio as well as minimizing random errors. The time delay is dependent on the thickness of the sample. The sampling rate, of 250 Ms/sec, makes it possible to measure time delays within the sample to a precision of about 4 nanoseconds [Peterson, 1996]. It was found that a signal took about 200 μsec to travel the entire distance of the waveguide setup. For this reason, a delay of 190 μsec is used to ensure the initial rise was visible. The signal processing is described in chapter 4. A schematic drawing of the instrument setup is shown in figure 2.23.
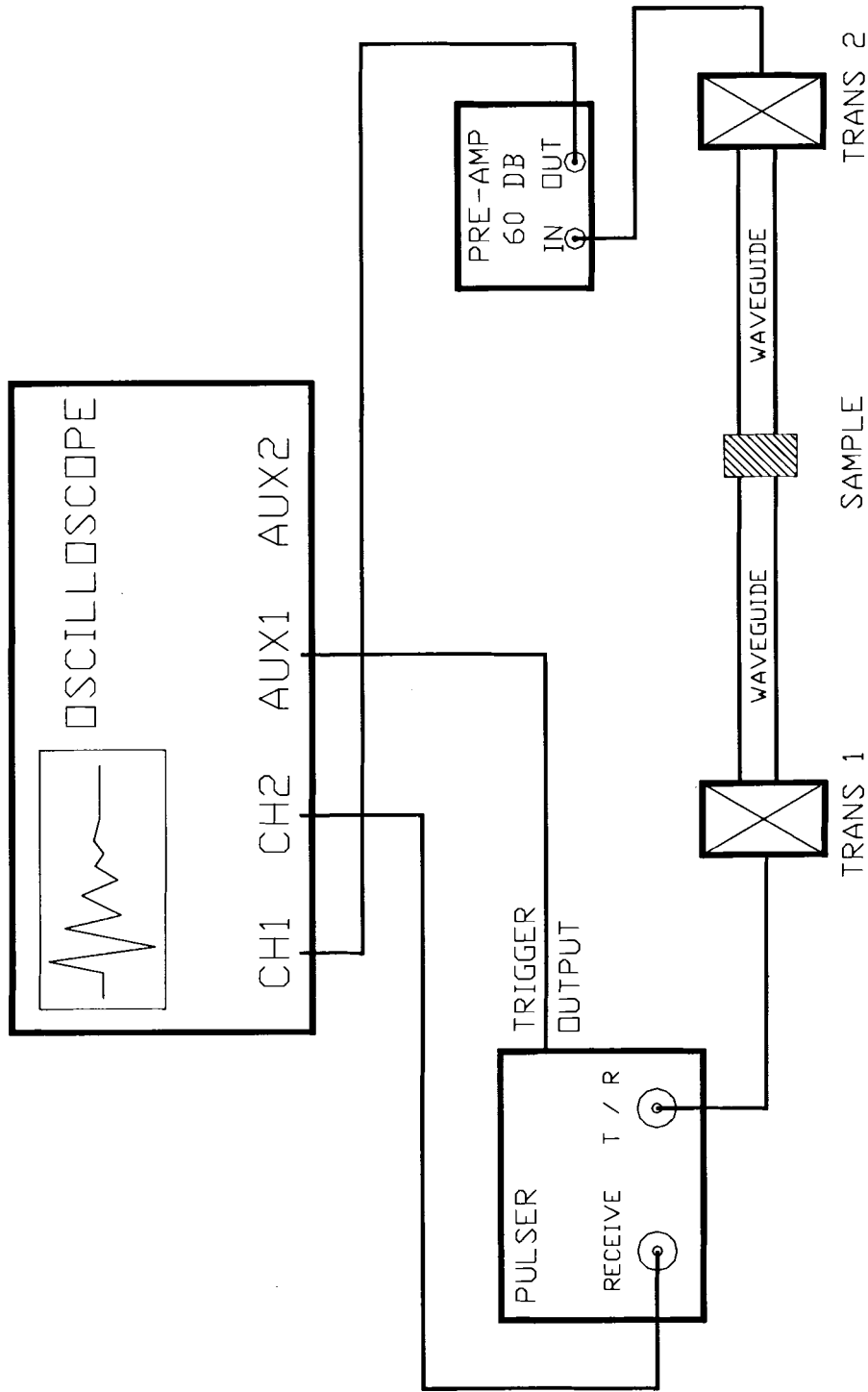
Figure 2.23. Schematic drawing of instrumental setup used in this work.

2.8.2 Acquiring Six Signals

Six signals are needed for signal processing at each temperature. Two through transmission signals and four pulse-echo signals are required at each temperature setting. The six signals are shown in figure 2.24 along with the notation used to describe them.
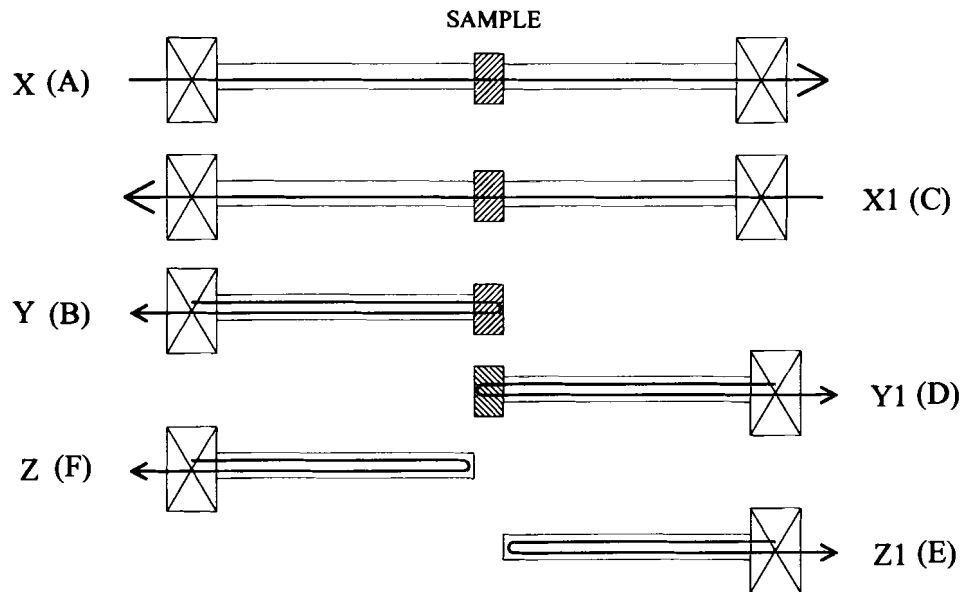
Figure 2.24. The six signals needed for future signal processing.

The signals X and X1 are through transmission signals obtained when the air cylinders are extended and the waveguides are in contact with the sample. Signals Y and Y1 are the pulse-echo signals obtained with the waveguides extended and in contact with the sample. Signals Z and Z1 are the pulse-echo signals obtained from the free end of the waveguides when the air cylinders are retracted from the sample. A, B, C, D, E and F denote the post-scripts of the recorded data files saved at each temperature and is the order of which each signal is recorded. The naming conventions for the six signals along with some example signals recorded through a C/C sample can be seen in appendix.

It is important when extending and retracting the waveguides to monitor the pressure in the air cylinders. Initial pressure should be limited to 5-8 lbs when extending and retracting the waveguides. The fused quartz waveguides have low toughness and will shatter if brought in to the sample too quickly while extending or retracting the waveguides. Once the waveguides have been extended and have contacted the sample, added pressure can then be applied. In most of the experiments in this work, a total of 25psi is used to provide consistent pressure between waveguides and sample once the two were in contact.

Chapter 3

EXPERIMENTAL PREPARATIONS AND PROCEDURES

The main objective of this work is to evaluate the dynamic elastic properties of a carbon-carbon (C/C) composite at elevated temperatures. The design and setup of the apparatus capable of measuring the modulus of a sample was previously described in chapter 2. The experimental procedures required to measure the modulus change with temperature will be discussed. Sample and furnace preparation along with the testing parameters and final measurements will be discussed in the sections that follow.

3.1   Sample Preparation and Measurements

Fiber Materials Incorporated (FMI) in Biddeford Maine produced the C/C composite sample material that was the primary focus of this work. Additional commercially produced carbon-carbon material was obtained from Goodfellow in Berwyn Pennsylvania. The original block of C/C obtained through Applied Thermal Sciences (Sanford, ME) was 123.825mm x 122.238mm by 41.275mm (~5 x 5 x 1.5 inches). The uncut block is shown in figure 3.1. Sections of C/C were initially cut from the original block using a tile saw (MK Diamond Products, model MK101, Torrance CA). The final specimens were cut from these sections using a low speed diamond wheel saw (South Bay Technology Inc., model 650, San Clemente CA). The opposing sides of the test specimens are cut as close to parallel as possible in order obtain accurate data. Signal complexity due to anisotropy and accuracy of the measurements from the ultrasonic signal are reduced if opposite sides of the specimens are not parallel.

51

Figure 3.1. The original C/C composite block obtained from FMI.

The size of each specimen was kept constant throughout the cutting process. The most important dimension to note was the thickness of each specimen. The thickness has a direct effect when calculating wave velocity through a specimen. Keeping the overall dimensions of all C/C composite specimens similar simplifies the experiments and calculations. The thickness of each specimen was cut to 10mm ($\pm$. 01mm). The height and width of the samples were cut to 20mm and 22mm ($\pm$ .01mm) respectively.

All of the specimen dimensions are carefully measured using calipers (Cole Parmer, #EW-97231-02, Vernon Hills IL), accurate to 0.01mm, recorded and placed in a small, labeled plastic bag. The bags were labeled with the date that the sample was tested. Each specimen is weighed, using a tabletop scale (Davis Instruments, model SV-200 Baltimore MD) accurate to 0.01 gm. The density of each specimen is calculated by dividing the mass of the specimen by the total volume of the specimen. The volume is calculated from the measured dimensions. Data for the test samples is given in the appendix. Three-dimensional drawings were made using AutoCAD to record the

locations of the test specimens. Some of the test specimens that were cut from the original block are shown in figure 3.2. Once these specimens have been cut, measured and recorded, they are ready to be tested.
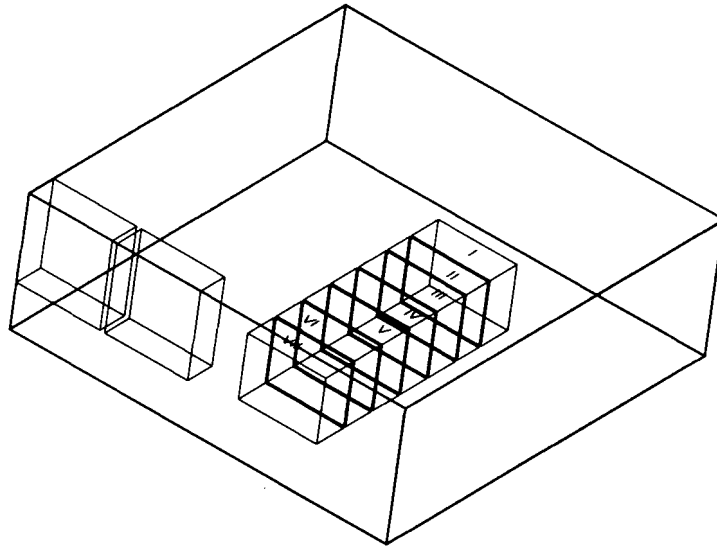
Figure 3.2. Sketch of original C/C block and locations of a few test specimens.

3.2   Furnace Preparations and Procedures

Assembly and atmospheric sealing of the furnace is critical in this work. For example, the o-ring gaskets located between each faceplate and endcaps, described in chapter 2, are coated with high vacuum grease (Dow-Corning #976, Midland MI). Figure 3.3 is a picture of a faceplate from the endcap setup that contains an o-ring gasket and applied vacuum grease.
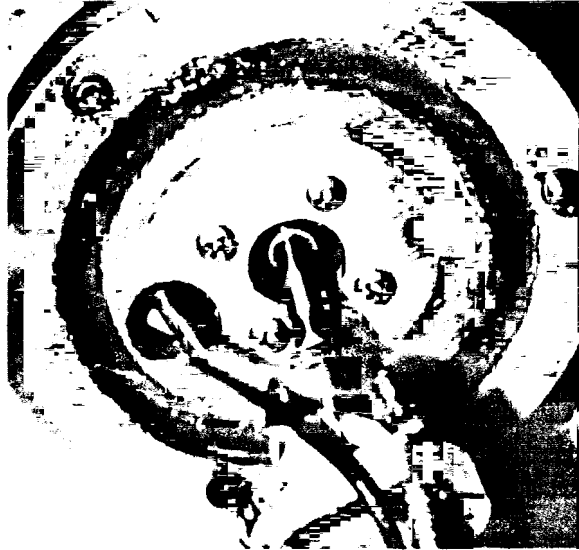
Figure 3.3. O-ring gasket with applied vacuum grease.

Once the vacuum grease has been applied to the endcap and air cylinder faceplate, the transducer is placed into the transducer-housing clamp and the waveguide is secured against the transducer with a setscrew. A small portion of vacuum grease is used as coupling between the transducer and waveguide. This is the only location where any coupling is used. A detailed sketch of the transducer and waveguide setup can be seen in section 2.5.3. Figure 3.4 is a photo of the transducer-housing clamp that holds the transducer in contact with the secured waveguide.
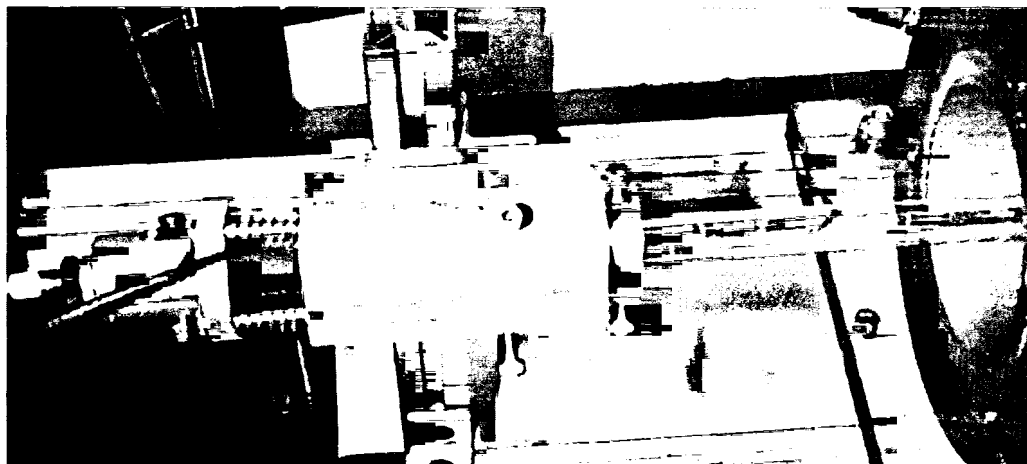
Figure 3.4. Transducer housing clamp and waveguide.
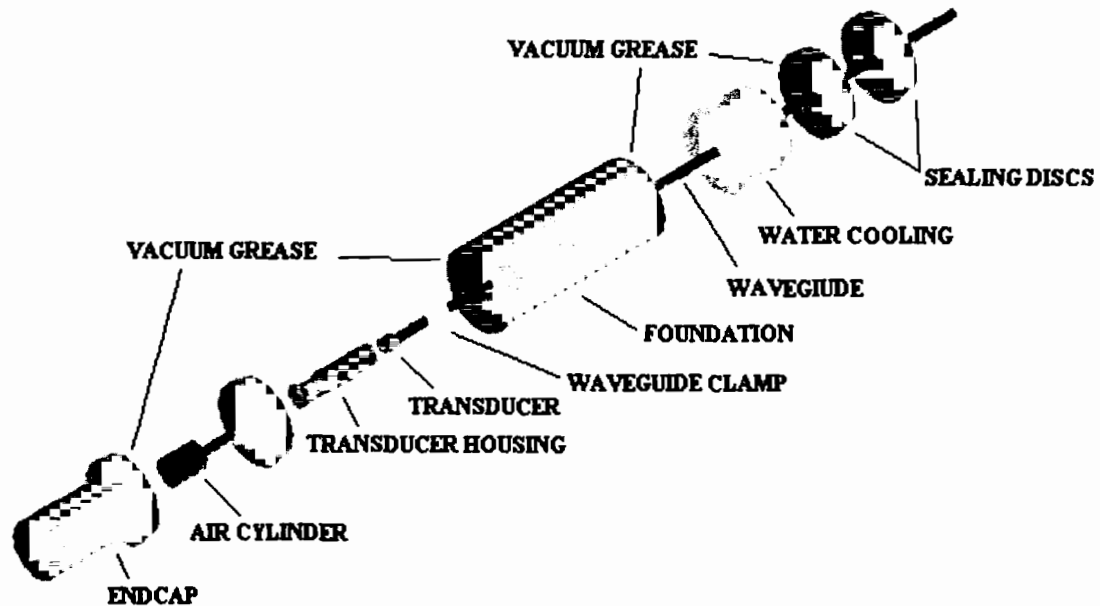
Figure 3.5. An exploded 3-dimensional view of the endcap setup (LHS).

After the transducer and waveguide have been assembled, the endcap containing the air cylinder is fastened to the endcap housing foundation. With vacuum grease applied to the remaining o-ring gaskets, the rest of the endcap setup, including the water-cooling system is secured to the endcap housing foundation. A three-dimensional exploded drawing of is shown in figure 3.5. Once the endcap setup is secured and sealed, the specimen is placed inside the furnace tube. A photograph of the procedure to load the specimen into the furnace tube is shown in figure 3.6.
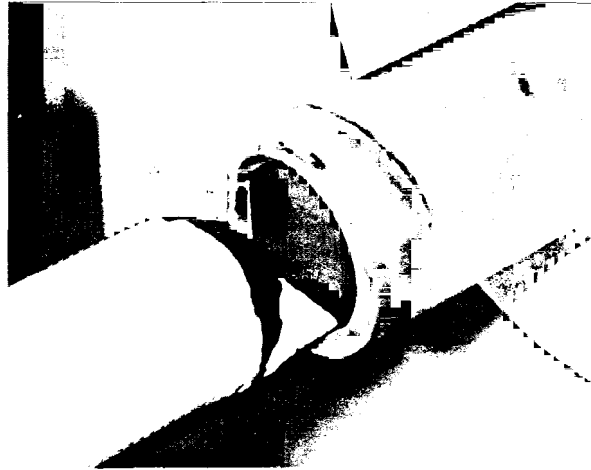
Figure 3.6. C/C composite sample loaded into furnace tube.

The entire endcap setup on the left hand side of the furnace was designed to slide away from the furnace to allow a specimen to be positioned at the opening of the furnace tube. Once the specimen is positioned inside at the end of the furnace tube, the entire endcap setup is then slowly slid back towards the furnace and the waveguide, sample and alumina tube slide into the furnace tube. Figure 3.7 shows the endcap setup withdrawn from the furnace and the alumina tube entering the furnace tube.
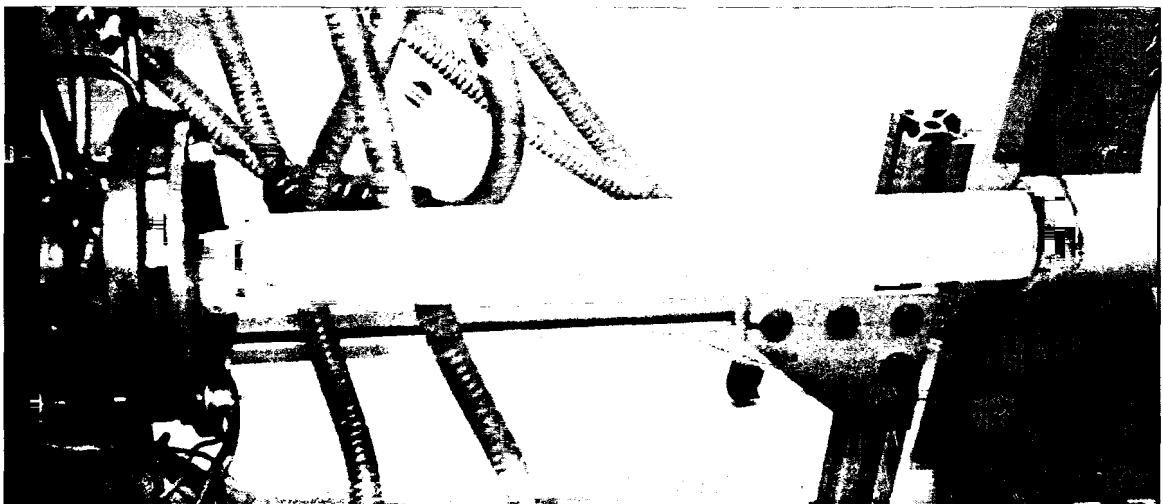
Figure 3.7. Actual alumina tube entering the furnace tube.

The platform at the end of the alumina tube, described in section 2.6, guides the specimen to the center of the furnace tube while holding it in position. A sketch of the alumina tube and specimen can also be seen in section 2.6.

After the endcap setup and specimen have been slid into the furnace, the two faceplates that seal the endcap to the furnace tube, described in section 2.5.4, are fastened together. These two faceplates force a high temperature Kalrez Perfluoroelastomer o-ring (McMaster-Carr, Dayton NJ) to compress around the furnace tube and seal the furnace. The left hand image in figure 3.8 is the high temperature o-ring that compresses around the furnace tube. The right hand image shows the endcap setup and faceplates sealed around the furnace tube.
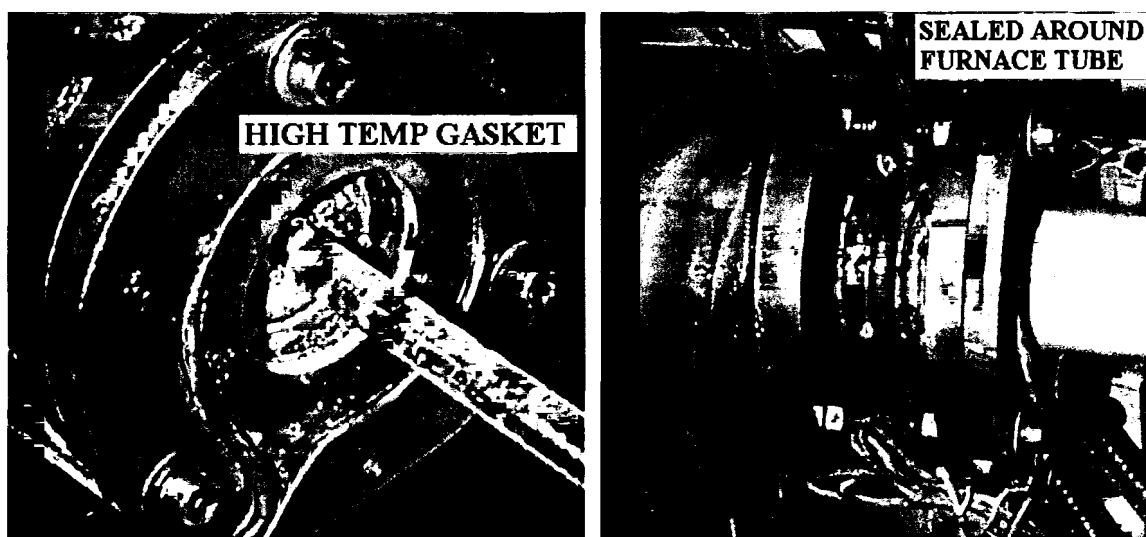
Figure 3.8. High temperature gasket and faceplates sealed around furnace tube.

3.3　Inert Atmosphere Procedures

After the entire endcap setup is secured together and sealed around the furnace tube, the furnace atmosphere must be evacuated and back filled with an inert gas. Each water-cooling system on the endcap setup has a small tube that extends from the inner

atmosphere of the furnace to the outside atmosphere of the setup. These are the fittings that are used to evacuate and backfill the furnace. The atmosphere within the furnace is evacuated using a medium vacuum pump (Marvac Scientific, Model #R-10, Concord CA) to 100kPa or 14.5psi. A control valve was placed within the vacuum line that is closed once the atmosphere has been fully evacuated. With the control valve closed, the atmosphere is then back filled with an inert gas. The valve is closed to prevent the inert gas from flowing out the vacuum line.

In this work, nitrogen is the inert gas that is used to back fill the atmosphere and supply the pressure to the air cylinders. A flowmeter is placed on the nitrogen supply line to help monitor the flow of gas to the atmosphere. The primary purpose of the flowmeter is to aid in the detection of leaks from the furnace. If gas was detected flowing through the meter once the atmosphere was completely back filled, then a leak was present. These leaks are then found and repaired. A pressure regulator is also placed within the nitrogen supply line to keep the pressure in the line slightly above atmospheric. If the gas pressure in the nitrogen supply line is not maintained above atmospheric pressure, any small leak within the setup is likely to contaminate the furnace atmosphere with oxygen.

A secondary task of the inert gas flowmeter is to monitor the amount of gas allowed into the furnace atmosphere. Any desired gas could be easily connected to the supply line that flows through the flowmeter and into the furnace setup. This flow can be adjusted to a desired rate with a valve located on the flowmeter. Experiments with oxidizing material will require that the amount of gas that passes through this flowmeter

be monitored. Flowing gas can be used to compare the degree of oxidation that corresponds to a particular level of change in material properties and material weight.

Once the atmosphere has been evacuated and back filled, the process is repeated a second time. Repeating this process ensures that only inert gas is present in the furnace. A schematic drawing of the vacuum and pressure system along with the air cylinder setup is shown in figure 3.9 on the following page. This is the setup configuration used to control the atmosphere in the furnace. The only sealed penetrations through the furnace and endcaps are the inert gas supply line, the vacuum line, the two transducer cables for the ultrasonic system and the air cylinder inlets. Now the six signals can be recorded in an inert atmosphere.
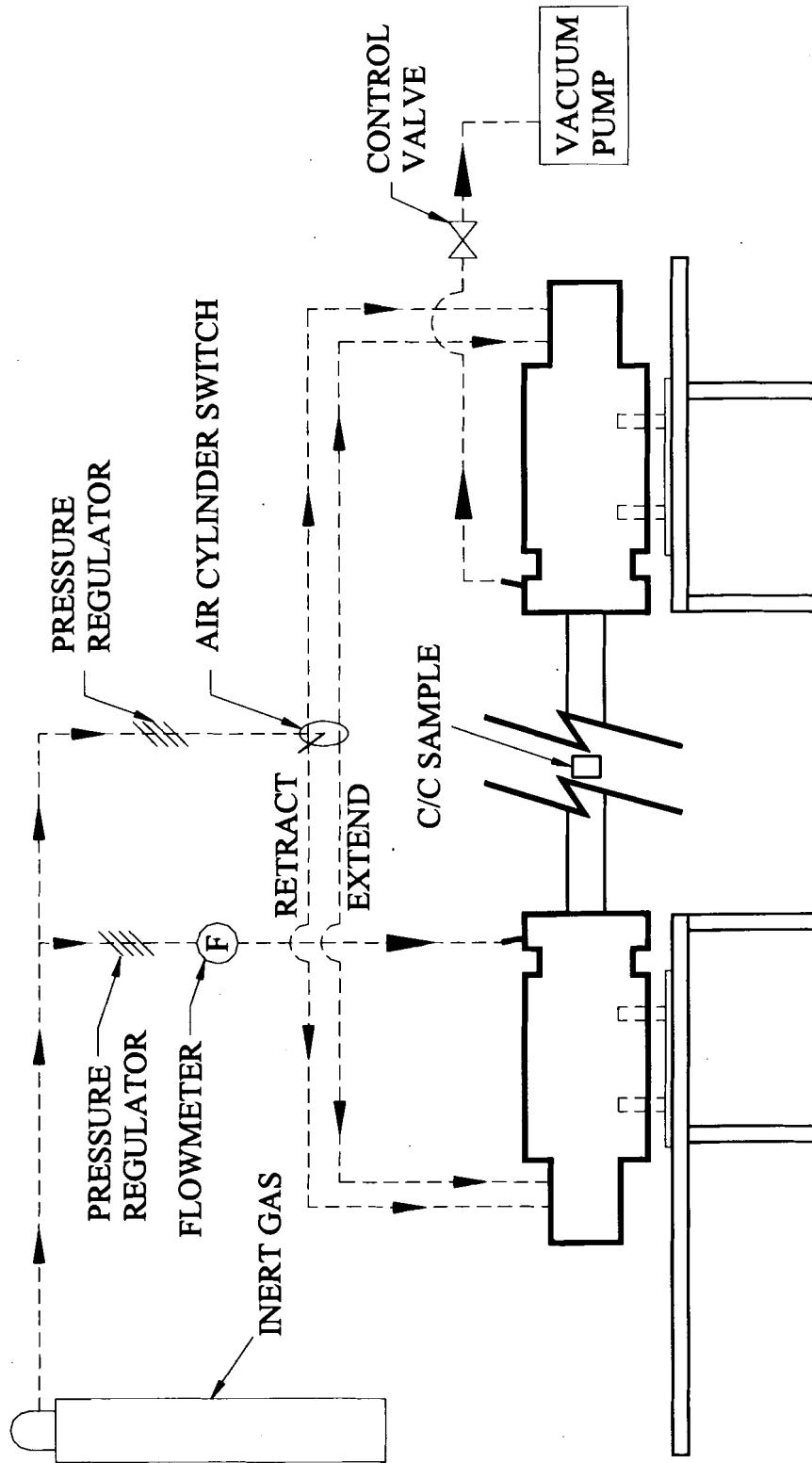
Figure 3.9. Schematic drawing of inert gas atmosphere setup.

3.4 Oxidation Procedures

The apparatus in this work is capable of controlling and monitoring the oxidation process of the C/C composite samples. The oxidation experiments are performed much like the inert atmosphere experiments. The atmosphere is evacuated and backfilled with the inert gas twice, as described in section 3.3, and gradually heated to 700°C. The six signals are recorded before any oxidation occurs. Once the signals have been recorded the atmosphere is evacuated again and medical air is connected to the atmosphere supply line while the vacuum pump remains running. Air is allowed to flow through the setup at 0.8scfm for 10-minute increments. After the completed time, the inert gas is reconnected to the atmosphere supply line and the vacuum pump remains running for one minute and then shut down and the six signals are recorded. The process is repeated until 120minutes of air has flowed through the setup. After the experiment is complete, the furnace is allowed to cool and then the specimen is weighed and recorded. A second oxidation procedure is performed on a different C/C sample that is similar to the previous, but the specimen is allowed to cool, removed from the furnace and weighed at every 20-minute increment.

3.5 Measurements and Observations

After elevated temperature testing has been performed on the sample, the sample is removed from the furnace. Initial visual observations including loss of matrix from the composite or marks on the surface of the sample from the waveguides are made. Marks found on the composite inflicted from the waveguides can impact the results and should be noted. After these observations are recorded, the sample is weighed in the same

manner as prior to the temperature testing. Loss in sample weight is normally used to quantify oxidation of C/C composites. A gain in weight is likely to be caused by alumina residue on a C/C sample and the alumina cement from the alumina tube guides.

After the sample has been weighed, the dimensions are recorded as prior to testing. Changes from the initial sample geometry would suggest localized oxidation of the sample. The left hand specimen in figure 3.10 is a C/C sample that was tested up to $1100^{\circ}C$ in a contaminated atmosphere. Oxidation is visible from the exposed carbon fibers and absence of carbon matrix. The right hand block is shown for comparison. This is a similar C/C sample that was held at $1100^{\circ}C$ but did not oxidize due to careful control of the atmosphere making sure to keep an inert atmosphere. This sample is much smoother and did not lose carbon matrix.
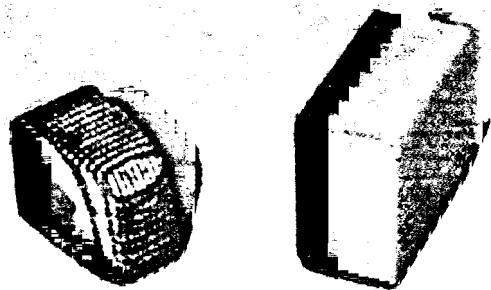
Figure 3.10. Oxidized (left) and non-oxidized C/C composite samples.

Chapter 4

SIGNAL PROCESSING

4.1   Introduction

It is necessary to perform appropriate signal processing to evaluate the dynamic properties of a C/C composite. The waveguides result in a complex signal that must be interpreted. The ultrasonic signal requires almost 200μsec to propagate through two waveguides and a 10mm thick sample. An example of a signal recorded through a C/C composite sample at 1100°C is shown in figure 4.1. Pulse echo signals from the free end of the waveguide also recorded at 1100°C. An example of a pulse-echo signal is shown in figure 4.2.
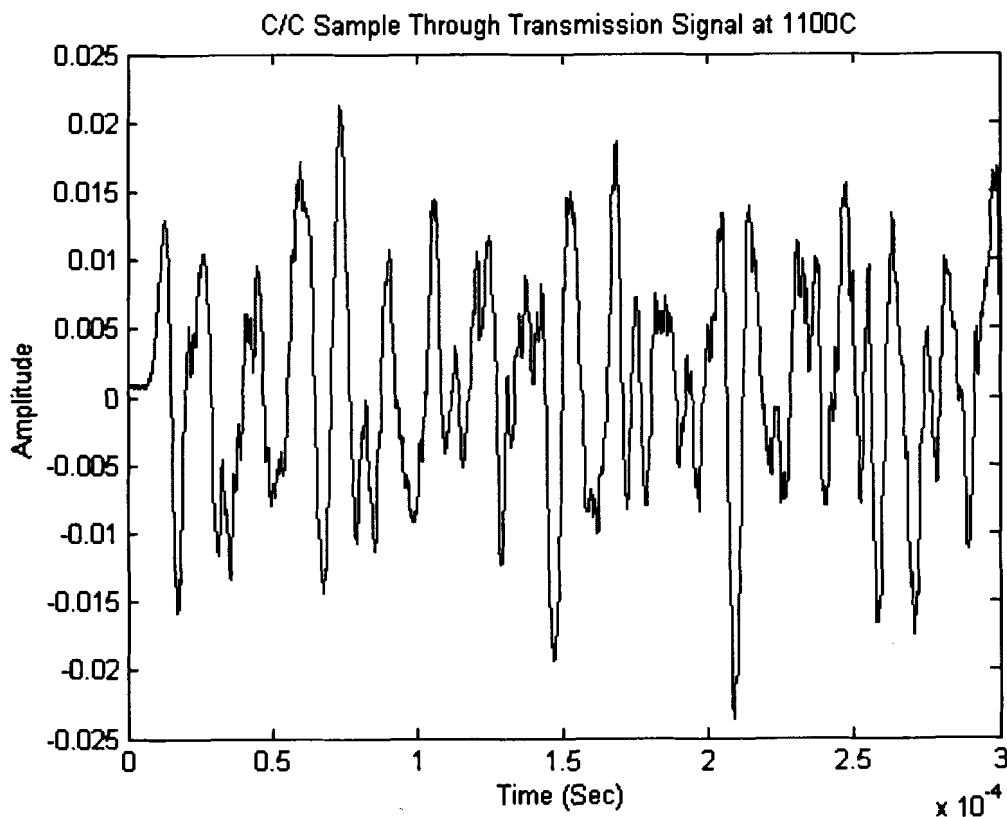
Figure 4.1. A transmission signal through a C/C sample at 1100°C.
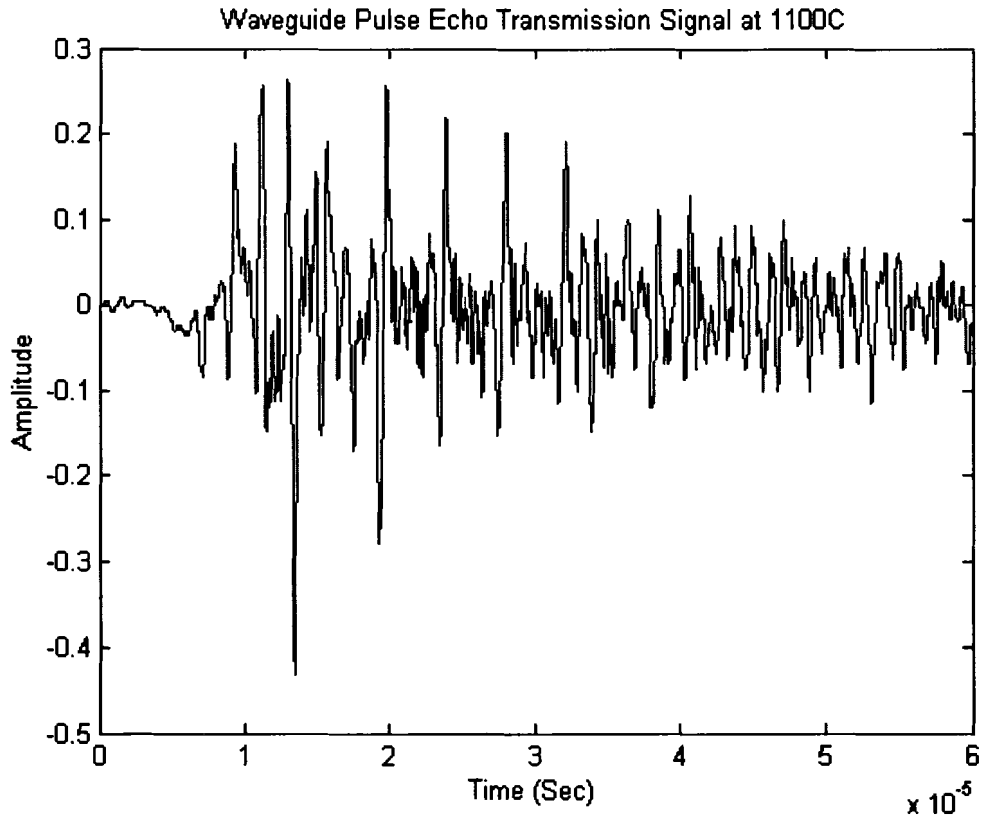
Figure 4.2. A pulse-echo transmission from the free end of the waveguide at 1100°C.

A 190μsec time delay occurs before the start of the data shown in figure 4.1 and in figure 4.2. No data is shown in this time interval because the range of the oscilloscope, at a sufficient sampling rate, is less than the total amount of time a signal propagates through the setup.

The received signal contains electronic noise from the initially transmitted signal along with reflections generated from within the sample. Most significantly, the dry coupling between waveguides and sample result in a low signal-to-noise ratio and very high attenuation. The top image of figure 4.3 was recorded from the system after transmission through a stainless steel sample. Significant noise is evident in the received signal. The bottom signal in figure 4.3 was recorded through a C/C composite sample, which has less noise in the received signal. The received signal requires processing in

order to extract the first arrival from the multiple reflections and to lower the signal to noise ratio. This data will then be used to generate the dynamic property changes of a sample with change in temperature.
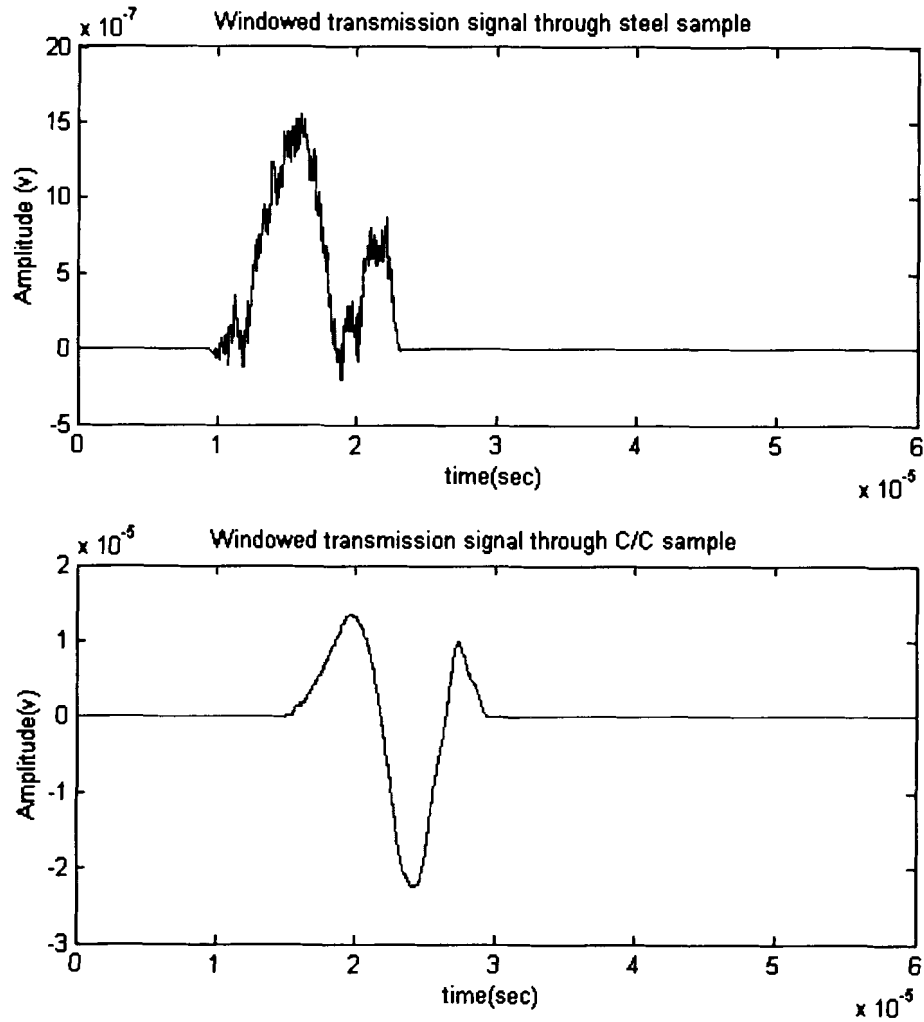
Figure 4.3. Windowed through transmission signals for stainless steel (top) and carbon-carbon (bottom) used for signal-to-noise comparison.

4.2   Processing Recorded Data

The complexity of the signal shown in figure 4.1 makes it difficult to extract the desired dynamic properties of the sample. Windowing is needed to isolate the first part of the recorded signal from the reflections from within the sample. The first part of the

65

signal is a directly transmitted signal that has propagated through the entire setup. From the initial portion of the signal, the change in modulus as a function of temperature can be determined.

The window used to isolate the signal of interest is a Hanning window. A Hanning window is computed from the following equation:

$$
w(x) = \begin{cases} 0 & x < A \\ .5(1\text{-}\cos(2\pi x/B)) & A \leqslant x \leqslant B \\ 1 & B < x \leqslant (D\text{-}B) \\ .5(1\text{-}\cos(2\pi x/B)) & (D\text{-}B) < x \leqslant D \\ 0 & x > D \end{cases}
$$

(4.1)

where w(n) is an n-point Hanning window. The Hanning window can be adjusted to fit the length of any signal. However, the desired length should be kept constant when windowing a group of signals. The accuracy of the velocity calculations using the cross-correlation process is dependent on the consistency of the signal windowing technique.

The unprocessed through-transmission signals are graphed using MathCAD and the first two peaks are located. Then the peaks of the through-transmission signals (Signal X and X1 in section 3.3.2) are windowed using a MatLab program that applies a Hanning window and generates an output file. The output file will be used in the cross-correlation. The MatLab program used to window the signals, is included in the appendix. In this program, the number of data points before the start of the Hanning

66

window, the width of the Hanning window, the number of data points between the Hanning window and the end of the Hanning window are input for each signal.

The pulse-echo signals from the free end of the waveguide must also be windowed (Signal Z and Z1 in section 3.3.2). The pulse-echo signals are windowed around the first 5 or 6 peaks using the same method as the through transmission windowing but with a slightly more narrow Hanning window. Figure 4.4 shows an unwindowed through-transmission signal and the Hanning window. The lower trace in figure 4.4 is the windowed signal that will be used in the cross-correlation. From these windowed signals it will be possible to calculate the time delay between two signals recorded at different temperatures.
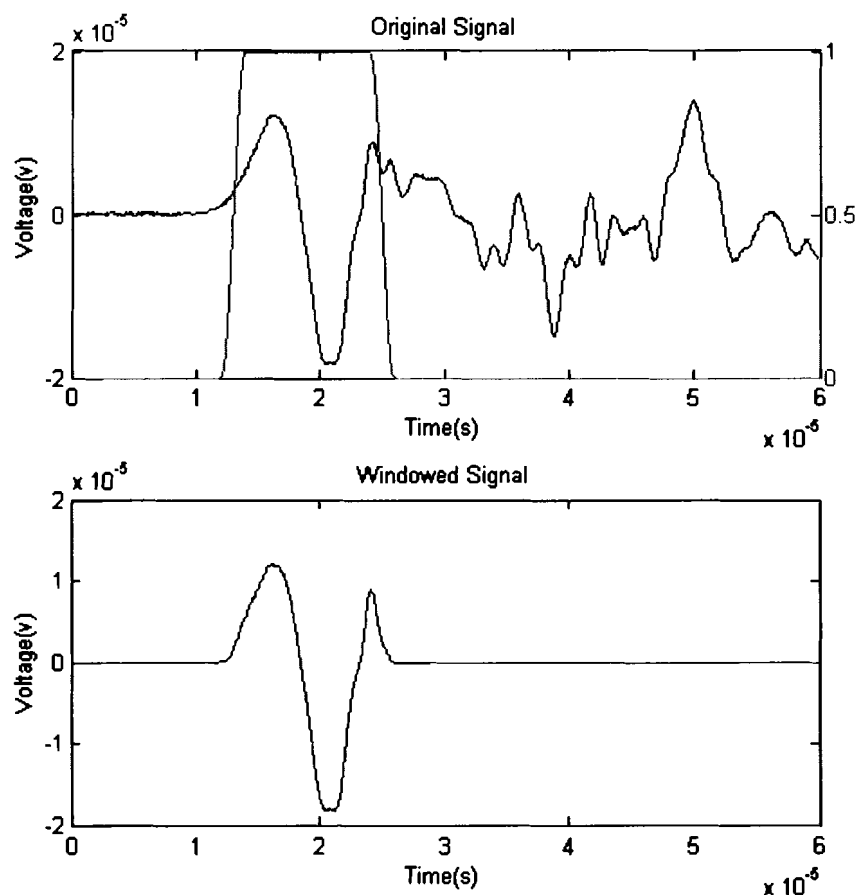
Figure 4.4. A C/C through transmission signal (X) before and after windowing.

Figure 4.5 shows a pulse-echo signal and the Hanning window. The lower trace in figure 4.5 is the windowed signal that will be used in the cross-correlation.
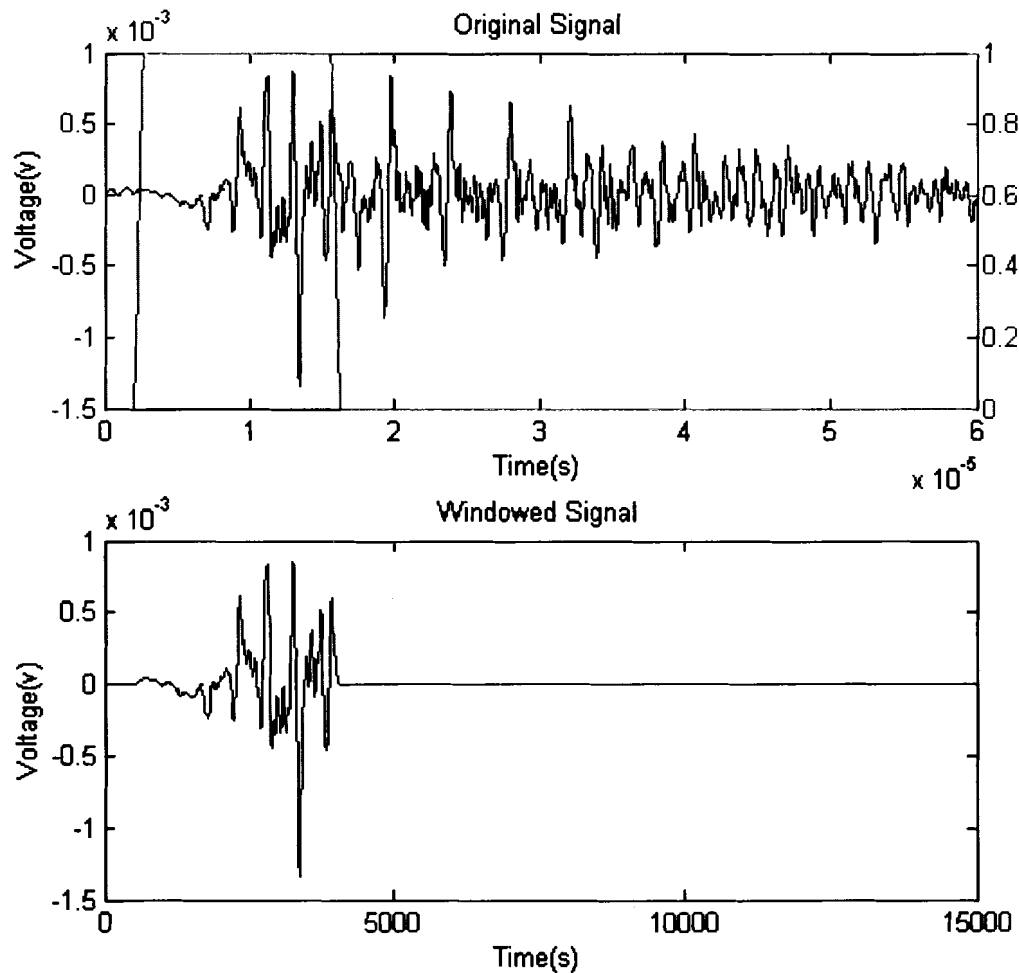
Figure 4.5. A pulse-echo signal (Z) before and after windowing.

4.3   Cross-Correlation

The relative arrival time of an ultrasonic signal is obtained from the cross-correlation of known to an unknown signal. The known signal is recorded under standard conditions with a reference specimen using the apparatus described in chapter 2. The unknown signals are from samples recorded at different temperatures. The cross

correlation of the known signal and the unknown signal is then calculated from [Peterson, 1996]:

$$C_r(t) = \sum_{t=-\infty}^{\infty} R(\tau)S(\tau - t)$$ (4.2)

The relative delay between the two signals corresponds to the point of maximum amplitude, τ_a, of the cross correlation of the two signals. The accuracy of the arrival time of the unknown signal obtained using this method is dependent on the sampling rate of the recorded signal. The consistency of the location of the Hanning window will also have an effect on the accuracy of the cross-correlation program.

A signal through a C/C composite sample is cross-correlated with a signal through a piece of aluminum to calculate the wave velocity through the C/C composite. The pulser, preamp and oscilloscope have the same settings for each signal. The two signals are cross-correlated and a relative time delay is found. The arrival time for the signal through the aluminum is calculated using known properties. The relative time delay is then added to the calculated reference arrival time to obtain the arrival time through the C/C composite sample. This time is used in the calculation of the wave velocity through a C/C composite sample at room temperature. The time at room temperature will be the reference point when calculating the change in time with change in temperature.

4.4 Modulus Calculations

The change in the modulus of a sample with change in temperature is obtained from the change in ultrasonic velocity. The change in velocity is calculated by dividing the width of the sample by the time for a signal to propagate through the sample. The relative time delay is obtained by using four of the signals at each temperature (X, X1, Z

69

and Z1 discussed in section 3.3.2). After windowing, a cross-correlation program finds the relative change in time between two signals. The relative time delay through a sample with change in temperature is calculated using the following:

$$\Delta t_{sample} = \frac{(\Delta t_X + \Delta t_{X1}) - (\Delta t_Z + \Delta t_{Z1})}{2}$$ (4.3)

where Δt_X is the relative time delay between $X(T_1)$ and $X(T_2)$, Δt_{X1} is the relative time delay between $X1(T_1)$ and $X1(T_2)$, Δt_Z is the relative time delay between $Z(T_1)$ and $Z(T_2)$, Δt_{Z1} is the relative time delay between $Z1(T_1)$ and $Z1(T_2)$, and Δt_{sample} is the relative time delay through the sample between T_1 and T_2. The modulus is calculated from the relative delay through the sample. Preliminary experiments were performed on type 316L stainless steel. The temperature dependence of the modulus was compared to handbook values [Bernstein, 1977]. Equation 2.5 is rearranged to solve for the change in Young's modulus of a stainless steel sample with change in temperature (equation 2.6).

The C/C composite specimens studied in this work are an anisotropic material. Tests on the C/C composites are performed such that waves propagate along one of the primary axes. A primary axis will be assumed to be an axis that lies parallel with one of the orthogonal carbon fibers. Propagating the signals through a primary axis of the C/C samples gives the following relationship for the velocity:

$$c = \sqrt{\frac{C_{11}}{\rho}}$$ (4.4)

where c is the wave velocity through the sample, ρ is the material density and C_{11} is the normal modulus in the x_1 direction. Equation 4.3 is rearranged to give:

$$\Delta C_{11} = C_{11}(T_1) - C_{11}(T_2) = \left[[\rho(T_1)] \cdot [c(T_1)]^2 - [\rho(T_2)] \cdot [c(T_2)]^2 \right]$$ (4.5)

where T_1 is the lower temperature, T_2 is the higher temperature and c is the wave velocity through a sample at these temperatures. The density, ρ is found for both of these temperatures. If no oxidation occurs in the C/C samples, it will be assumed that the density of the material will stay constant. During oxidation, however, the C/C composite sample will lose some of its primary matrix and the density of the material will change. Drastic loss of material and significant changes in material density are experienced at temperatures higher than 700°C [Savage, 1993]. This change must be considered in order to obtain an accurate measure of the modulus change within an oxidizing environment.

Initially, the density of the material will be calculated by dividing the mass of the sample by the product of the dimensions of the sample. This is the sample density that will be used when calculating the change in the modulus of the sample when no oxidation occurs. The accuracy of calculating the modulus change is dependent on the measured signal time change through the sample.

4.5 Material Attenuation using Deconvolution

Another dynamic material property of concern is the attenuation of ultrasound through the material studied. An ultrasound is propagated through a medium and the intensity of the ultrasound is measured at two points, x_1 and x_2. Attenuation is used to describe the total reduction in the intensity of the ultrasound through the medium. Attenuation results from the absorption of energy by the medium between the two points and from the deflection of the energy from the path of the ultrasound by reflection, refraction, diffraction and scattering [Cracknell, 1980].

The absorption involves the conversion of ultrasound into energy such as heat or displacement. The absorption of the ultrasound is dependent on the nature of the medium and can therefore be beneficial when studying the physical properties of the medium. The reflection, refraction, diffraction and scattering losses are dependent on the geometry and boundaries of the medium. If the porosity of a medium increases with temperature, the attenuation of the medium will increase due to reflections generated from the pores. Calculating the attenuation of a C/C composite material is not one of the objectives in this work, however, showing that the attenuation change of the material can be calculated will be useful for future work.

The attenuation of a specimen is calculated using six signals (X, X1, Y, Y1, Z and Z1 in section 3.3.2). A deconvolution method is used in order to separate the effects of the sample from the other effects generated within the system from the temperature changes. Deconvolution is required since a larger number of parts in the proposed setup are affected by heat and other changes that occur during an experiment [Peterson, 1994]. Examples of these changes are the variation in coupling between the waveguides and transducers, waveguides and sample and changes in wave velocity within the waveguides. To calculate a value for the material attenuation through a sample from an ultrasonic signal, the magnitude of the spectrum of these six signals must be obtained.

A fast Fourier transform is performed on each windowed signal that yields the spectra, $X(\omega)$, $X1(\omega)$, $Y(\omega)$, $Y1(\omega)$, $Z(\omega)$ and $Z1(\omega)$ from their respective signal. In mathematical form, the signals may be shown as the convolution of the contributing response functions (multiplication in the frequency domain) [Peterson, 1994]:

$$X = A_{lt}(\omega)H_{tb}(\omega)H_{b}(\omega)T_{bs}(\omega)H_{s}(\omega)T_{sb}(\omega)H_{b}(\omega)H_{bt}(\omega)A_{2r}(\omega) \tag{4.6a}$$

$$Y = A_{lt}(\omega)H_{tb}(\omega)H_{b}(\omega)R_{bs}(\omega)H_{b}(\omega)H_{bt}(\omega)A_{1r}(\omega) \tag{4.6b}$$

$$Z = A_{lt}(\omega)H_{tb}(\omega)H_{b}(\omega)R_{bo}(\omega)H_{b}(\omega)H_{bt}(\omega)A_{1r}(\omega) \tag{4.6c}$$

where $A_n(\omega)$ = response spectrum of transducer n (transmit or receive mode, respectively), $H_{tb}(\omega)$ = spectrum of coupling response from transducer to waveguide, $H_b(\omega)$ = spectrum of response of waveguide, $T_{bs}(\omega)$ = spectrum of transmission response of dry coupling between waveguide and sample, $R_{bs}(\omega)$ = spectrum of reflection response of dry coupling between waveguide and sample, $R_{bo}(\omega)$ = Spectrum of reflection response of free end of waveguide (assumed equal to -1) and $H_s(\omega)$ = spectrum of response of sample. The other three signals, X1, Y1 and Z1 are represented in the same manner however the transmitting and receiving transducers are reversed.

These six spectra are used along with equation 4.6 in order to solve for the response of the sample:

$$H_s(\omega) = \sqrt{\frac{X(\omega) \cdot X1(\omega)/Z(\omega) \cdot Z1(\omega)}{\left[1 - \left|\frac{Y(\omega)}{Z(\omega)}\right|^2\right] \cdot \left[1 - \left|\frac{Y1(\omega)}{Z1(\omega)}\right|^2\right]}} \tag{4.7}$$

The amplitude of H_s is the attenuation of the through-transmission signal with other effects from the system removed. Similarly, the phase of H_s is the time delay as a result of the C/C sample. This calculation of the time delay will not be as accurate as the one obtained from the cross-correlation program, however, it can be used to compare the two.

Chapter 5

RESULTS

In the following sections initial proof of concept tests are described which were performed on stainless steel samples. Tests that were performed on carbon-carbon in both an inert and in an oxidizing environment are also described.

5.1   Stainless Steel

Two, 316L stainless steel samples were tested in-situ from room temperature up to 1100°C in an inert atmosphere. The change in the arrival time of an ultrasonic signal propagating through the samples was measured using the cross-correlation (equation 4.3). Figure 5.1 shows the time delay that was calculated at various temperatures through the stainless steel sample relative to room temperature. The time delay is obtained from the change in time from the four signals acquired (X, X1, Z and Z1) (also shown in figure 5.1). The delay time for the stainless steel samples is shown in figure 5.2.

From the time delay, the change in modulus of the stainless steel sample was calculated for two samples using equation 2.6. The calculated modulus change with change in temperature for both stainless steel samples is compared to values obtained from the *Handbook of Stainless Steels* [Bernstein, 1977] shown in figure 5.3. The remaining data from the stainless steel experiments is shown in the appendix.
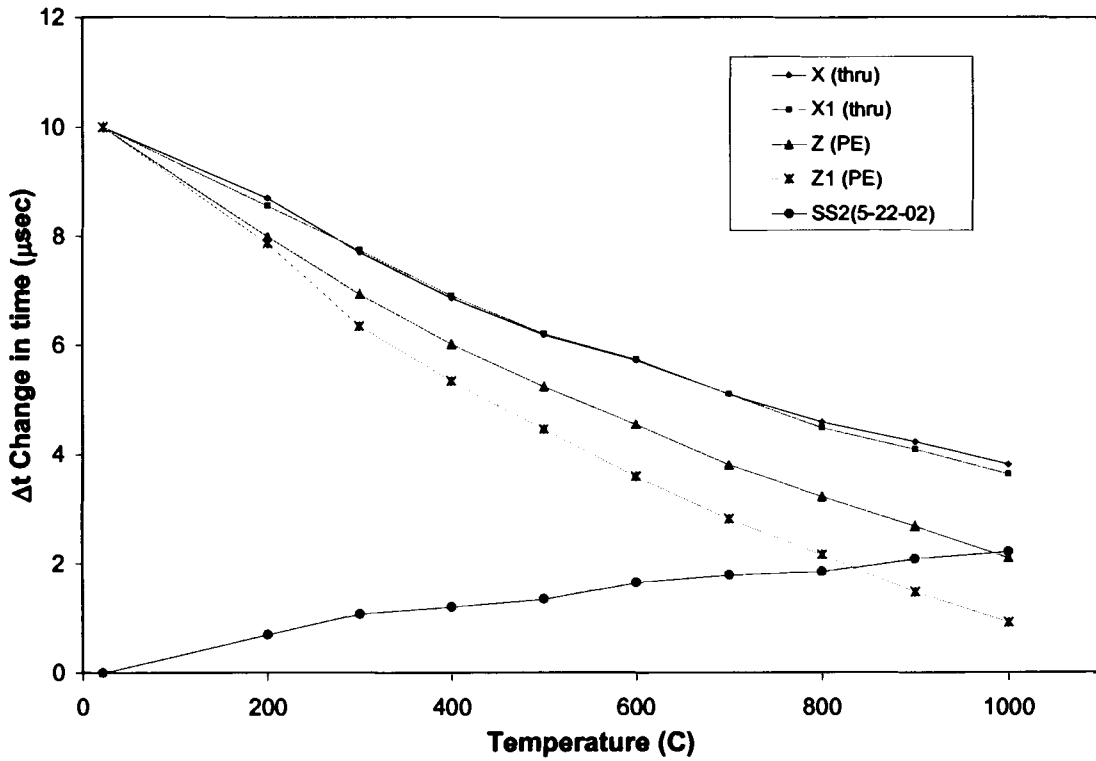
Figure 5.1. Change in sample time of a type 316L stainless steel sample.
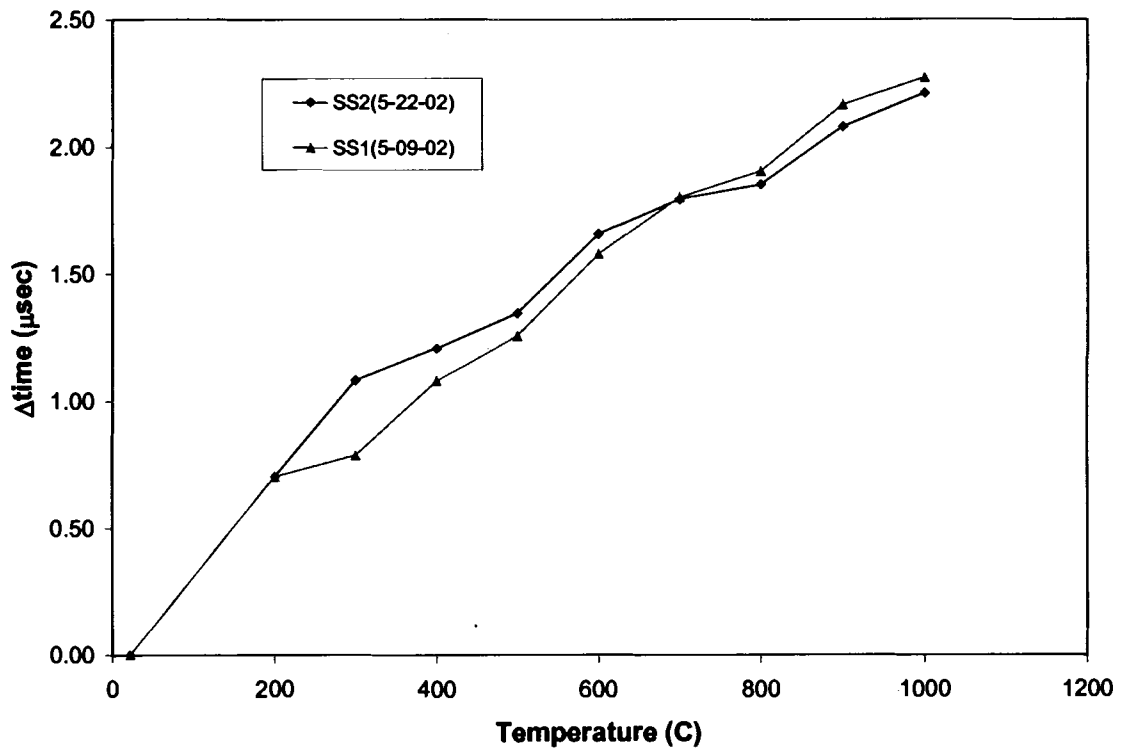
Figure 5.2. Change in signal time in both stainless steel samples with temperature.

75
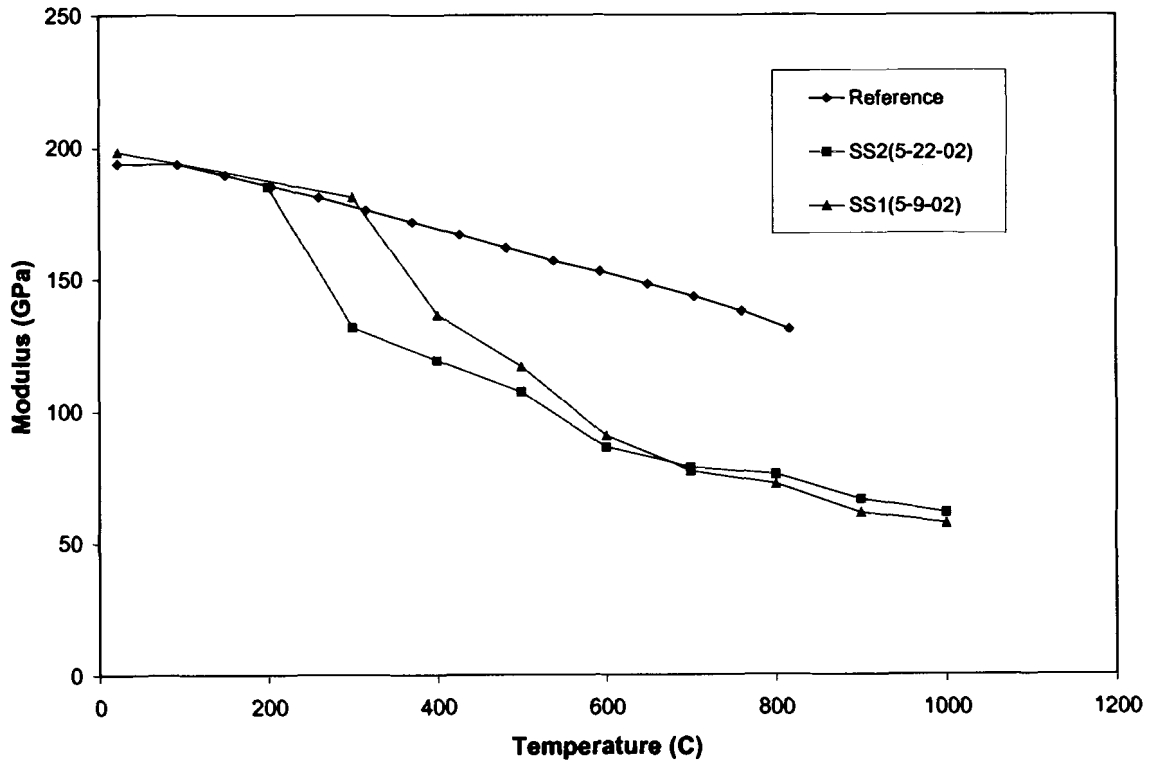
Figure 5.3. Modulus change of stainless steel samples.

5.2 Carbon - Carbon

Multiple samples of C/C composites were tested in both an inert and in a controlled oxidizing atmosphere. A drawing that shows the location of the C/C samples cut from the original block obtained from FMI is shown in figure 5.4.
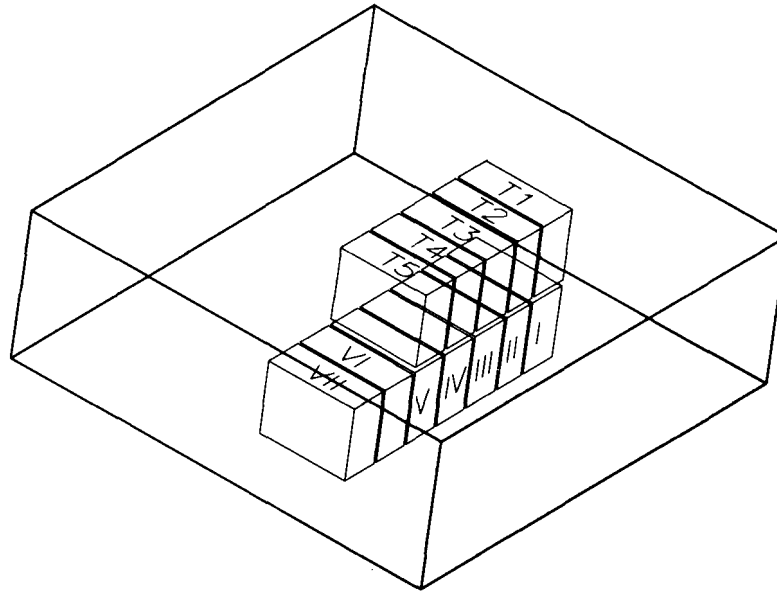
Figure 5.4. Location of C/C samples cut from original block obtained from FMI.

A single C/C composite sample from FMI, was tested four times in an inert atmosphere to show the repeatability of the experiment. A total of four different C/C composite samples from FMI were also tested in an inert atmosphere to show sample-to-sample variation. Two C/C composite samples, also from FMI, were also tested to show the change in modulus during controlled oxidation and compared to the oxidation reaction of a commercially produced carbon-carbon sample (Goodfellow, #C413050, Berwyn PA). Figure 5.5 shows the change in time through one C/C composite sample extracted from the change in time from the four signals (X, X1, Z and Z1). The other C/C composite sample time graphs are shown in the appendix.
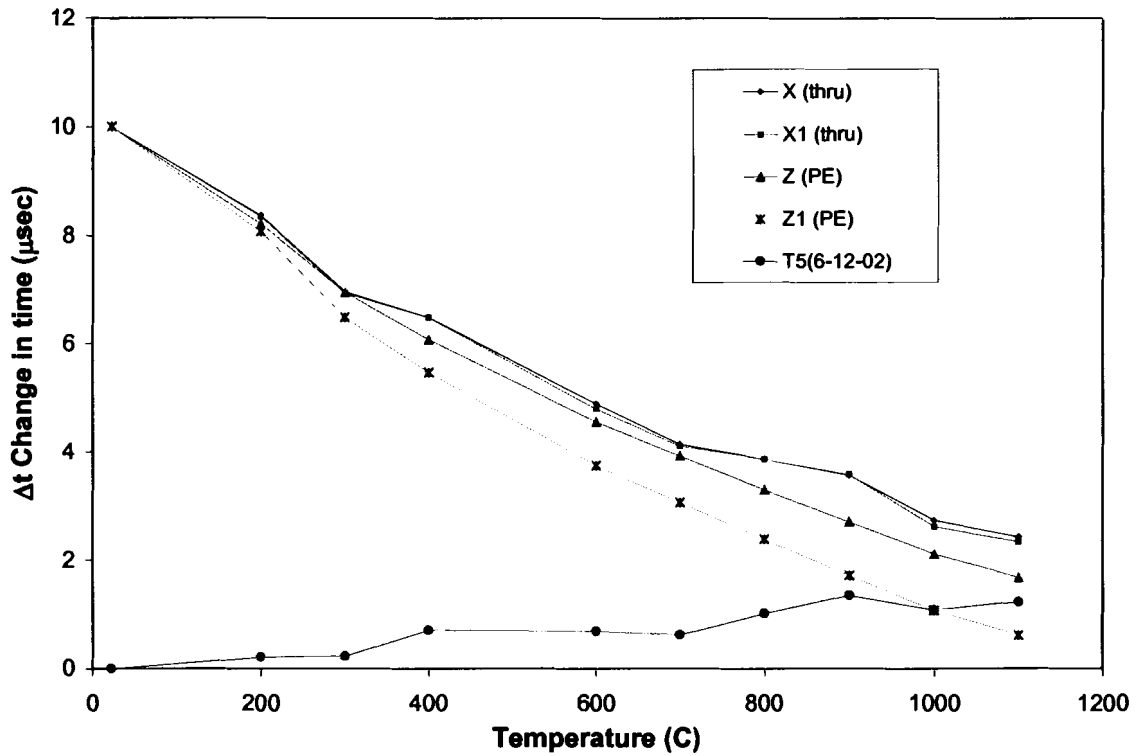
Figure 5.5. Change in time of a single C/C composite sample along with changes in
delay time found for each of the four component signals.

5.2.1 Repeatability

Tests were performed on a single C/C composite sample with four repetitions to
show the uncertainty of the calculated data. The change in modulus of the C/C sample,
measured in an inert atmosphere is shown in figure 5.6 from the four separate tests.
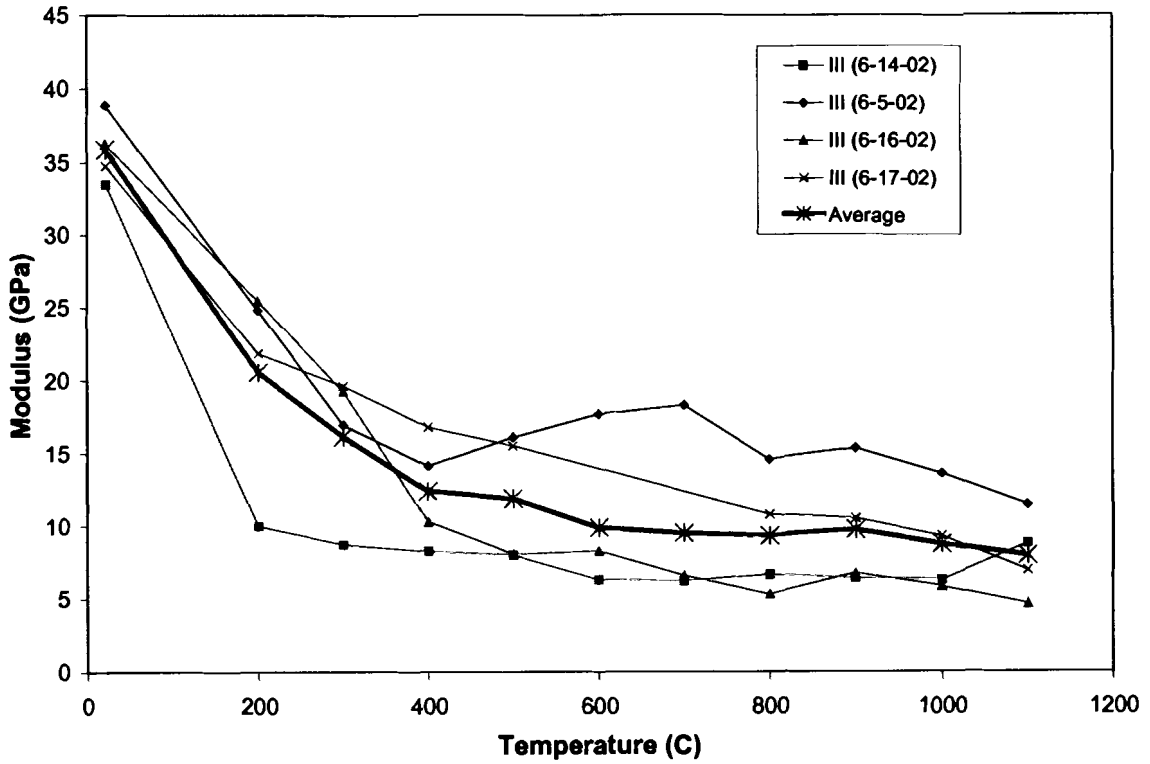
Figure 5.6. Modulus change calculations of C/C sample CCIII from four tests.

5.2.2 Sample–to–Sample Variation

The change in modulus of four C/C samples measured in an inert atmosphere is shown in figure 5.7 to illustrate the sample – to – sample variation. The change in modulus of the commercial C/C composite sample is shown in figure 5.8.
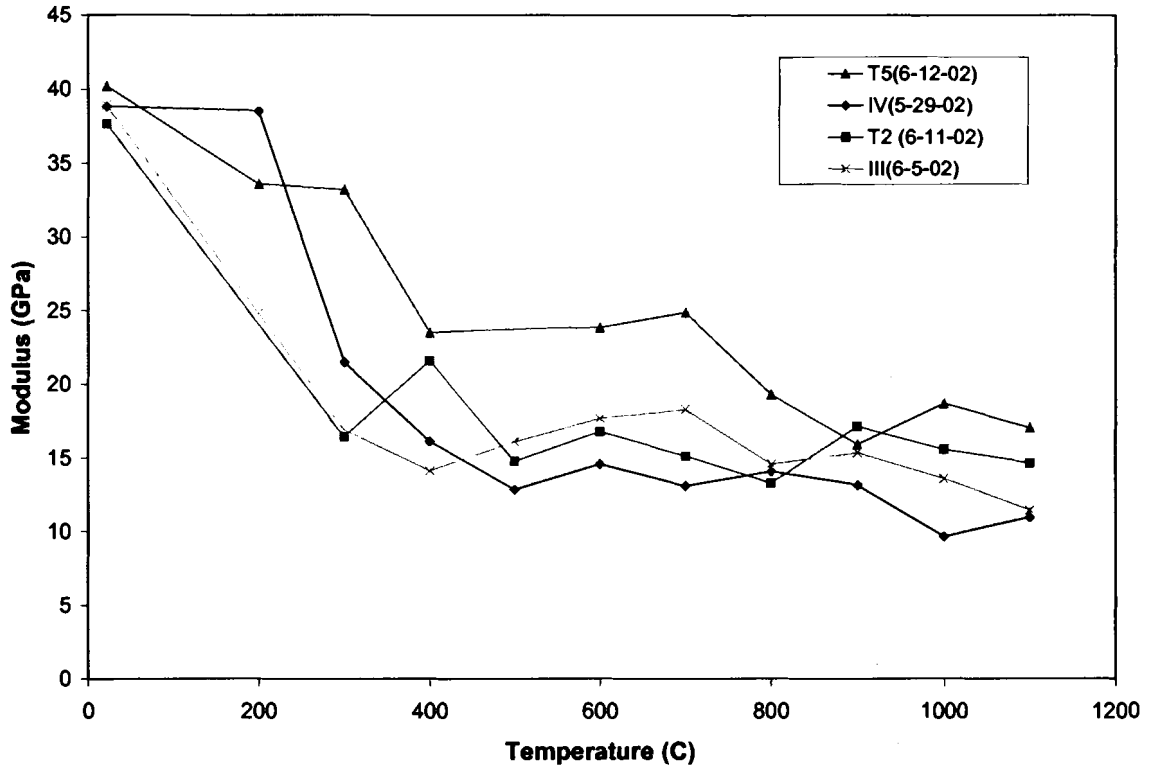
Figure 5.7. Modulus change from four C/C composite samples.
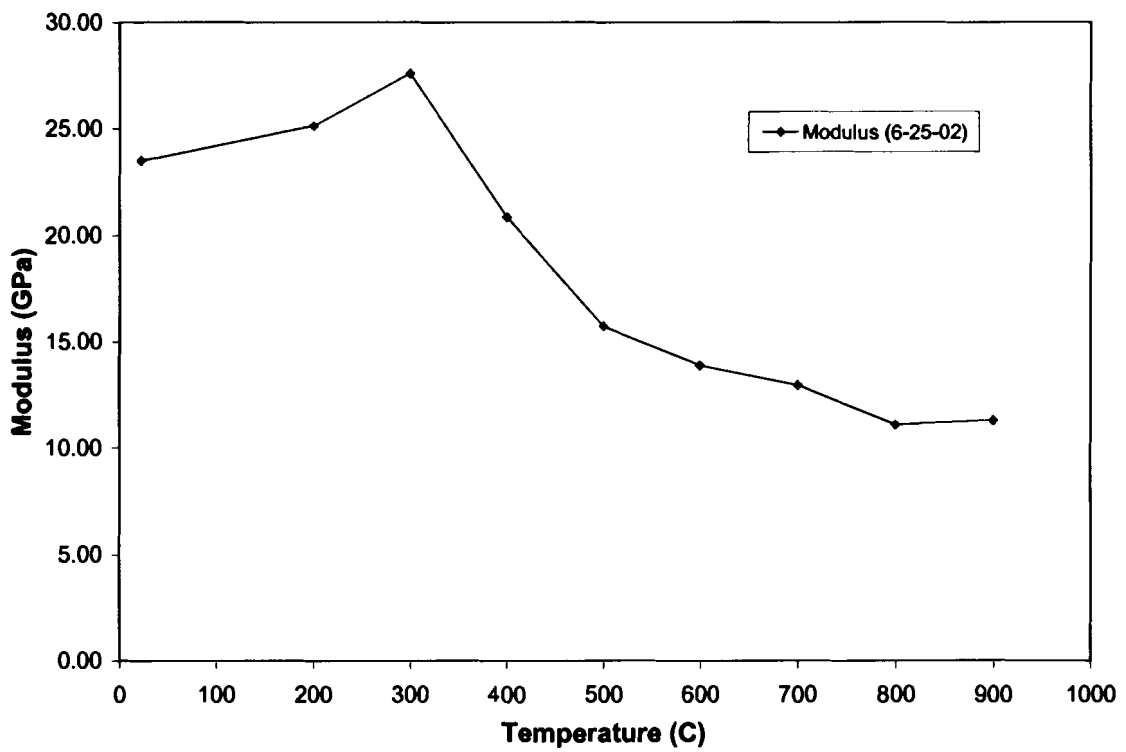
Figure 5.8. Modulus change from the commercial C/C sample.

80

5.2.3 Oxidation

The change in modulus of three C/C samples was monitored during controlled oxidation. Measurements were recorded after medical air was flowed at a rate of 0.8scfm through the seal furnace at 700°C. The air was flowed for 10 minutes and then switched to the inert atmosphere. In the inert atmosphere the in-situ measurements were then performed. The sample was then weighed at every 20-minute increment until a total of 120 minutes of air exposure occurred. The oxidation of the C/C samples from FMI is illustrated in figure 5.9 by the weight loss. The resulting modulus change of the C/C sample periodically removed from the furnace is compared to a sample that was not weighed at every 20-minute increment also in figure 5.9. The left hand image of figure 5.10 shows the C/C sample before oxidation and the right hand image shows the sample after exposed to 120 minutes of air at 700°C. The modulus change from oxidation of the commercial C/C sample is shown in figure 5.11. The data for the remaining C/C samples are shown in the appendix.
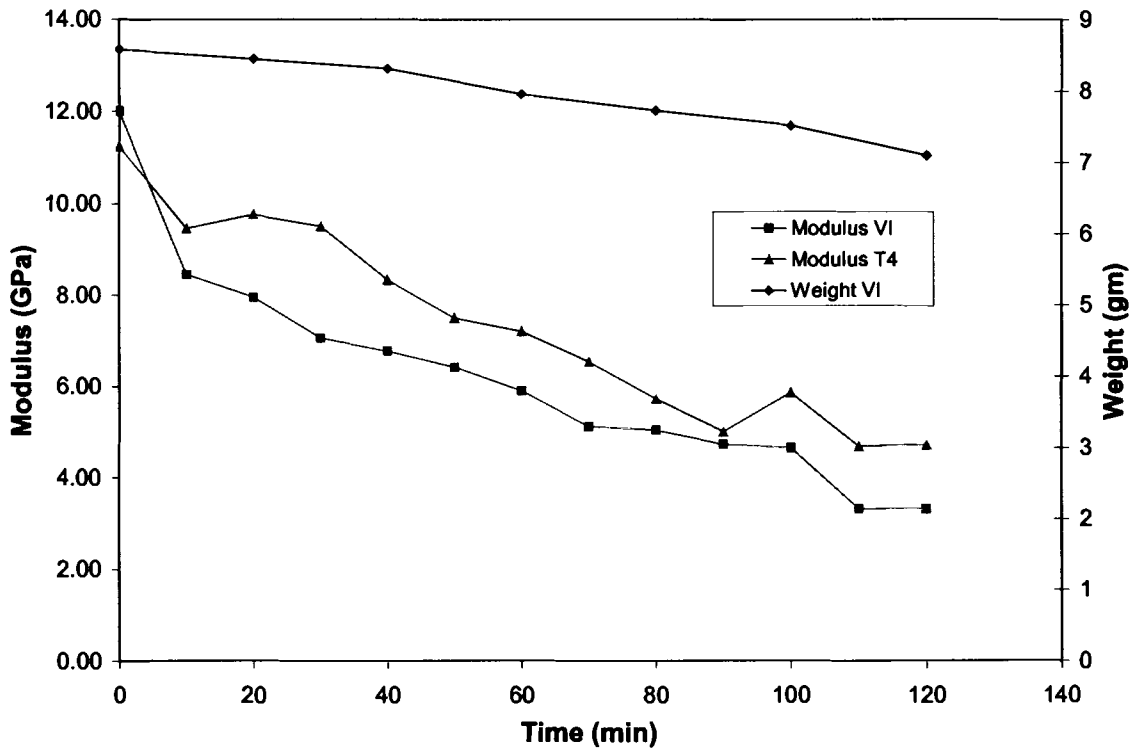
Figure 5.9. Modulus and weight change during oxidation of two C/C samples at 700°C.
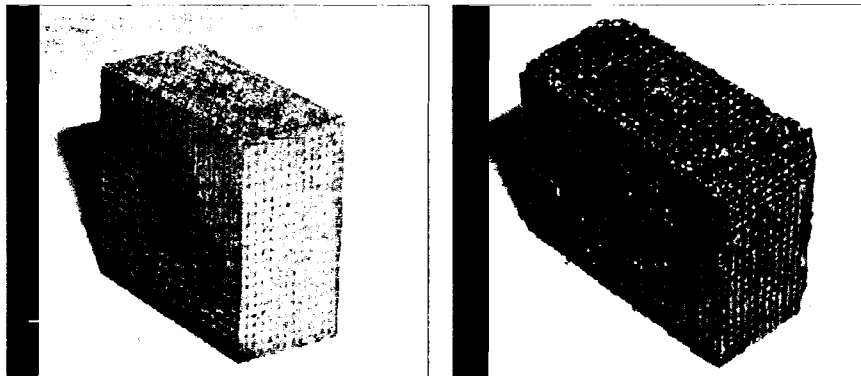
Figure 5.10. C/C composite sample from FMI before (left) and after oxidation.
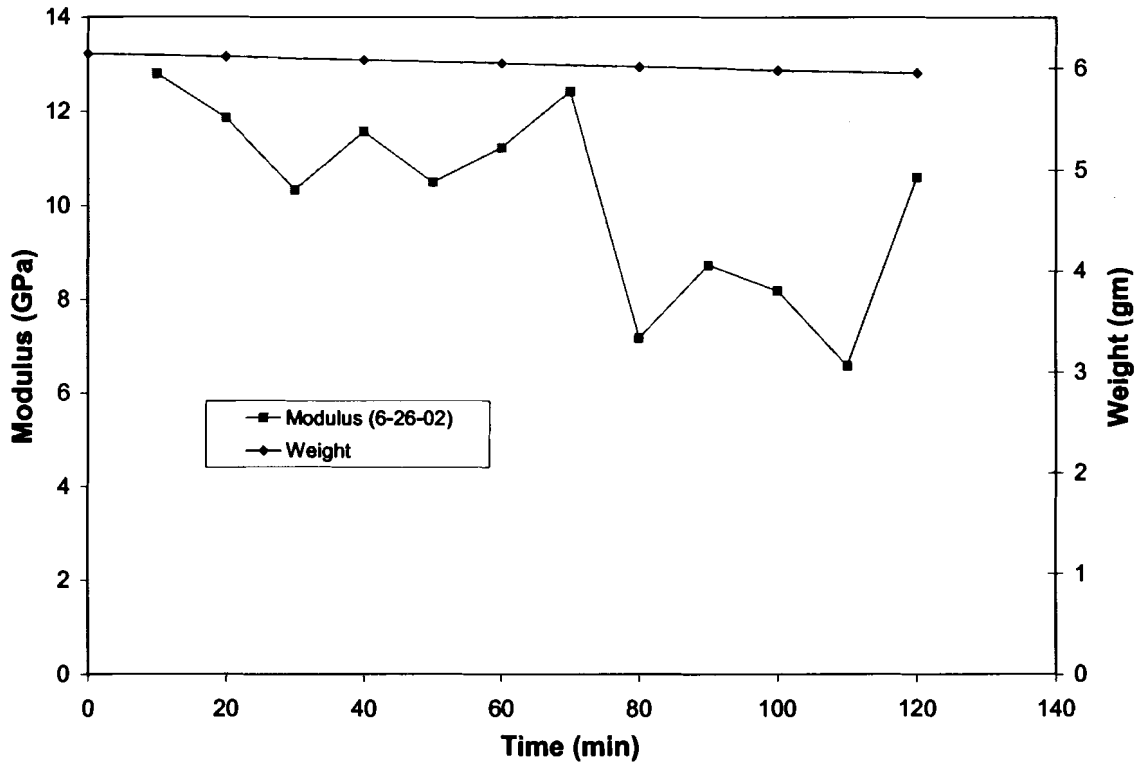
Figure 5.11. Modulus change during oxidation of the commercial carbon composite
sample at 700°C.

5.3   Discussion of Results

5.3.1   Stainless Steel

The change in modulus of the stainless steel samples was calculated and
compared to reference book values to prove that the waveguide technique works. The
modulus change for the two stainless steel samples is shown in figure 5.3 along with the
reference values. The initial room temperature modulus values were calculated by cross-
correlating a signal through the steel sample with a signal through an aluminum reference
sample. The cross-correlation between the two signals gave a time delay that was then
added to the arrival time of the signal through the aluminum. This gave the actual arrival
time through the steel sample at room temperature that was used to calculate the initial
room temperature modulus. The slope of the monitored samples is different than the

slope of the reference values by about 15%. Due to the close similarity between the two, it can be concluded that the proposed technique can qualitatively measure the change in modulus of a sample with change in temperature.

5.3.2 Carbon - Carbon

The change in modulus with change in temperature of C/C composite samples is monitored by measuring the change in the arrival time of a signal with change in temperature. The change in signal arrival time is obtained from the four acquired signals shown in figure 5.4. An increase in the arrival time through a sample is a result of a slower wave velocity through the sample. A slower wave velocity can be the result of a decreasing modulus and/or an increasing density. All of the C/C composites experienced a drastic reduction in modulus until 400°C, but then remained consistent up to 1100°C. The coefficient of thermal expansion for carbon was found to be much less than 10^{-6} per °C for the temperature range experienced in this work. It is assumed that the density of the material will not change with temperature because the expansion coefficient is negligible. It is suggested that the modulus changed and not the density of the material due to no weight gain or loss and the dimensions of the sample remained the same. The results show that the C/C composites retain their elastic properties at temperatures above 400°C in an inert atmosphere.

The repeatability of the testing method described in this work was also studied. Figure 5.5 shows the results of four separate tests performed on the same C/C composite sample while in an inert atmosphere. The general trend of each test shows an initial drop in the modulus until 400°C and then remained consistent up to 1100°C. The weight of

the sample was recorded and found to be the same before and after the testing using the same scale accurate to 0.01 grams. Weighing the sample before and after ensured that no oxidation had occurred during testing. Testing the same C/C sample several times can have the same effect on the sample as heat-treating. Depending on the heat treatment of C/C composites, the reaction of the modulus with temperature change will vary [Savage, 1993]. This would help explain the variation between the four test results of the same sample. Also, variation in the testing setup, such as alumina fiber build-up on the free-end of the waveguides, would also contribute to the variation in results by interfering with the through-transmission signals. The free-end of the waveguides were cleaned between each test, but could have experienced the alumina build up during intermittent contact with the sample.

The change in modulus of four different C/C composites samples from FMI, shown in figure 5.6 and the commercial C/C sample, shown in figure 5.7, was also monitored in an inert atmosphere. Figure 5.6 shows the sample-to-sample variation of modulus change with temperature change. These results also show the initial decrease in modulus up to 400°C and then a consistent modulus up to 1100°C. However, the commercial C/C sample had an initial increase in modulus up to 300°C and then decreased until 900°C, shown in figure 5.7. The difference in modulus change between the two samples could be explained by the difference in manufacturing techniques. The densities of the FMI samples were 27% larger than the commercial samples. The different densities will yield a different initial modulus value for C/C samples of the same geometry.

The modulus change along with the change in weight of two C/C composites shown in figure 5.8 was monitored during controlled oxidation. The weight was monitored to measure the degree of oxidation. The modulus initially decreased drastically within the first 20 minutes of airflow, followed by a steady decrease for the remainder of the test. The left hand image in figure 5.10 shows the C/C sample before oxidation and the right hand image shows the sample after oxidation. The surface of the sample appears to have lost the primary matrix of the material exposing the carbon fiber weave. As a result, the modulus decreased by almost 77% as the specimen experienced a 17.25% weight loss. This shows that the C/C composite samples lose a significant amount of their modulus during 120 minutes of oxidation.

The modulus of other C/C composites obtained from the same manufacturer did not change from room temperature up to 800°C. These results were obtained from compression testing using extensometers while in an uncontrolled oxidizing environment [Walls, 2002]. These C/C specimens had a smaller volume on average compared to the specimens in this work by 55%. However, the specimens experienced a 45% weight loss while in the uncontrolled oxidizing environment at 600°C after 120 minutes. The larger specimens in this work only experienced on average a 17% weight loss after 120 minutes of exposure to a controlled airflow. The difference between these results could be explained by the qualitative measurements performed on the specimens as well as the difference in specimen size and testing procedures.

The modulus change during oxidation of the commercial C/C sample is shown in figure 5.9. The signals through this sample were much more complex compared to the

signals through the FMI samples, mainly due to the rough surfaces of the samples. The amplitudes of the received signals were smaller as was the signal to noise ratio compared to the FMI samples. This could account for the erratic change in modulus yet almost no change in weight during the oxidation test. If no weight loss were experienced during the oxidation process, it would be expected that no decrease in modulus would occur.

The time delay through the quartz waveguides was calculated using the pulse-echo signals that were recorded during a temperature test while in an inert atmosphere as well as the during an oxidation test. Calculating the time delay through the quartz shows how the waveguides experience their own material changes with temperature. The material changes within the waveguides may contribute to any inaccuracies during signal measurements. Figure 5.12 shows the time delay within the quartz waveguides during temperature testing in an inert atmosphere. This data is compared to the time delay through the quartz during an oxidation test at 700°C, also on the same graph. The time delay through the quartz during the oxidation test remains consistent for the duration of the test while at 700°C suggesting that the material is not changing with time. However, the time delay through the waveguides changes with increase in temperature suggesting that the modulus of the material is also increasing. These results are consistent with data that was referenced [Fukuhara, 1999]. Figure 5.13 shows the time delay within the quartz comparing measured pulse-echo signal time delays with the time delays measured from transmission signals through a C/C sample.
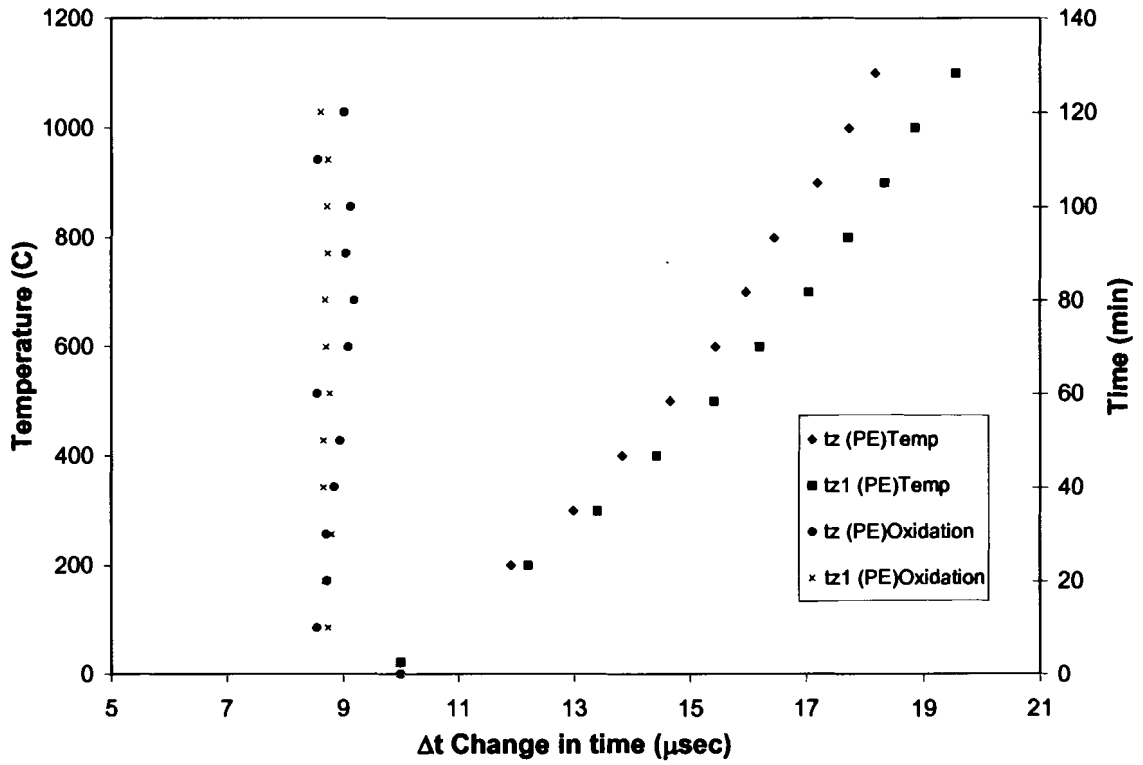
Figure 5.12. Time delay changes in quartz during temperature changes and oxidation.
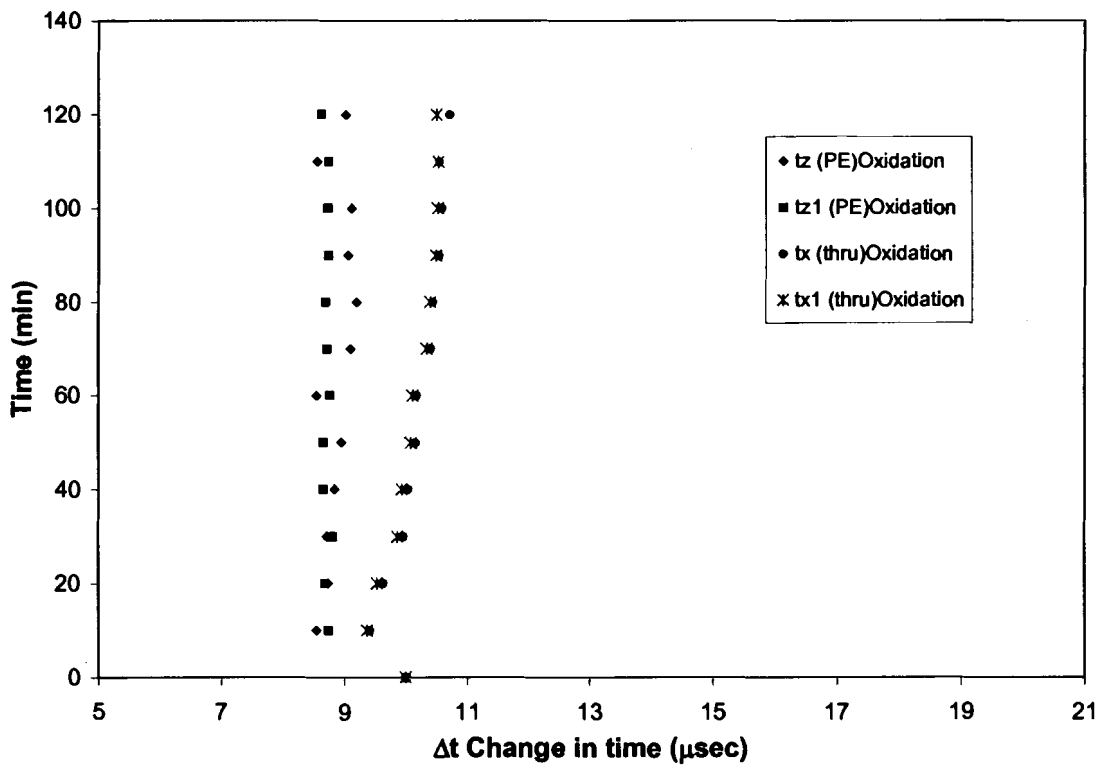
Figure 5.13. Time delay changes through quartz and sample during oxidation.

Chapter 6

CONCLUSIONS

6.1   Summary

A method was developed to measure the ultrasonic wave velocity of materials at temperatures up to 1100°C in a controlled oxidizing atmosphere. A high temperature apparatus was designed to create a controlled atmosphere that is capable of testing a 10mm thick sample in either an inert or in an oxidizing environment. The method developed makes use of solid cylindrical waveguides to monitor the change of elastic properties and the oxidation reaction of carbon-carbon composites with change in temperature.

The apparatus was designed to allow ultrasonic measurements to be performed on a sample while in a controlled oxidizing atmosphere with varying temperatures. The apparatus encloses the ultrasonic transducers within the atmosphere and outside of the furnace. Waveguides are used to transmit the signal through a sample located inside the controlled atmosphere furnace. Extensive signal processing was performed using MatLab to obtain quantitative information from the experimental apparatus. The change in Young's modulus of a C/C composite was monitored with change in temperature in an inert atmosphere and during controlled oxidation at 700°C for 120 minutes.

Verification of the method was based on testing using stainless steel samples with known change in modulus and by repeatability testing using carbon composites. Experiments were performed using two type 316L stainless steel samples. The modulus change with temperature of the stainless steel samples calculated using this method was

within 15% of the modulus change of the handbook values. The resulting similarities between the calculated data and the reference data suggest that this technique can qualitatively measure the change in modulus of a sample.

There are many factors that contribute to the calculated error within the experiments. A large portion of the error is generated from the significant change in modulus with change in temperature of the waveguides. The modulus of fused quartz slightly increases with temperature almost 7% from room to 1100°C [Fukuhara, 1999]. An increase in modulus will have an affect on wave velocity through the waveguides and consequently will affect the wave velocity through the sample. Although the effects of the waveguides are removed using four signals and equation 4.3, accurately extracting the small time change through the sample from the larger time change through the waveguides is difficult. For this reason, an alternative waveguide material is suggested.

An ideal material for waveguides would be diamond. Diamond has a large modulus that remains relatively constant within the temperature range experienced in this work. Also, the loss coefficient of diamond is 0.0002, compared to the fused quartz value of 0.002, [Granta, 2000]. The overall extremely high cost of diamond did not make it a possible choice for waveguide material in this work. Sapphire is recommended for waveguide material due to a consistent modulus value at higher temperatures along with a low loss coefficient that is equal to quartz and relatively low cost (1100$/lb) compared to diamond (100000$/lb).

Another factor that may contribute to the calculated error in the experiments would be the sampling rate. The sampling rate in this work was 250 mega samples per second. This sampling rate is capable of recording a 4ηsec time change within a signal. This time delay is equivalent to a 0.17124Gpa modulus change within a sample. A time change smaller than 4ηsec would not be recorded. The average modulus change in the stainless steel was 20GPa per degree Celsius and in the C/C specimens was 2GPa per degree Celsius. Therefore, the accuracy of this technique is limited by factors other than the sampling rate used to record the data. Testing a material that has a modulus change much smaller than the changes in this work would require a higher sampling rate in order to obtain or increase the accuracy of the measurements.

Testing the same C/C composite sample four times was another method used in this work to verify the accuracy of this method. However, the results show significant error between the four tests of the same C/C specimen. The sample from each test experienced on average a 78% modulus decrease plus or minus 8% when heated from room temperature up to 1100°C while in an inert atmosphere.

The spectrum of the input signal (figure 6.1) is compared to the spectrum of a received through transmission signal (figure 6.2) to show the differences between the two. The spectrum of the input signal was acquired using a small reference sample made from aluminum and the spectrum from the received through transmission was acquired from a signal through the entire setup containing a C/C specimen. The spectrum of the transmitted signal shows significantly less energy at high frequencies than the input spectrum, which reduces the time resolution of the cross-correlation. To increase the

accuracy, received signals that are shorter in time with greater frequency content is required. Ideally, the received output spectrum should resemble the input spectrum.

Response of Transducers
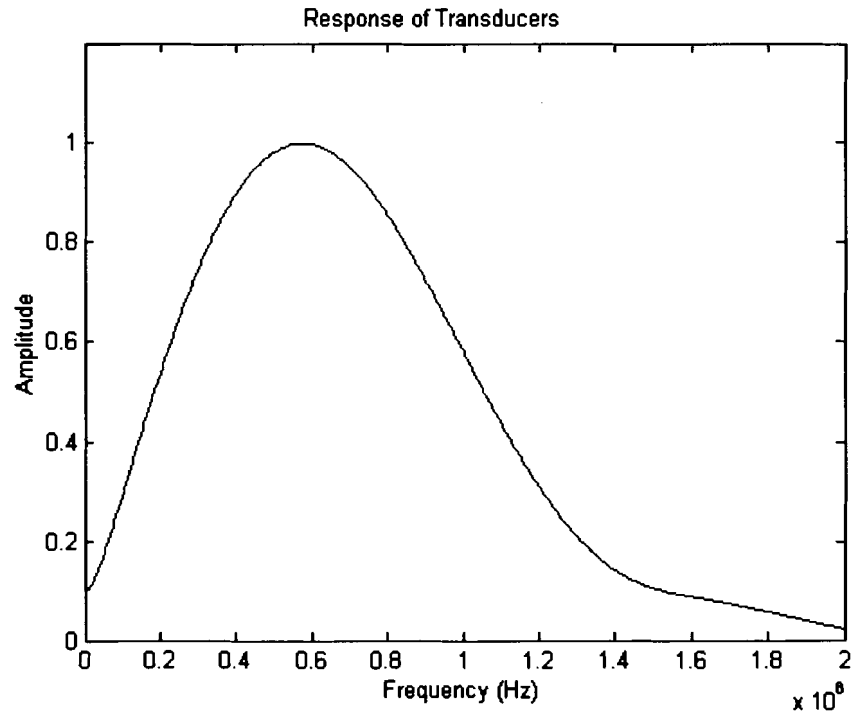
Figure 6.1. Spectrum of the input signal.

Output Spectrum
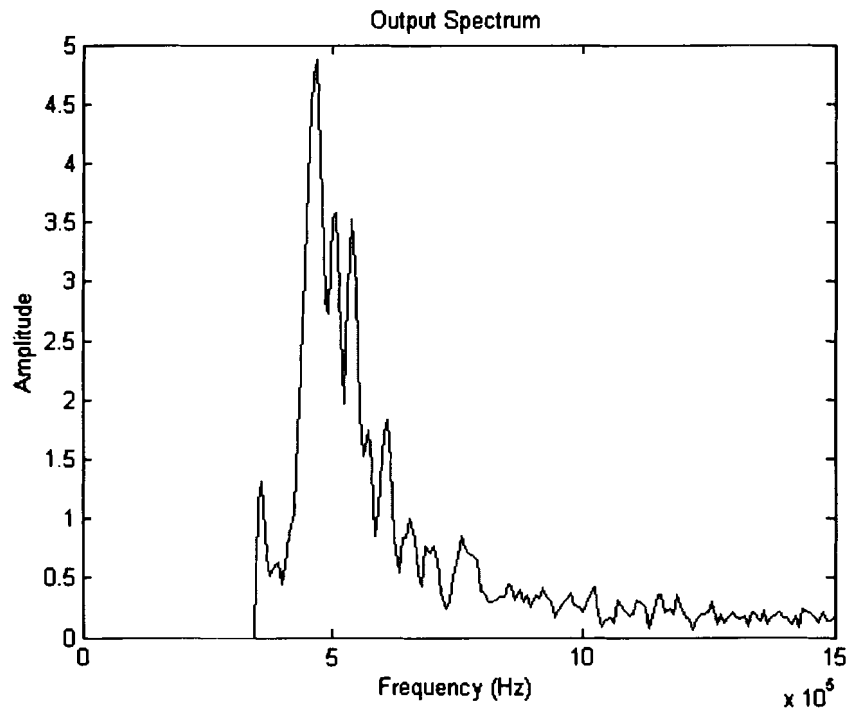
Figure 6.2. Spectrum of received through transmission signal.

Tests were also performed on four different C/C composite samples in an inert atmosphere to monitor the change in modulus with change in temperature. The general change in modulus of the C/C composites was found to initially decrease from room temperature up to 400°C and then remained relatively constant up to 1100°C. The overall modulus decrease was found to fall within the error range generated by the repeatability study. The initial decrease might suggest that the material is undergoing heat-treating. The consistency of the modulus change after the initial decrease suggests that the carbon composites can retain the modulus at elevated temperatures while in an inert atmosphere. The changes in the modulus at temperatures from room to 1100°C of all the specimens tested were well within the 8% range.

Oxidation tests were also performed on C/C composites so that the change in modulus could be compared to weight loss studies. The change in modulus of the C/C samples was found to steadily decrease to almost 30% while only experiencing a 17.25% weight loss after exposed to a controlled oxidizing environment at 700°C. The large decrease in modulus even with modest weight loss might suggest that the matrix of the material is disbanding. The bond between the matrix and the fibers might be weakened thus decreasing the modulus. Therefore the weight loss is unlikely to show the sufficient material sensitivity to oxidation. Alternatively, the modulus is better to weight studies when categorizing the oxidation of carbon composites.

6.2   Future Work and Recommendations

The results of this work and future work using this technique should be compared to other C/C composite results that are obtained from high temperature mechanical testing. A high temperature compression-testing machine has recently become available that has the ability to test C/C specimens in either an inert or in a controlled oxidizing environment. The comparison of the results between the two testing procedures may aid in the understanding of the oxidation reaction and the modulus change of C/C composites with change in temperature.

Further coupling studies should be conducted with the described setup to decrease the percent of error generated from the modulus calculations from the repeatability study. Dry coupling was used for these experiments to avoid contamination of the samples during testing. A gold leaf could be used as coupling between the waveguides and sample but further knowledge is required to understand the effects that the gold leaf may have on the modulus calculations. Other possible couplings should be researched and tested to help improve the waveguide-to-sample contact.

Future experiments should be performed on multiple C/C composites to acquire a better understanding of the oxidation reaction and the effects on modulus. The oxidation reaction of C/C composites increases rapidly at higher temperatures; therefore higher temperature oxidation studies are recommended. Different components of the existing furnace could be used to achieve higher temperatures than those experienced in this work.

The modulus information acquired from the recorded signals is dependent on the accuracy of the signal processing. Each of the four windowed signals (X, X1, Z, and Z1) must be cross-correlated individually with the signals from the previous temperature. It took the cross-correlation program, written in MatLab, approximately two and a half minutes to run for one signal that contained 15000 data points. The development of automated signal processing would be highly beneficial in future studies. Software that could record and process the signals without additional programming would greatly decrease the amount of time needed to generate the material property changes of the samples. Most importantly, techniques must be developed to reduce the length and complexity of the received signal. A signal that has compact support in the time domain is likely to significantly improve the accuracy of the technique presented.

BIBLIOGRAPHY

Ashby, M.F., <u>Materials Selection in Mechanical Design</u>, 2nd edition, 1999, Butterworth-Heinemann

Bernstein, I. M., & Peckner, D., <u>Handbook of Stainless Steels</u>, 1977, McGraw Hill Inc.

Cracknell, A.P., <u>Ultrasonics</u>, 1980, Wykeham Publication

Demarest, H., <u>Journal of Acoustic Society of America</u>, vol 49, 1971

Dual, J., *Dynamic Methods for Measuring the Elastic Properties of Solids*, <u>Handbook of Elastic Properties of Solids, Liquids and Gases</u>, vol. I, 2001

Fukuhara, M., & Sampei, A., *Effects on high-temperature elastic properties on α-/β-quartz phase transition of fused quartz*, <u>Journal of Materials Science Letters</u>, vol. 18, 1999, Kluwer Academic Publishers

Gauthier, M.M., *Carbon-Carbon Composites*, <u>Engineering Materials</u>, Handbook Desk Edition, 1995

Granta Design Limited, *Cambridge Engineering Selector III*, Cambridge, United Kingdom, 2000

Huger, M., Fargeot, D., & Gault, C., *High Temperature Measurement of Ultrasonic Wave Velocity in Refractory Materials*, <u>15th European Conference on Thermophysical Properties</u>, 1999

Kimura, S., Yasuda, E., & Tanabe, Y., *Microstructure and Fracture Behavior of Unidirectionally Reinforced Carbon Fiber/Carbon Composites*, <u>Progress in Science and Engineering of Composites International Conference</u>, 1982

Kline, Ronald A., *Properties of Solids*, <u>Handbook of Elastic Properties of Solids, Liquids and Gases</u>, vol. II, 2001

Ohno, I., <u>Journal of Physical Earth</u>, vol 24, 1976

Peterson, M.L., Bunker, S., & Puckett, A., *Evaluation of Dynamic Properties of Composites in an Oxidizing Environment*, <u>Quantitative Nondestructive Evaluation Technical Conference</u>, vol. 21, 2002

Peterson, M.L., *A Method for Increased Accuracy of the Measurement of Relative Phase Velocity*, <u>Ultrasonics</u>, vol. 35, 1996

Peterson, M.L., *A Signal Processing Technique for Measurement of Multimode Waveguide Signals: An Application to Monitoring Reaction Bonding in Silicon Nitride*, Nondestructive Evaluation, 1994, Springer-Verlag New York Inc.

Rozak, G.A., Mechanical Behavior of Carbon-Carbon Composites, NASA Contractor Report # 174767, 1984

Savage, G., Carbon-Carbon Composites, 1993, Chapman and Hall

Sun, M., *Optimal Recovery of Elastic Properties for a General Anisotropic Material through Ultrasonic Measurements*, Masters Thesis, 2002, The University of Maine

Walls, J., *High Temperature Compression Testing of an Advanced Carbon-Carbon Composite in an Oxidizing Atmosphere*, Masters Thesis, 2002, The University of Maine

APPENDIX A – Experimental Procedures

Inert Atmosphere

1. Weigh and measure sample.

2. Place sample in furnace tube.

3. Slide alumina guide slowly, such that it pushes the sample until the whole alumina guide is in the furnace tube.

4. Fasten the three bolts, around the sealing faceplate, to seal the setup.

5. Make sure the atmosphere supply line valve is in correct position.

6. Evacuate using vacuum pump then close vacuum regulator.

7. Fill with inert gas until flowmeter does not register.

8. Open vacuum regulator and evacuate again, then close regulator.

9. Fill with inert gas again and leave supply line open.

10. Turn on water to cooling system and check for leaks.

11. Acquire six signals at room temperature.

12. Acquire signals at every $100^\circ C$ increment.

13. Allow furnace to cool gradually before removing the sample with a shop vacuum and hose.

14. Weigh sample and record any observations.

Controlled Oxidizing Environment

1. Repeat steps 1 – 10 of the inert atmosphere procedures.

2. Gradually heat furnace to desired oxidation temperature.

3. Acquire six signals at time = 0.

4. Open vacuum pump regulator and turn vacuum pump on.

5.   Switch gas supply line to a compressed medical air tank.

6.   Record flowmeter and let the air flow for 10 minutes.

7.   Switch gas supply line back to the inert gas leaving the vacuum pump running for an additional minute.

8.   Close vacuum regulator and shut off the vacuum pump.

9.   Record six signals.

10. Repeat steps 4 – 9 until either no signal can be acquired or until desired amount of airflow has been reached.

11. Allow furnace to gradually cool before removing sample.

12. Weigh sample and record any observations.

APPENDIX B – Signal Processing MatLab Programs

Cross-Correlation Preparation (Through Transmission) – "XprepThru"

```
clear W2
ref=textread('D:\Shaun\Thesis\Carbon\CCIII(6-5-02)\500\FiveA.dat');

ref(:,2) = ref(:,2)-ref(10,2);    %Lines up verticle to zero
ref(:,2) = ref(:,2)./(1000);      %Divides by 1000 because of Pre-Amp set on 60db

A = 1700;       %Number of zeroes at beginning of signal
B = 400;        %1/2 of the Hanning Window used judged by looking at plot of signal
C = 5700;       %Data point to end window
D = 14995;      %Total number of Data points recorded

W1 = hanning(2*B);
W2(1:A)=0;
W2((A+1):(A+B))=W1(1:B);
W2((A+1+B):(C-B))=1;
W2((C-B+1):C) = W1((B+1):(2*B));
W2((C+1):D) = 0;

newref(:,2)=ref(:,2).*W2';      %Windows Amplitude column in ref
newref(:,1)=ref(:,1);           %Copies over time column

y=[newref(:,1)';newref(:,2)'];

fid=fopen('D:\Shaun\Thesis\Carbon\CCIII(6-5-02)\XPrepOut\500\FiveA.dat','w');
fprintf(fid,'%8.4e %8.4e\n',y);
status=fclose(fid);

subplot(3,1,1);
plot(ref(:,2));
title('Original Signal');
xlabel('Time(s)');
ylabel('Voltage(v)');

subplot(3,1,2);
plot(W2);
title('Hanning Window');

subplot(3,1,3);
plot(newref(:,2));
title('Windowed Signal');
xlabel('Time(s)');
ylabel('Voltage(v)');
```

Cross-Correlation Preparation (Pulse-Echo Transmission) – "XprepPE"

```
clear W2
ref=textread('D:\Shaun\Thesis\Carbon\CCIII(6-5-02)\ 500\FiveF.dat');

ref(:,2) = ref(:,2)-ref(10,2); %Lines up verticle to zero
ref(:,2) = ref(:,2)./(10^2.5); %Divides by 10^2.5 because of Pulser Pre - Amp set on 50db

A = 3100;        %Number of zeroes at beginning of signal
B = 200;         %1/2 of the Hanning Window used judged by looking at plot of signal
C = 6700;        %Data point to end window
D = 14995;       %Total number of Data points recorded

W1 = hanning(2*B);
W2(1:A)=0;
W2((A+1):(A+B))=W1(1:B);
W2((A+1+B):(C-B))=1;
W2((C-B+1):C) = W1((B+1):(2*B));
W2((C+1):D) = 0;

newref(:,2)=ref(:,2).*W2';    %Windows Amplitude column in ref
newref(:,1)=ref(:,1);         %Copies over time column

y=[newref(:,1)';newref(:,2)'];

fid=fopen('D:\Shaun\Thesis\Carbon\ CCIII(6-5-02)\XPrepOut\500\FiveF.dat','w');
fprintf(fid,'%8.4e %8.4e\n',y);
status=fclose(fid);

subplot(2,1,1);               %Plots Hanning window over original
plotyy(ref(:,1),ref(:,2),ref(:,1),W2);
title('Original Signal');
xlabel('Time(s)');

subplot(2,1,2);               %Plots new signal
plot(newref(:,2));
title('Windowed Signal');
xlabel('Time(s)');
ylabel('Voltage(v)');
```

Program to Graph New Signals– "NewsigCheck"

```
%This program lets you look at any graphs you specify.
clear;

REF1=textread('D:\Shaun\Thesis\Carbon\ CCIII(6-5-
02)\XPrepOut\Room\RoomA.DAT');
REF2=textread('D:\Shaun\Thesis\Carbon\CCIII(6-5-02)\XPrepOut\200\TWOC.DAT');
REF3=textread('D:\Shaun\Thesis\Carbon\CCIII(6-5-02)\XPrepOut\300\THREEC.DAT');
REF4=textread('D:\Shaun\Thesis\Carbon\CCIII(6-5-02)\XPrepOut\400\FOURC.DAT');
REF5=textread('D:\Shaun\Thesis\Carbon\CCIII(6-5-02)\XPrepOut\500\FIVEC.DAT');
REF6=textread('D:\Shaun\Thesis\Carbon\CCIII(6-5-02)\XPrepOut\600\SIXC.DAT');
REF7=textread('D:\Shaun\Thesis\Carbon\CCIII(6-5-02)\XPrepOut\700\SEVENC.DAT');
REF8=textread('D:\Shaun\Thesis\Carbon\CCIII(6-5-02)\XPrepOut\800\EIGHTC.DAT');
REF9=textread('D:\Shaun\Thesis\Carbon\CCIII(6-5-02)\XPrepOut\900\NINEC.DAT');
REF10=textread('D:\Shaun\Thesis\Carbon\CCIII(6-5-02)\XPrepOut\1000\TENC.DAT');
REF11=textread('D:\Shaun\Thesis\Carbon\CCIII(6-5-02)\XPrepOut\1100\ElevenC.dat');

subplot(11,1,1);
plot(REF1(:,2));
%axis([0 15000 -.00001 .00001]);
title('Thru Transmission Signal of CCIII(6-5-02) (A)');
ylabel(Room);

subplot(11,1,2);
plot(REF2(:,2));
%axis([0 15000 -.00001 .00001]);
ylabel('200');

subplot(11,1,3);
plot(REF3(:,2));
%axis([0 15000 -.00001 .00001]);
ylabel('300');

subplot(11,1,4);
plot(REF4(:,2));
%axis([0 15000 -.00001 .00001]);
ylabel('400');

subplot(11,1,5);
plot(REF5(:,2));
%axis([0 15000 -.00001 .00001]);
ylabel('500');

subplot(11,1,6);
plot(REF6(:,2));
```

```
%axis([0 15000 -.00001 .00001]);
ylabel('600');

subplot(11,1,7);
plot(REF7(:,2));
%axis([0 15000 -.00001 .00001]);
ylabel('700');

subplot(11,1,8);
plot(REF8(:,2));
%axis([0 15000 -.00001 .00001]);
ylabel('800');

subplot(11,1,9);
plot(REF9(:,2));
%axis([0 15000 -.00001 .00001]);
ylabel('900');

subplot(11,1,10);
plot(REF10(:,2));
%axis([0 15000 -.00001 .00001]);
ylabel('1000');

subplot(11,1,11);
plot(REF11(:,2));
%axis([0 15000 -.00001 .00001]);
ylabel('1100');
```

Cross-Correlation Program – "XcorrSingle"

```
clear;

Reference=textread('D:\Shaun\Thesis\Carbon\CCIII(6-5-02)\XPrepOut\500\FiveA.dat');
ref=Reference(:,2);

input=textread('D:\Shaun\Thesis\Carbon\CCIII(6-5-02)\XPrepOut\600\SixA.dat');
input1=input(:,2);

n=length(ref);

timearray=Reference(:,1);
interval=timearray(2)-timearray(1);

for m=2:n
    shift_y1=[input1(m:n);zeros(m-1,1)];
    cro1(m)=dot(ref,shift_y1);
```

```
    shift_y2=[ref(m:n);zeros(m-1,1)];
    cro2(m)=dot(input1,shift_y2);
end
cro1(1)=dot(ref,input1);
cro2(1)=dot(input1, ref);

[y1,index1]=max(cro1);
[y2,index2]=max(cro2);

if y1>y2
    y=y1;
    index_y=-index1;
    cro=cro1;
else
    y=y2;
    index_y=index2;
    cro=cro2;
end

delay=interval*(abs(index_y)-1)        %Displays time delay between signals
index_y                                 %Displays shift in signal

%If a negative "index y" then input signal is slower then reference signal
%If a positive "index y" then input signal is faster then reference signal
```

APPENDIX C – Samples of Non-Oxidized & Oxidized C/C Signals
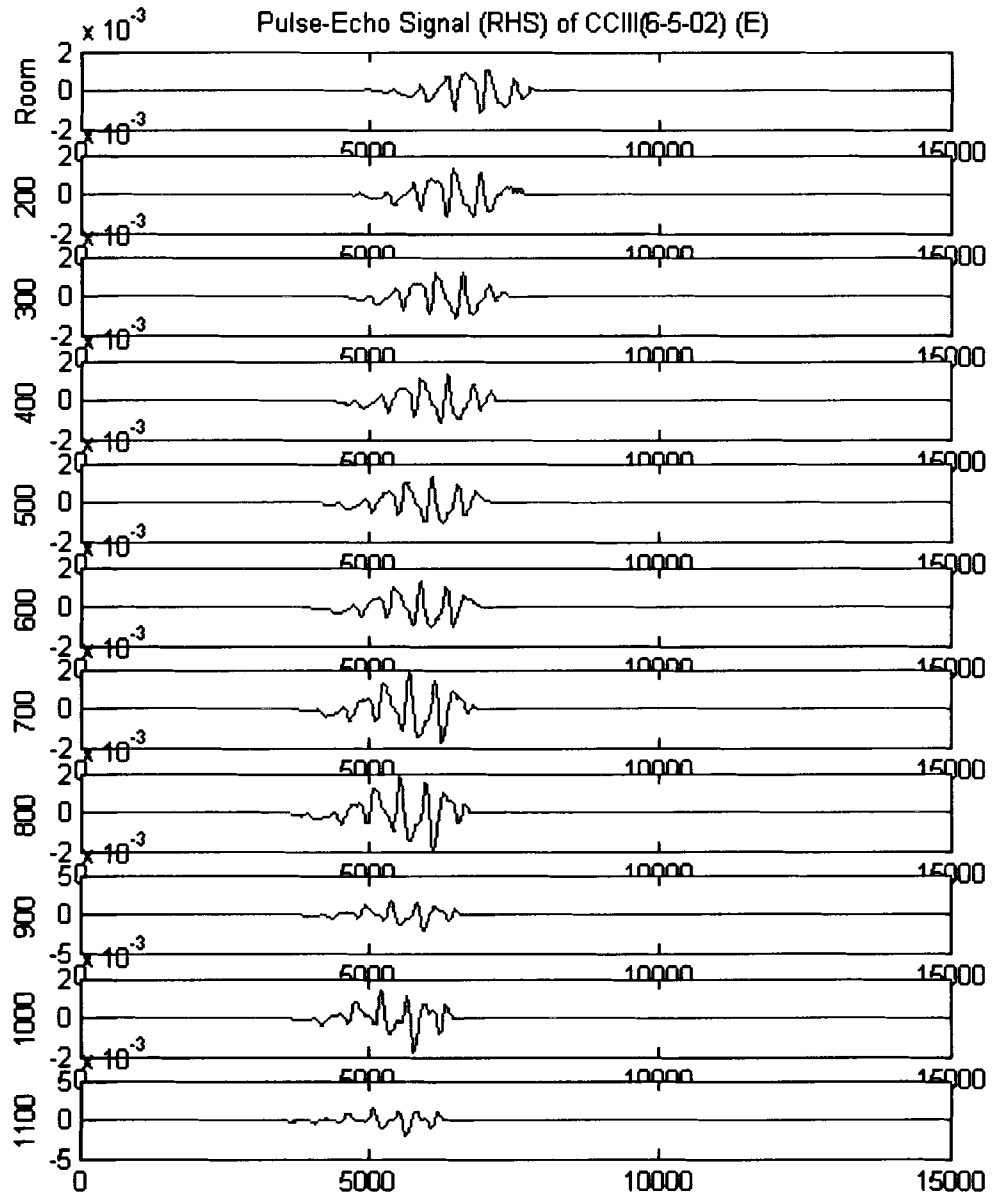
Figure C.1.   Sample of pulse-echo signals from free end of right hand waveguide shown with a temperature range of room to 1100°C.
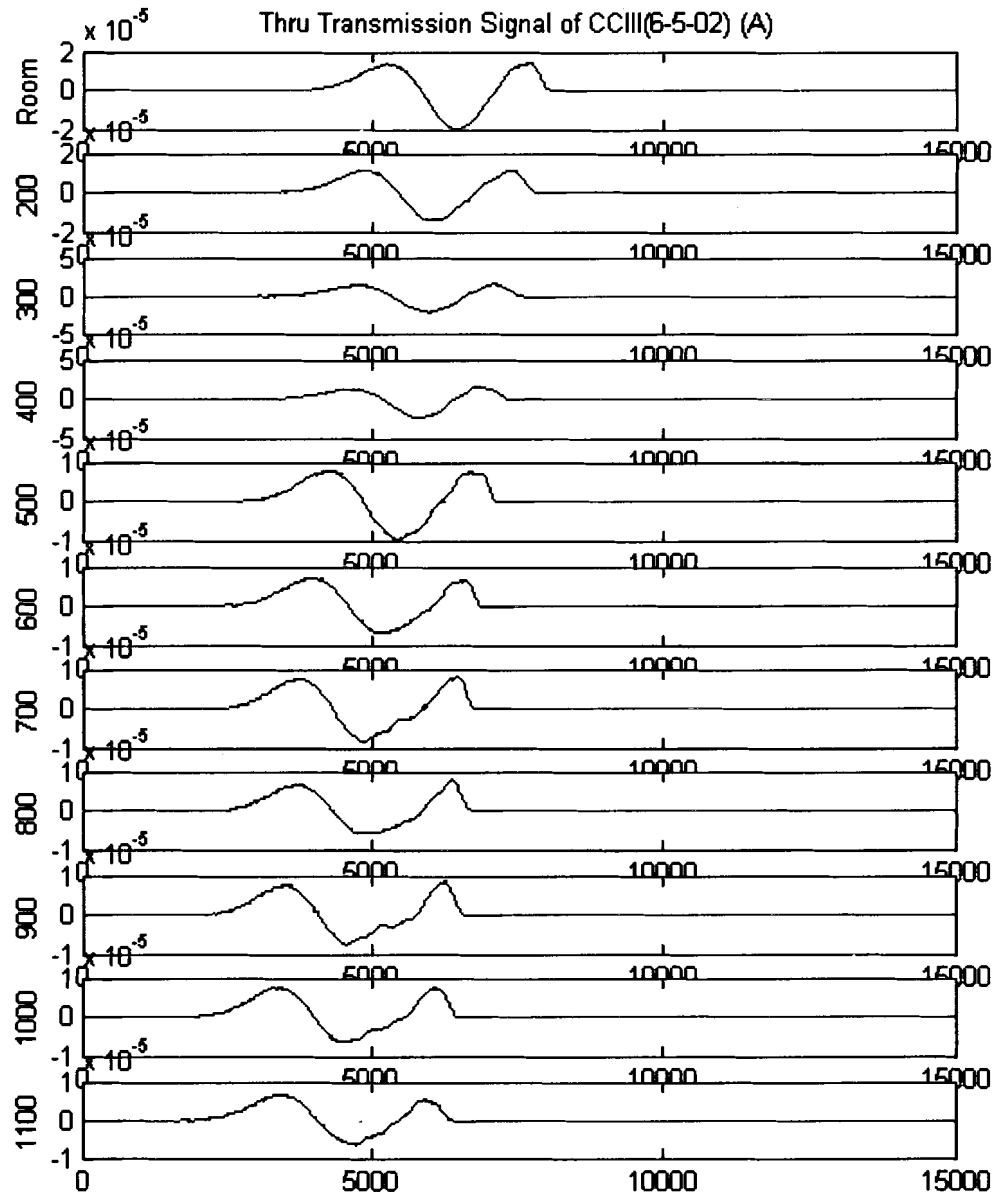
Figure C.2.   Sample of through-transmission signals through a C/C composite sample
in an inert atmosphere shown with a temperature range of room to 1100°C.
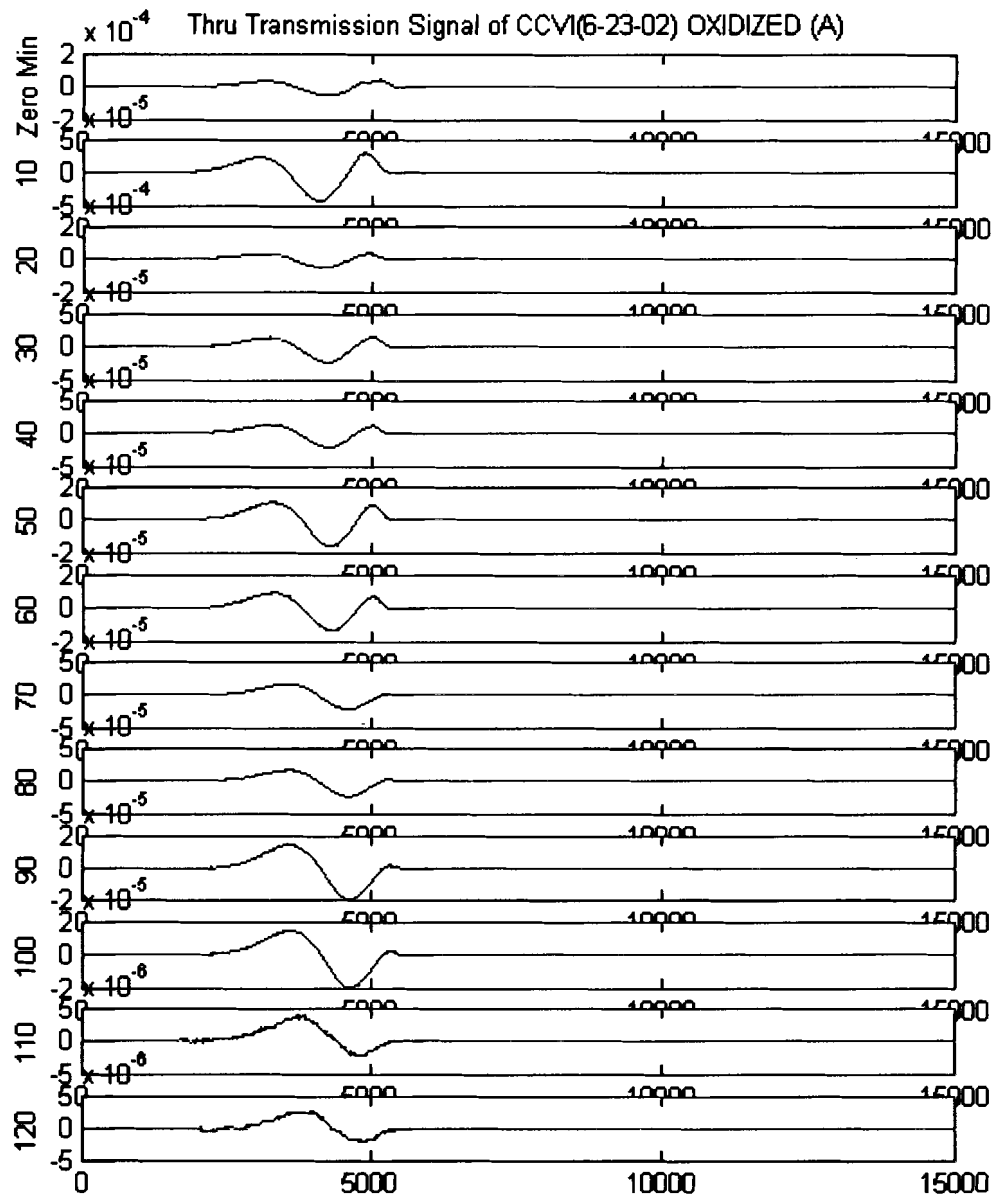
Figure C.3.   Sample of through-transmission signals through a C/C composite sample during oxidation at 700°C.

APPENDIX D – Sample Data Sheets

Temp	$t_{x\,(thru)}$	Total t_x	$t_{x1\,(thru)}$	Total t_{x1}	$t_{z\,(PE)}$	Total t_z	$t_{z1\,(PE)}$	Total t_{z1}	Δt_{sample}	Time$_{sample}$
C	μsec	μsec	μsec	μsec	μsec	μsec	μsec	μsec	μsec	μsec
22	0	10	0	10	0	10	0	10	0	0.0000
200	2.076	7.924	2.028	7.972	1.912	8.088	2.208	7.792	-0.008	0.0080
300	0.356	7.568	0.404	7.568	1.076	7.012	1.192	6.6	-0.754	0.7620
400	0.5	7.068	0.456	7.112	0.848	6.164	1.024	5.576	-0.458	1.2200
500	0.524	6.544	0.468	6.644	0.828	5.336	0.992	4.584	-0.414	1.6340
600	0.948	5.596	1.092	5.552	0.784	4.552	0.784	3.8	0.236	1.3980
700	0.588	5.008	0.376	5.176	0.52	4.032	0.84	2.96	-0.198	1.5960
800	0.688	4.32	0.74	4.436	0.48	3.552	0.676	2.284	0.136	1.4600
900	0.464	3.856	0.64	3.796	0.736	2.816	0.628	1.656	-0.13	1.5900
1000	-0.204	4.06	-0.0084	3.8044	0.544	2.272	0.512	1.144	-0.6342	2.2242
1100	0.912	3.148	0.78	3.0244	0.456	1.816	0.696	0.448	0.27	1.9542

	(m)		kg/m³
Sample Thickness:	0.00994	**Sample Density:**	1935.39
Sample Height:	0.02014		
Sample Width:	0.02199		
Sample Weight (g):	8.52		

Sample (5-29-02)

Temp	ρ	Δt_{sample}	Time	Wave Speed	Modulus
°C	kg/m³	sec	sec	m/s	Gpa
22	1935.39	0	2.22E-06	4477.477	38.80032
200	1935.39	-8.0000E-09	2.23E-06	4461.400	38.52218
300	1935.39	-7.5400E-07	2.98E-06	3333.333	21.50433
400	1935.39	-4.5800E-07	3.44E-06	2889.535	16.15937
500	1935.39	-4.1400E-07	3.85E-06	2579.139	12.87413
600	1935.39	2.3600E-07	3.62E-06	2747.374	14.60845
700	1935.39	-1.9800E-07	3.82E-06	2604.822	13.13181
800	1935.39	1.3600E-07	3.68E-06	2701.087	14.12036
900	1935.39	-1.3000E-07	3.81E-06	2608.924	13.17320
100	1935.39	-6.3420E-07	4.44E-06	2236.623	9.68176
1100	1935.39	2.7000E-07	4.17E-06	2381.295	10.97475

Figure D.1. Sample of a C/C data sheet [CCIV(5-29-02)] (no oxidation).

Time	Weight	$t_{x\,(thru)}$	Total t_z	$t_{x1\,(thru)}$	Total t_{x1}	$t_{z\,(PE)}$	Total t_z	$t_{z1\,(PE)}$	Total t_{z1}	Δt_{sample}	Time$_{sample(6\text{-}24\text{-}02)}$
min	gm	μsec	μsec	μsec	μsec	μsec	μsec	μsec	μsec	μsec	μsec
0	7.68	0	10	0	10	0	10	0	10	0	0.0000
10		-0.36	10.36	-0.384	10.384	-0.292	10.292	0.216	9.784	-0.334	0.3340
20		0.072	10.288	0.12	10.264	-0.148	10.44	0.156	9.628	0.092	0.2420
30		0.168	10.12	0.132	10.132	-0.009	10.449	0.368	9.26	-0.0295	0.2715
40		-0.112	10.232	-0.072	10.204	0.004	10.445	0.34	8.92	-0.264	0.5355
50		-0.04	10.272	-0.096	10.3	-0.02	10.465	0.312	8.608	-0.214	0.7495
60		0.016	10.256	0.044	10.256	-0.016	10.481	0.204	8.404	-0.064	0.8135
70		-0.224	10.48	-0.184	10.44	-0.044	10.525	0.048	8.356	-0.206	1.0195
80		-0.176	10.656	-0.168	10.608	0.048	10.477	0.228	8.128	-0.31	1.3295
90		-0.288	10.944	-0.324	10.932	-0.072	10.549	0.112	8.016	-0.326	1.6555
100		0.6	10.344	0.568	10.364	0.08	10.469	0.168	7.848	0.46	1.1955
110		-0.624	10.968	-0.64	11.004	-0.124	10.593	0.004	7.844	-0.572	1.7675
120	6.58	0.188	10.78	0.2	10.804	0.05	10.543	0.02	7.824	0.159	1.6085

	(m)		kg/m³
Sample Thickness:	0.0095	**Sample Density:**	1992.63
Sample Height:	0.01887		
Sample Width:	0.0215		
Sample Weight (g):	7.68		

		Constant Sample (6-24-02)					Removed Sample (6-23-02)
Time	Weight	ρ	Δt_{sample}	Time	Wave Speed	Modulus	Modulus
min	gm	kg/m³	sec	sec	m/s	Gpa	Gpa
0	7.68	1992.63	0	2.22E-06	4279.279	36.48955	38.9817602
10	7.59	1968.85	-3.3400E-07	2.55E-06	3719.655	27.24067	21.5857503
20	7.50	1945.07	9.2000E-08	2.46E-06	3858.652	28.96045	19.6885362
30	7.41	1921.28	-2.9500E-08	2.49E-06	3812.964	27.93293	16.4439003
40	7.31	1897.50	-2.6400E-07	2.76E-06	3447.650	22.55422	15.5427883
50	7.22	1873.71	-2.1400E-07	2.97E-06	3199.192	19.17715	14.5027459
60	7.13	1849.93	-6.4000E-08	3.03E-06	3131.696	18.14324	12.949272
70	7.04	1826.15	-2.0600E-07	3.24E-06	2932.551	15.70461	10.5835412
80	6.95	1802.36	-3.1000E-07	3.55E-06	2676.433	12.91087	10.4181654
90	6.86	1778.58	-3.2600E-07	3.88E-06	2451.297	10.68723	9.61003117
100	6.76	1754.80	4.6000E-07	3.42E-06	2781.438	13.57580	9.42396037
110	6.67	1731.01	-5.7200E-07	3.99E-06	2382.445	9.82531	5.96804838
120	6.58	1707.23	1.5900E-07	3.83E-06	2481.390	10.51191	6.0104281

Figure D.2. Sample of a C/C data sheet [CCT4(5-24-02)] (with oxidation).
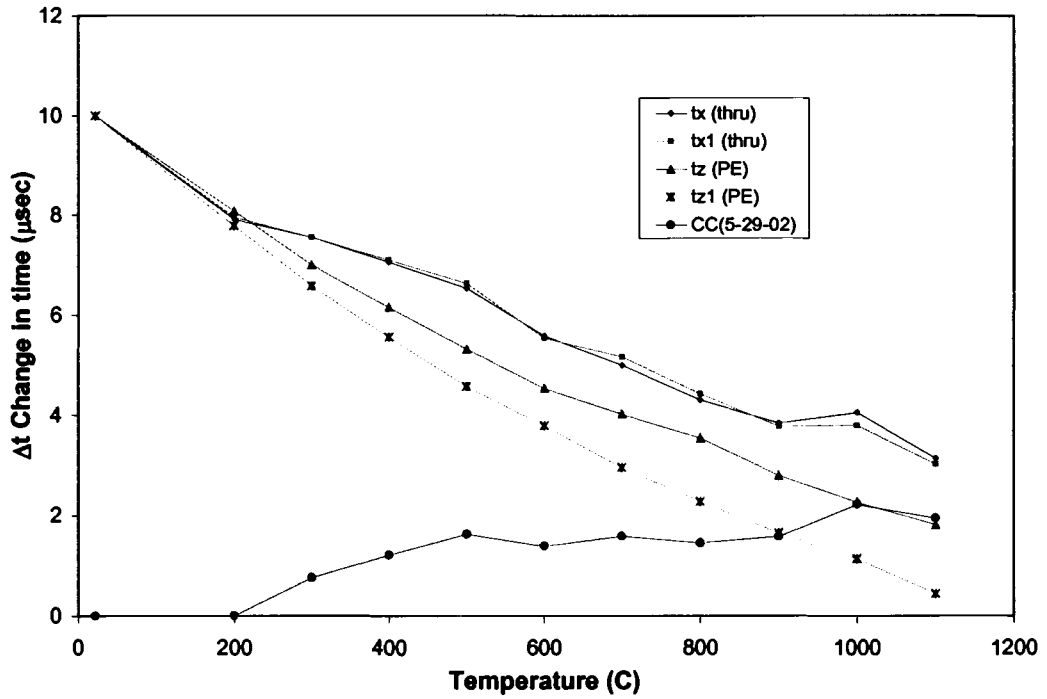
Figure E.1. Change in signal arrival time of CCIV(5-29-02) (inert).
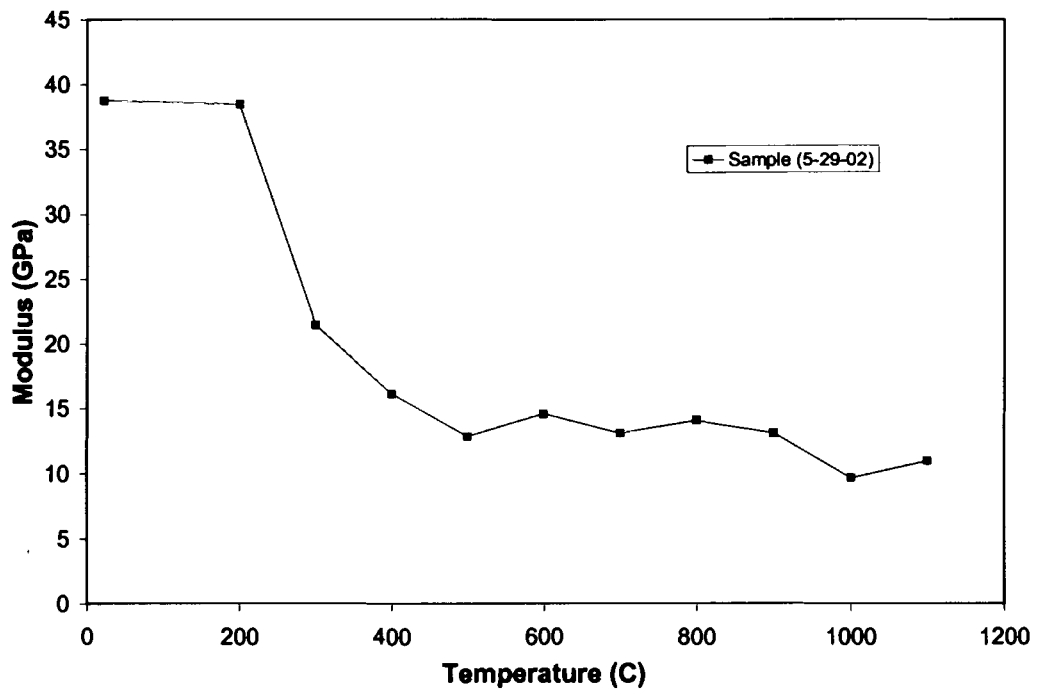
Figure E.2. Change in modulus of CCIV(5-29-02) (inert).
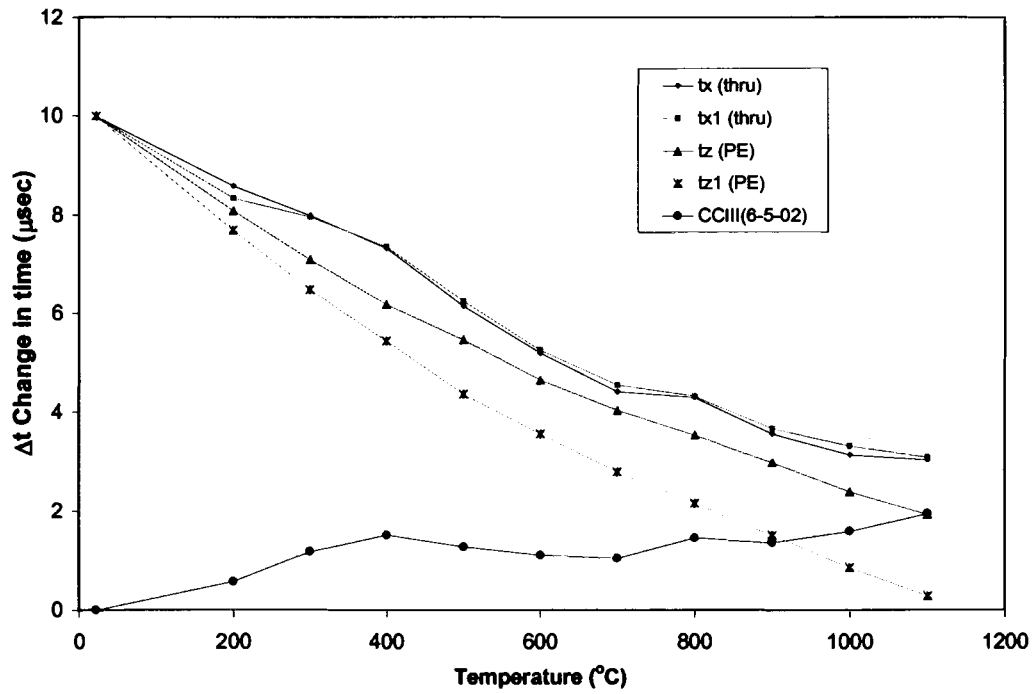
Figure E.3. Change in signal arrival time of CCIII(6-5-02) (inert).
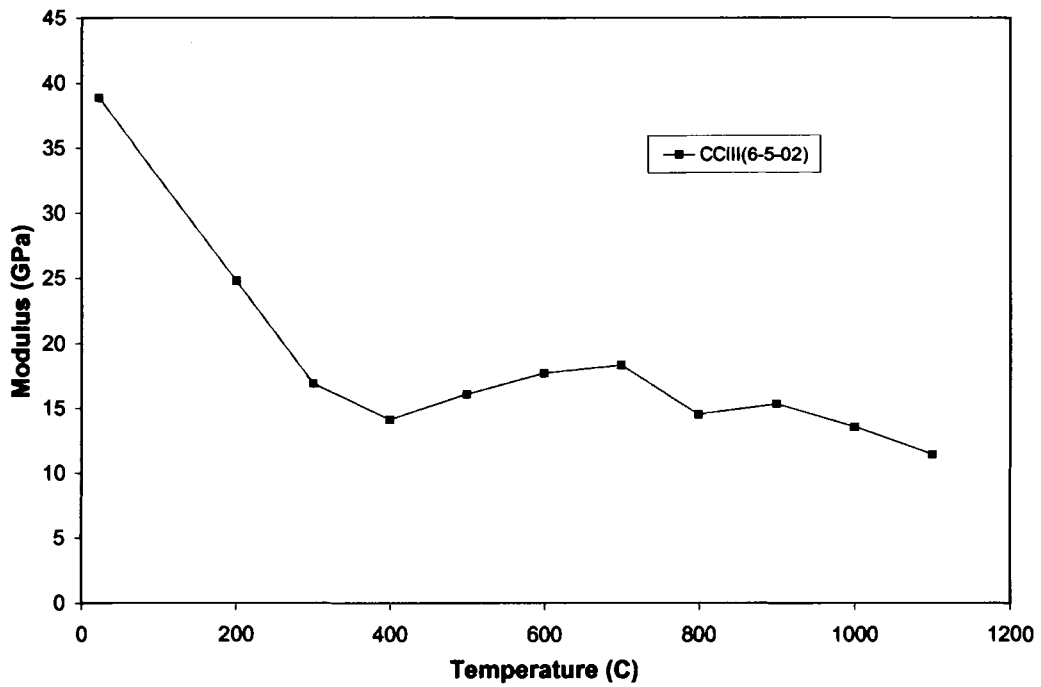
Figure E.4. Change in modulus of CCIII(6-5-02) (inert).

111
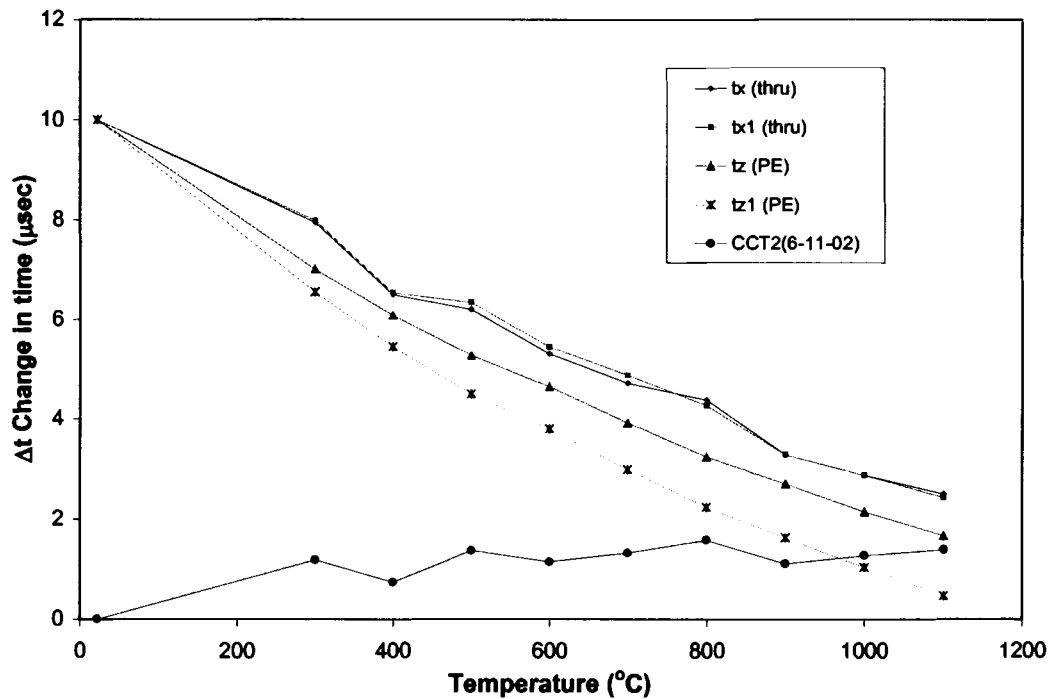
Figure E.5. Change in signal arrival time of CCT2(6-11-02) (inert).
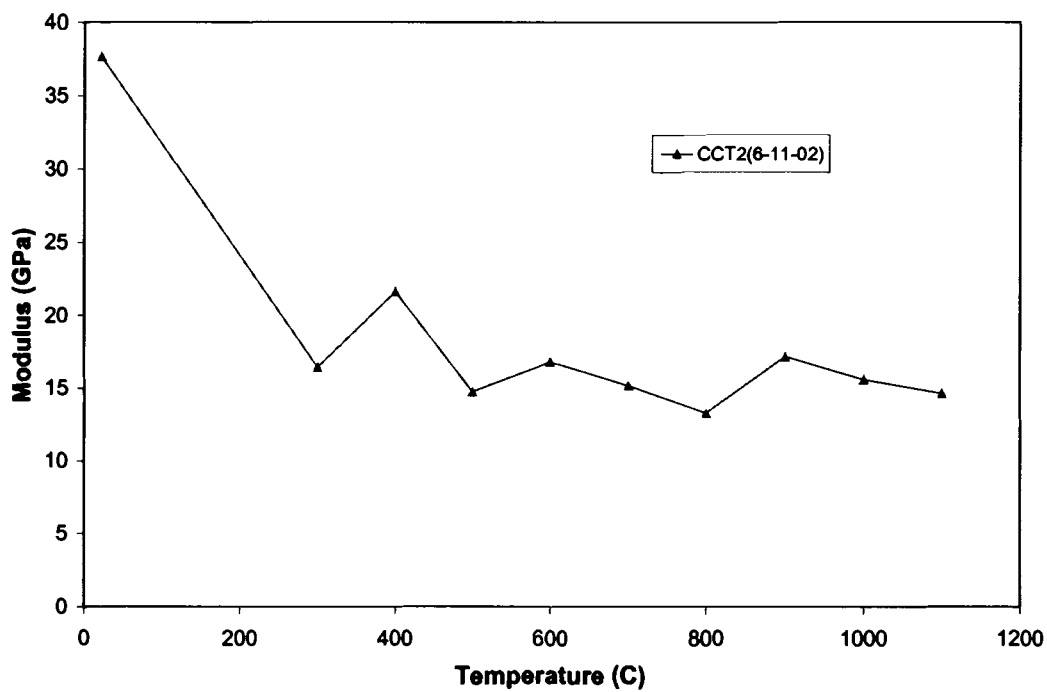
Figure E.6. Change in modulus of CCT2(6-11-02) (inert).

112
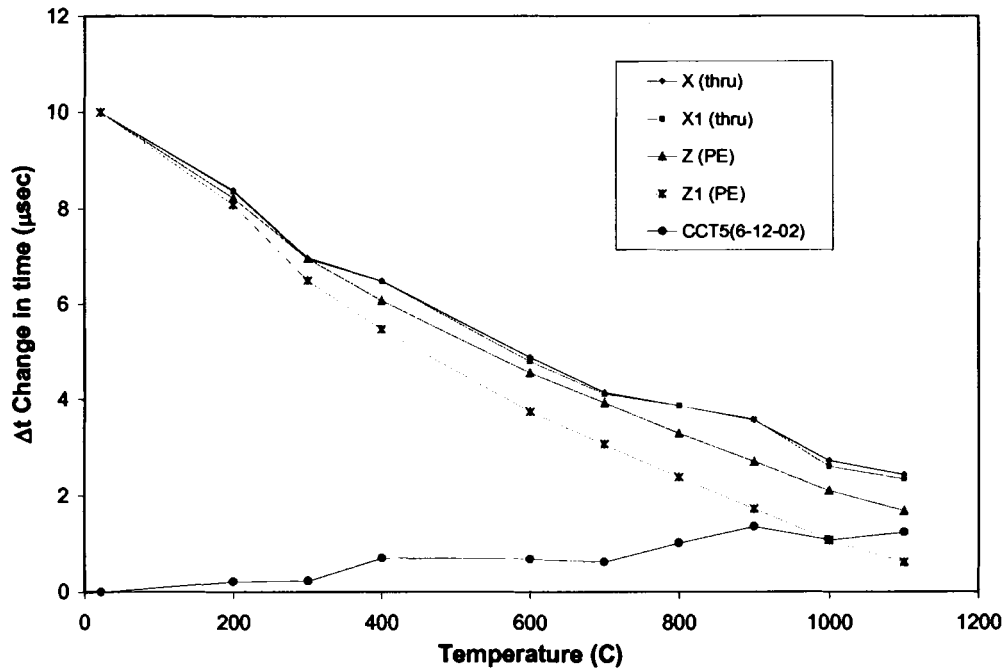
Figure E.7. Change in signal arrival time of CCT5(6-12-02) (inert).
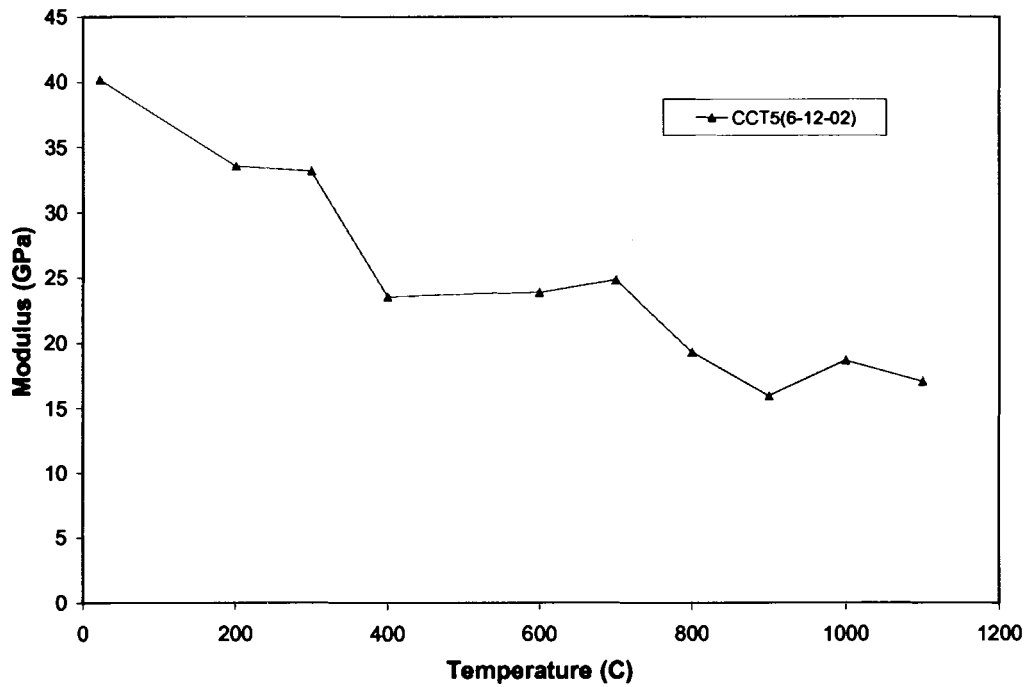
Figure E.8. Change in modulus of CCT5(6-12-02) (inert).
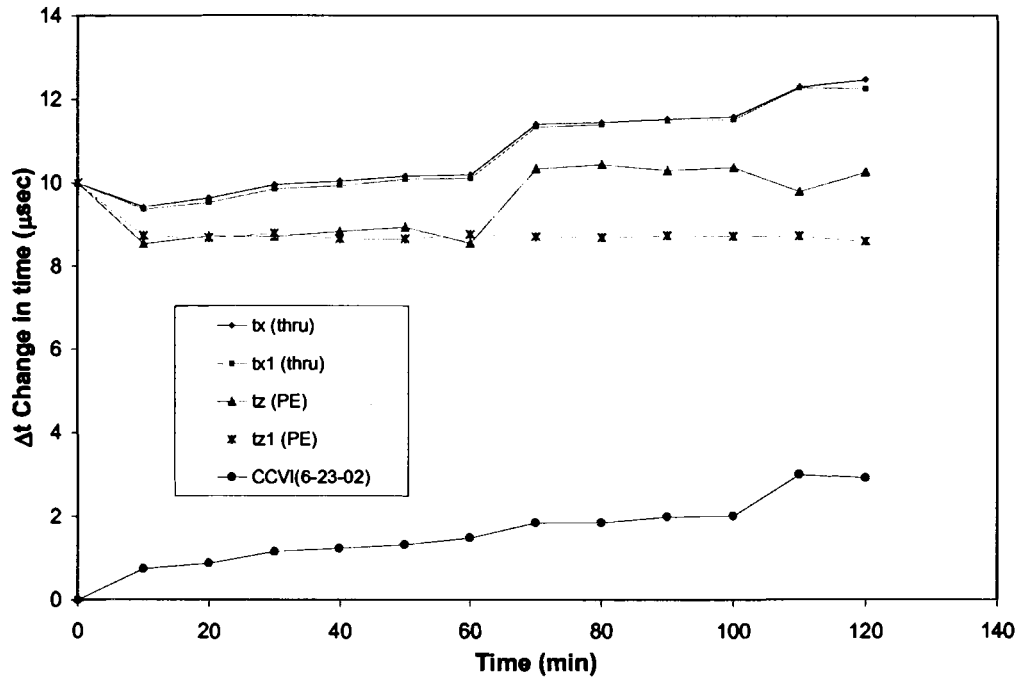
Figure E.9. Change in signal arrival time of CCVI(6-23-02) (oxidation).
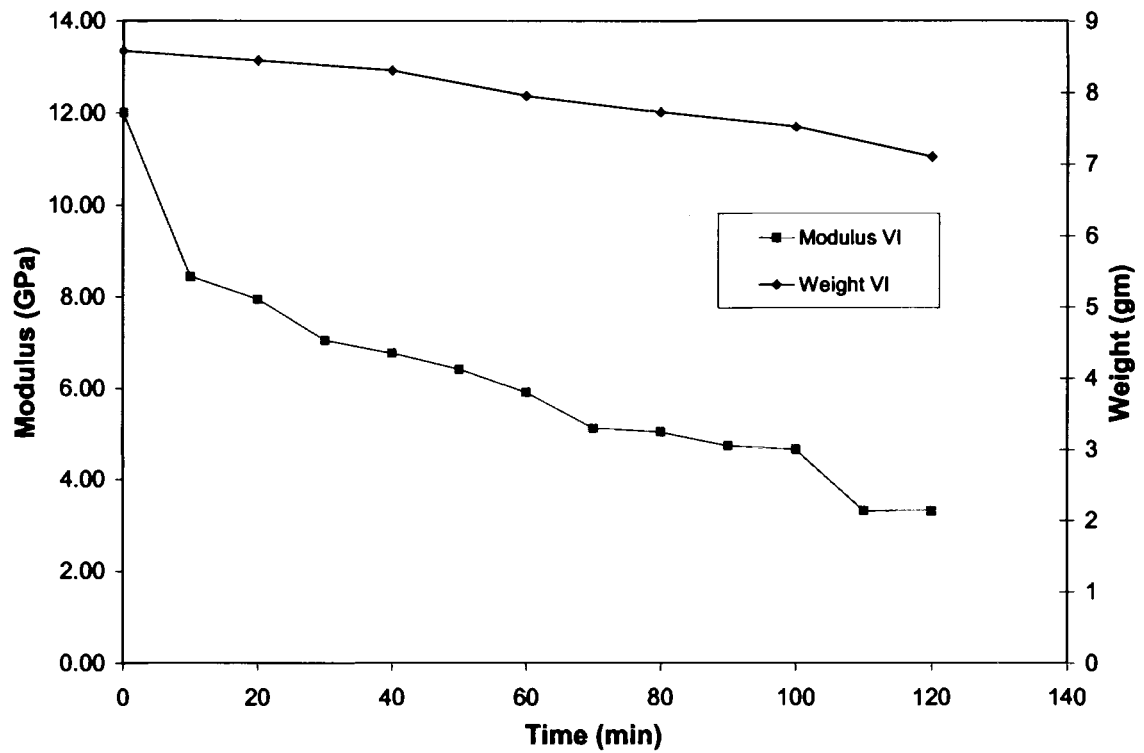
Figure E.10. Change in modulus of CCVI(6-23-02) (oxidation).

114
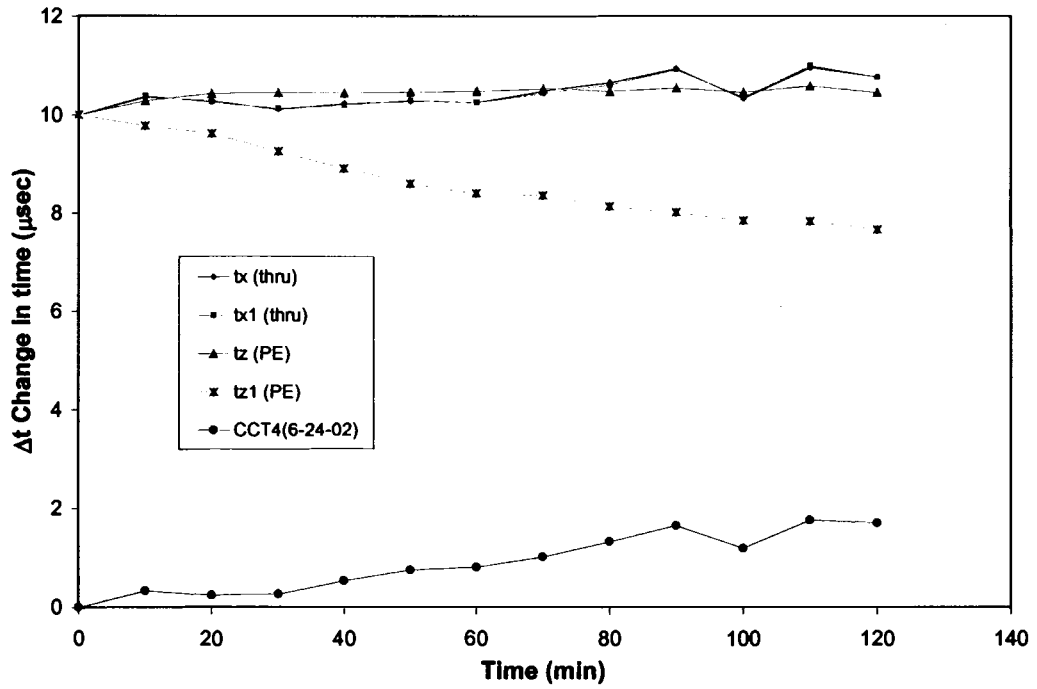
Figure E.11. Change in signal arrival time of CCT4(6-24-02) (oxidation).
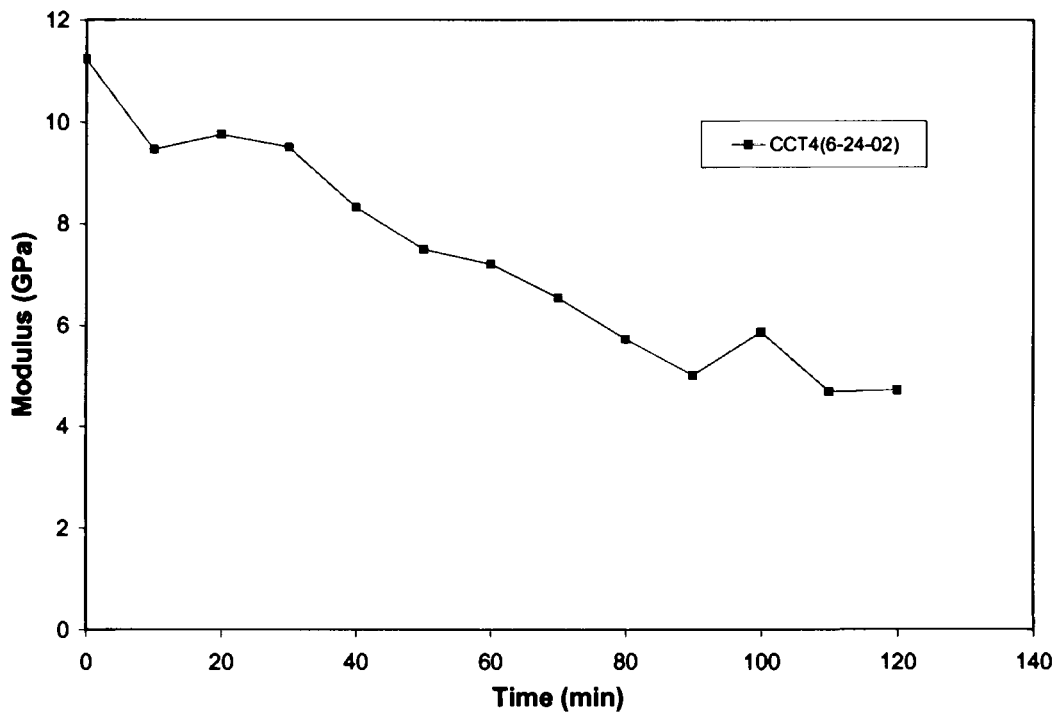
Figure E.12. Change in modulus of CCT4(6-24-02) (oxidation).
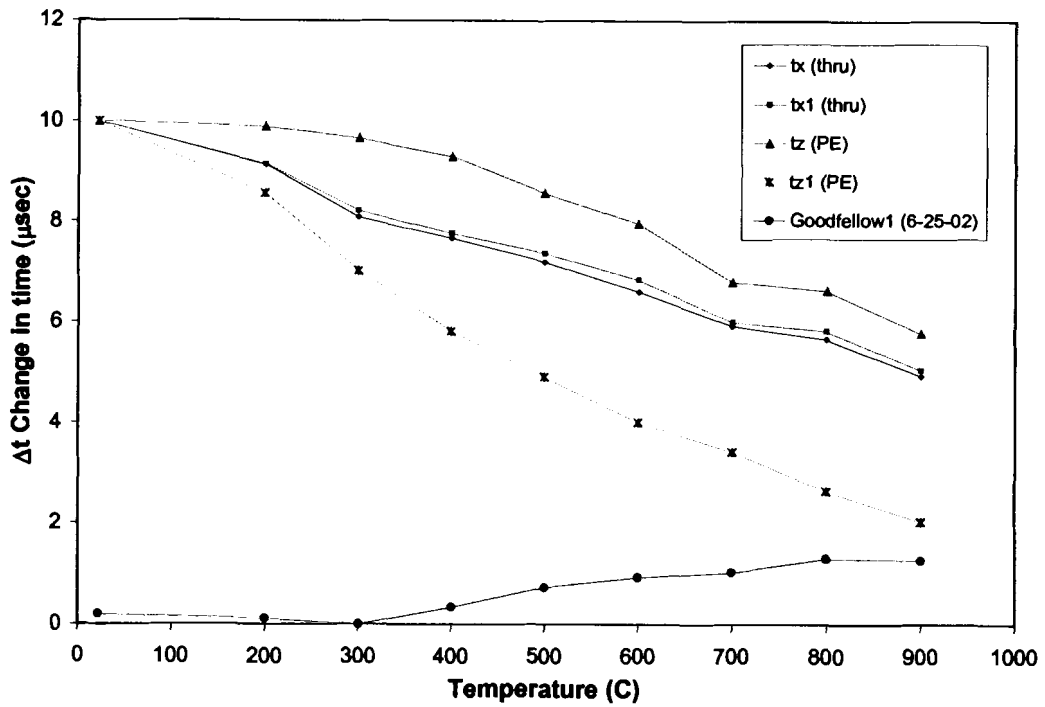
Figure E.13. Change in signal arrival time of Goodfellow1 (6-25-02) (inert).
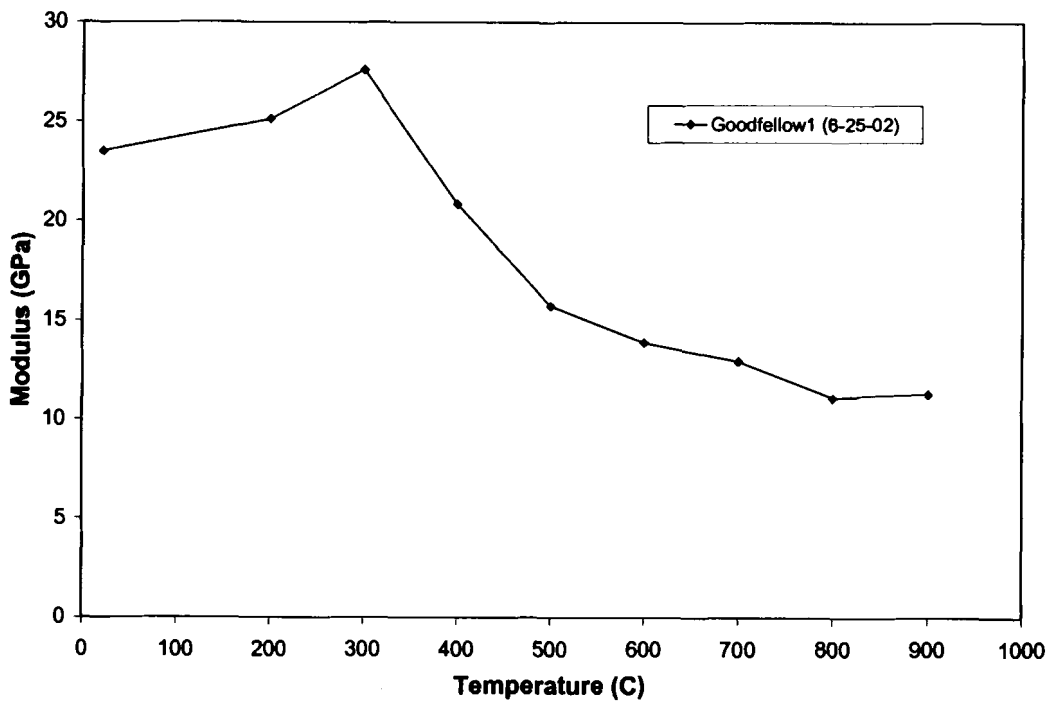
Figure E.14. Change in modulus of Goodfellow1 (6-25-02) (inert).

116
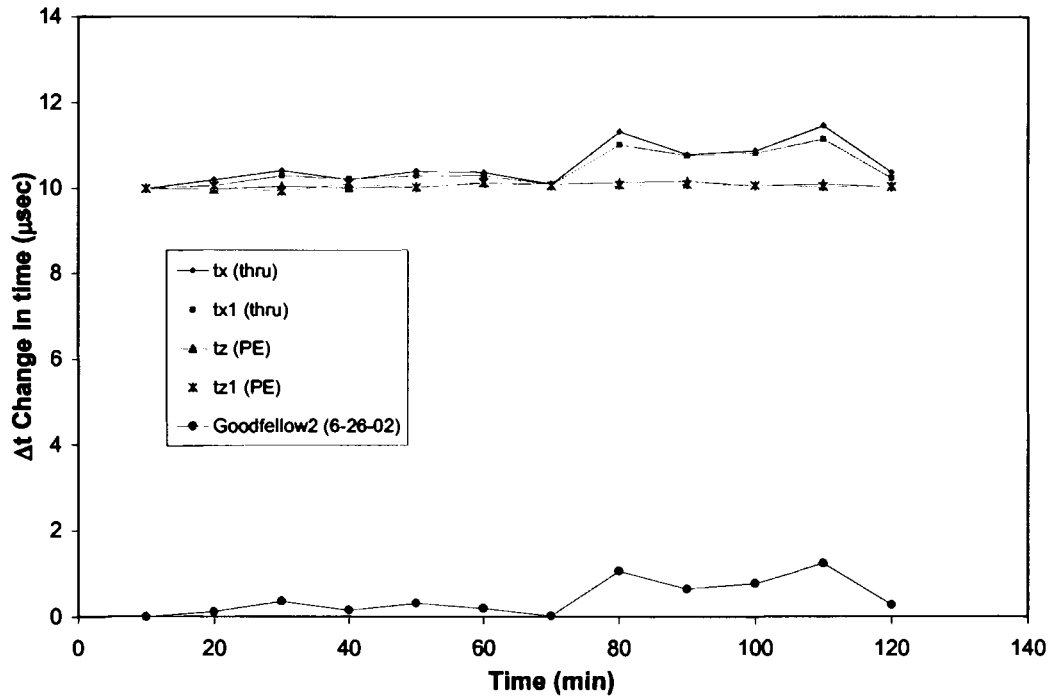
Figure E.15. Change in signal arrival time of Goodfellow2 (6-26-02) (oxidation).
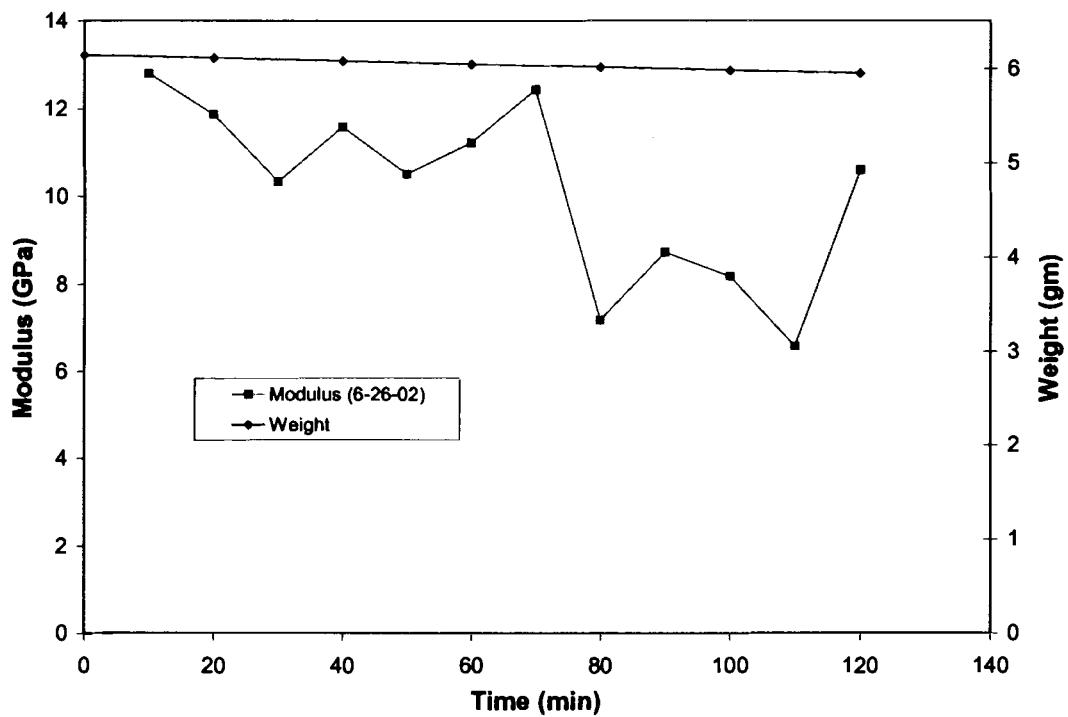
Figure E.16. Change in modulus of Goodfellow2 (6-26-02) (oxidation).

APPENDIX F – Furnace Materials

Waveguides:

Material: Fused quartz

Order from: Quartz Scientific Inc.
819 East St.
Fairport Harbor, OH 44077

Part number: QR10

Description: 10mm diameter x 4' long clear fused quartz

Alumina Guides:

Material: Alumina fiber

Order from: Zircar Ceremics
110 North Main St.
Florida, NY 10921

Part number: ASH

Description: 1.25" O.D. x 0.390" I.D. x 12" long ASH insulation cylinder

Furnace Tube:

Material: High dense Mullite

Order from: Earthwaterfire.com
An Anderson & Company Ltd.

Part number: EWF.610

Description: 40mm x 32mm x 1000mm long Mullite tube

BIOGRAPHY OF THE AUTHOR

Shaun Patrick Bunker was born in Augusta, Maine on July 14, 1978. He graduated from Cony High School in Augusta, ME in 1996. He attended The University of Maine at Orono and graduated in May, 2001 with a Bachelor of Science degree in Mechanical Engineering. While enrolled at the university, Shaun became a member of Pi Tau Sigma, national mechanical engineering honor society, Tau Beta Pi, national engineering honor society, Golden Key, national academic honor society, and the Francis Crowe, engineering graduate honor society. He is a co-author of the technical paper titled: *Evaluation of Dynamic Properties of Composites in an Oxidizing Environment*, published in the Review of Quantitative Nondestructive Evaluation, vol. 21, 2002, by the American Institute of Physics. Shaun is a candidate for the Master of Science degree in Mechanical Engineering from The University of Maine in August, 2002.